EXPLORATORY STUDY OF THE OPERATIONAL CONDITIONS OF A BELL MODEL 205A-1 HELICOPTER IN USFS SERVICE

A Thesis by

Thomas D. Dalton

Bachelor of Science, Embry-Riddle Aeronautical University, 2008

Submitted to the Department of Aerospace Engineering
and the faculty of the Graduate School of
Wichita State University
in partial fulfillment of
the requirements for the degree of
Master of Science

December 2011

© Copyright 2011 by Thomas D. Dalton

All Rights Reserved

EXPLORATORY STUDY OF THE OPERATIONAL CONDITIONS OF A BELL MODEL 205A-1 HELICOPTER IN USFS SERVICE

The following faculty members have examined the final copy of this thesis for form and content and recommend that it be accepted in partial fulfillment of the requirement for the degree of Master of Science with a major in Aerospace Engineering.

_____
Linda Kliment, Committee Chair

_____
Kamran Rokhsaz, Committee Member

_____
Abu Asaduzzaman, Committee Member

ACKNOWLEDGMENTS

This work was partially funded by the Federal Aviation Administration under the grant 08-G-016. The authors would like to acknowledge the technical support provided by HBM-nCode and the United States Forest Service.

ABSTRACT

For this exploratory study, flight data of a Bell Model 205A-1 helicopter, flying under contract to the United States Forest Service, is analyzed to investigate its operational conditions. Usage of the helicopter, specifically the missions performed, and phases occurring within those missions, is determined; as well as finding the magnitude and classification of vertical loads that occurred in the course of operation. As a result, it is determined that the helicopter was required to carry out seven distinguishable types of missions; and within those missions, the helicopter performed ten flight phase types, three of which were mission specific. A program code is written to determine these phases and mission types. Data is presented to show the flight usage of the helicopter for all mission types, as well as the specific phases occurring within those missions. Due to placement of the accelerometers in the nose of the aircraft, separation of gust and maneuver loads is difficult. A method is presented to classify vertical loads into three categories based upon roll and pitch rates of the helicopter. Flight load data is presented to help understand the loading the helicopter experiences through its overall flights along with the maximum and minimum loads experienced in individual flight phases.

TABLE OF CONTENTS

Chapter Page

1. INTRODUCTION 1

A. Background 1
B. Literature Review 1
C. Thesis Structure 2

2. METHODS OF ANALYSIS 3

A. Aircraft Analyzed 3
B. Available Flight Data 4
C. Flight Data Files and Data Handling 5
D. Aircraft Usage 5
1. Phase Separation and Identification 7
2. Mission Identification 9
3. Phase Separation and Mission Identification Program Architecture 12
E. Flight Loads 14
1. Normal Load Identification 14
2. Normal Load Classification 14
F. Aircraft Usage Statistics 16

3. RESULTS AND DISCUSSION 19

A. Available Data 19
B. Aircraft Usage 19
1. Mission Usage Results 19
a. Bucket Mission Usage Data 19
b. Ferry Mission Usage Data 25
c. Passenger Mission Usage Statistics 30
d. Reconnaissance Mission Usage Statistics 35
e. Helitorch Mission Usage Statistics 41
f. Longline Mission Usage Statistics 46
g. Rappel Mission Usage Statistics 51
2. Phase Usage Results 56
a. Stationary Phase Usage Statistics 57
b. Start of Flight Phase Usage Statistics 59

TABLE OF CONTENTS (continued)

Chapter Page

c. Climb Phase Usage Statistics 62
d. Cruise Phase Usage Statistics 65
e. Descent Phase Usage Statistics 67
f. Start of Landing Phase Usage Statistics 70
g. Hover Phase Usage Statistics 72
h. Bucket Fill Phase Usage Statistics 75
i. Bucket Drop Phase Usage Statistics 78
j. Helitorch Burn Phase Usage Statistics 80

D. Flight Loads 83
1. General Usage Results and Comparisons 83
2. Gust, Maneuver, and Change of State Induced Loads 86
a. Gust Induced Vertical Flight Loads 87
b. Maneuver Induced Vertical Flight Loads 90
c. Maneuver and Change of State Induced Vertical Flight Loads 93

4. SUMMARY 97

5. CONCLUSIONS 98

6. RECOMMENDATIONS 100

REFERENCES 101

APPENDIX 103

LIST OF TABLES

Table Page

Table 1. Model 205A-1 Characteristics 3

Table 2. Data Collected by the Appareo Systems Data Recorder 4

Table 3. Flight Phase Separation Criteria 8

Table 4. Hover Identification Criteria 8

Table 5. Mission Classification Criteria 11

Table 6. Normal Load Factor Classification Criteria 16

Table 7. Extracted Usage Data Used for Graphical Presentation 17

Table 8. Extracted Usage Data for Tabular Presentation 18

Table 9. Bucket Mission Usage Statistics and Average Mission Profile 20

Table 10. Bucket Mission V_{NE} Exceedance Statistics 21

Table 11. Ferry Mission Usage Statistics and Average Mission Profile 26

Table 12. Ferry Mission V_{NE} Exceedance Statistics 26

Table 13. Passenger Mission Usage Statistics and Average Mission Profile 31

Table 14. Passenger Mission V_{NE} Exceedance Statistics 31

Table 15. Reconnaissance Mission Usage Statistics and Averaege Mission Profile 36

Table 16. Reconnaissance Mission V_{NE} Exceedance Statistics 36

Table 17. Helitorch Mission Usage Statistics and Average Mission Profile 41

Table 18. Helitorch Mission V_{NE} Exceedance Statistics 42

Table 19. Longline Mission Usage Statistics and Average Mission Profile 47

Table 20. Longline Mission V_{NE} Exceedance Statistics 47

Table 21. Rappel Mission Usage Statistics 52

Table 22. Rappel Mission V_{NE} Exceedance Statistics 52

Table 23. Usage Statistics of the Stationary Phase 57

Table 24. Usage Statistics of the Start of Flight Phase 59

Table 25. Usage Statistics of the Climb Phase 62

Table 26. Usage Statistics of the Cruise Phase 65

LIST OF TABLES (continued)

Table Page

Table 27. Usage Statistics of the Descent Phase....68

Table 28. Usage Statistics of the Start of Landing Phase....70

Table 29. Usage Statistics of the Hover Phase....73

Table 30. Usage Statistics of the Bucket Fill Phase....75

Table 31. Usage Statistics of the Bucket Drop Phase....78

Table 32. Usage Statistics of the Helitorch Burn Phase....81

Table 33. Mission Average, Maximum, and Minimum Incremental Load Factor....84

Table 34. Phase Average, Maximum, Minimum Incremental Load Factor....85

Table 35. N_z Disturbance Comparisons....86

Table 36. Gust Induced Load Statistics by Mission Type....88

Table 37. Gust Induced Load Statistics by Phase Type....88

Table 38. Maneuver Induced Load Statistics by Mission Type....91

Table 39. Maneuver Induced Load Statistics by Phase Type....91

Table 40. Maneuver and Change of State Induced Load Statistics by Mission Type....94

Table 41. Maneuver and Change of State Induced Load Statistics by Phase Type....94

Table 42. Gust N_Z Peaks for Velocity vs N_Z for Reference 6....104

Table 43. Maneuver N_Z Peaks for Velocity vs N_Z for Reference 6....105

LIST OF FIGURES

Figure Page

Figure 1. Model 205A-1 Planform 3

Figure 2. Excerpt of Standard CSV Data File....5

Figure 3. Burn Phase Introduction Logic....9

Figure 4. Helicopter Ferry Mission Profile....10

Figure 5. Helicopter Initial Bucket Mission Profile....10

Figure 6. Helicopter Flight Track in Google™ Earth 12

Figure 7. Data Analysis Program Architecture....13

Figure 8. Peak-Between-Means and Time-Between-Means Logic 14

Figure 9. Maximum Indicated Airspeed and Coincident MSL Altitude for Bucket Missions....21

Figure 10. Maximum MSL Altitude and Coincident Indicated Airspeed for Bucket Missions....22

Figure 11. Maximum MSL Altitude and Coincident Flight Distance for Bucket Missions 22

Figure 12. Maximum Flight Duration and Coincident Flight Distance for Bucket Missions 23

Figure 13. Normal Probability Distribution of Flight Duration for Bucket Missions....23

Figure 14. Normal Probability Distribution of Flight Distance for Bucket Missions 24

Figure 15. Maximum and Minimum Pitch Angle and Coincident Indicated Airspeed for Bucket Missions 24

Figure 16. Maximum and Minimum Roll Angle and Coincident Indicated Airspeed for Bucket Missions....25

Figure 17. Maximum MSL Altitude and Coincident Indicated Airspeed for Ferry Missions 27

Figure 18. Maximum Indicated Airspeed and Coincident MSL Altitude for Ferry Missions 27

Figure 19. Maximum MSL Altitude and Coincident Flight Distance for Ferry Missions 28

Figure 20. Maximum Flight Duration and Coincident Flight Distance for Ferry Missions 28

Figure 21. Normal Probability Distribution of Flight Duration for Ferry Missions 29

Figure 22. Normal Probability Distribution of Flight Distance for Ferry Missions....29

Figure 23. Maximum and Minimum Pitch Angle and Coincident Indicated Airspeed for Ferry Missions 30

Figure 24. Maximum Roll Angle and Coincident Indicated Airspeed for Ferry Missions 30

Figure 25. Maximum MSL Altitude and Coincident Indicated Airspeed for Passenger Missions 32

Figure 26. Maximum Indicated Airspeed and Coincident MSL Altitude for Passenger Missions 32

LIST OF FIGURES (continued)

Figure Page

Figure 27. Maximum MSL Altitude and Coincident Flight Distance for Passenger Missions 33

Figure 28. Maximum Flight Duration and Coincident Flight Distance for Passenger Missions 33

Figure 29. Normal Probability Distribution of Flight Duration for Passenger Missions 34

Figure 30. Normal Probability Distribution of Flight Distance for Passenger Missions 34

Figure 31. Maximum and Minimum Pitch Angle and Coincident Indicated Airspeed for Passenger Missions 35

Figure 32. Maximum Roll Angle and Coincident Indicated Airspeed for Passenger Missions 35

Figure 33. Maximum MSL Altitude and Coincident Indicated Airspeed for Reconnaissance Missions 37

Figure 34. Maximum Indicated Airspeed and Coincident MSL Altitude for Reconnaissance Missions 37

Figure 35. Maximum MSL Altitude and Coincident Flight Distance for Reconnaissance Missions 38

Figure 36. Maximum Flight Duration and Coincident Flight Distance for Reconnaissance Missions 38

Figure 37. Normal Probability Distribution of Flight Duration for Reconnaissance Missions 39

Figure 38. Normal Probability Distribution of Flight Distance for Reconnaissance Missions 39

Figure 39. Maximum and Minimum Pitch Angle and Coincident Indicated Airspeed for Reconnaissance Missions 40

Figure 40. Maximum Roll Angle and Coincident Indicated Airspeed for Reconnaissance Missions 40

Figure 41. Maximum MSL Altitude and Coincident Indicated Airspeed for Helitorch Missions 42

Figure 42. Maximum Indicated Airspeed and Coincident MSL Altitude for Helitorch Missions 43

Figure 43. Maximum MSL Altitude and Coincident Flight Distance for Helitorch Missions 43

Figure 44. Maximum Flight Duration and Coincident Flight Distance for Helitorch Missions 44

Figure 45. Normal Probability Distribution of Flight Duration for Helitorch Missions 44

Figure 46. Normal Probability Distribution of Flight Distance for Helitorch Missions 45

Figure 47. Maximum and Minimum Pitch Angle and Coincident Indicated Airspeed for Helitorch Missions 45

Figure 48. Maximum and Minimum Roll Angle and Coincident Indicated Airspeed for Helitorch Missions 46

Figure 49. Maximum MSL Altitude and Coincident Indicated Airspeed for Longline Missions 48

Figure 50. Maximum Indicated Airspeed and Coincident MSL Altitude for Longline Missions 48

Figure 51. Maximum MSL Altitude and Coincident Flight Distance for Longline Missions 49

Figure 52. Maximum Flight Duration and Coincident Flight Distance for Longline Missions 49

LIST OF FIGURES (continued)

Figure Page

Figure 53. Normal Probability Distribution of Flight Duration for Longline Missions....50

Figure 54. Normal Probability Distribution of Flight Distance for Longline Missions....50

Figure 55. Maximum and Minimum Pitch Angle and Coincident Indicated Airspeed for Longline Missions....51

Figure 56. Maximum and Minimum Roll Angle and Coincident Indicated Airspeed for Longline Missions....51

Figure 57. Maximum MSL Altitude and Coincident Indicated Airspeed for Rappel Missions....53

Figure 58. Maximum Indicated Airspeed and Coincident MSL Altitude for Rappel Missions....53

Figure 59. Maximum MSL Altitude and Coincident Flight Distance for Rappel Missions....54

Figure 60. Maximum Flight Duration and Coincident Flight Distance for Rappel Missions....54

Figure 61. Normal Probability Distribution of Flight Duration for Rappel Missions....55

Figure 62. Normal Probability Distribution of Flight Distance for Rappel Missions....55

Figure 63. Maximum and Minimum Pitch and Coincident Indicated Airspeed for Rappel Missions....56

Figure 64. Minimum and Minimum Roll Angle and Coincident Indicated Airspeed for Rappel Missions....56

Figure 65. Maximum MSL Altitude and Coincident Ground Speed of the Stationary Phase....57

Figure 66. Maximum Ground Speed and Coincident MSL Altitude of the Stationary Phase....58

Figure 67. Maximum MSL Altitude and Coincident Phase Distance of the Stationary Phase....58

Figure 68. Maximum Phase Duration and Coincident Flight Distance of the Stationary Phase....59

Figure 69. Maximum MSL Altitude and Coincident Ground Speed of the Start of Flight Phase....60

Figure 70. Maximum Ground Speed and Coincident MSL Altitude of the Start of Flight Phase....60

Figure 71. Maximum MSL Altitude and Coincident Phase Distance of the Start of Flight Phase....61

Figure 72. Maximum Phase Duration and Coincident Phase Distance of the Start of Flight Phase....62

Figure 73. Maximum MSL Altitude and Coincident Ground Speed or Indicated Airspeed of the Climb Phase....63

Figure 74. Maximum Ground Speed or Indicated Airspeed of the Climb Phase....63

Figure 75. Maximum MSL Altitude and Coincident Phase Distance of the Climb Phase....64

Figure 76. Maximum Phase Duration and Coincident Phase Distance of the Climb Phase....64

Figure 77. Maximum MSL Altitude and Coincident Ground Speed or Indicated Airspeed of the Cruise Phase....66

Figure 78. Maximum Ground Speed or Indicated Airspeed and Coincident MSL Altitude of the Cruise Phase....66

LIST OF FIGURES (continued)

Figure Page

Figure 79. Maximum MSL Altitude and Coincident Phase Distance of the Cruise Phase 67

Figure 80. Maximum Phase Duration and Coincident Phase Distance of the Cruise Phase 67

Figure 81. Maximum MSL Altitude and Coincident Ground Speed and Indicated Airspeed of the Descent Phase ...68

Figure 82. Maximum Ground Speed or Indicated Airspeed and Coincident MSL Altitude of the Descent Phase 68

Figure 83. Maximum MSL Altitude and Coincident Phase Distance of the Descent Phase.....69

Figure 84. Maximum Phase Duration and Coincident Phase Distance of the Descent Phase 70

Figure 85. Maximum MSL Altitude and Coincident Ground Speed of the Start of Landing Phase.....71

Figure 86. Maximum Ground Speed and Coincident MSL Altitude of the Start of Landing Phase.....71

Figure 87. Maximum MSL Altitude and Coincident Phase Distance of the Start of Landing Phase 72

Figure 88. Maximum Phase Duration and Coincident Phase Distance of the Start of Landing Phase 72

Figure 89. Maximum MSL Altitude and Coincident Ground Speed of the Hover Phase.....73

Figure 90. Maximum Ground Speed and Coincident MSL Altitude of the Hover Phase.....74

Figure 91. Maximum MSL Altitude and Coincident Phase Distance of the Hover Phase 74

Figure 92. Maximum Phase Duration and Coincident Phase Distance of the Hover Phase 75

Figure 93. Maximum MSL Altitude and Coincident Ground Speed or Indicated Airspeed of the Bucket Fill Phase.76

Figure 94. Maximum Ground Speed or Indicated Airspeed and Coincident MSL Altitude of the Bucket Fill Phase.76

Figure 95. Maximum MSL Altitude and Coincident Phase Distance of the Bucket Fill Phase.....77

Figure 96. Maximum Phase Duration and Coincident Phase Distance of the Bucket Fill Phase 77

Figure 97. Maximum MSL Altitude and Coincident Ground Speed or Indicated Airspeed of the Bucket Drop Phase 78

Figure 98. Maximum Ground Speed or Indicated Airspeed and Coincident MSL Altitude of the Bucket Drop Phase 79

Figure 99. Maximum MSL Altitude and Coincident Phase Distance of the Bucket Drop Phase 79

Figure 100. Maximum Phase Duration and Coincident Phase Distance of the Bucket Drop Phase 80

Figure 101. Maximum MSL Altitude and Coincident Ground Speed of the Helitorch Burn Phase 81

LIST OF FIGURES (continued)

Figure Page

Figure 102. Maximum Ground Speed or Indicated Airspeed and Coincident MSL Altitude of the Helitorch Burn Phase 82

Figure 103 Maximum MSL Altitude and Coincident Phase Distance of the Helitorch Burn Phase 82

Figure 104. Maximum Phase Duration and Coincident Phase Distance of the Helitorch Burn Phase 83

Figure 105. Model 205A-1 and UH-1H Cumulative Load Factor Comparison 85

Figure 106. Gust, Maneuver, and Change of State Load Cumulative Load Factor Comparison 87

Figure 107. Maximum and Minimum Incremental Load Factors Due to Gusts and Coincident Ground Speed or Indicated Airspeed 89

Figure 108. Gust Induced Cumulative Load Factor Comparision by Mission Type 90

Figure 110. Maximum and Minimum Incremental Load Factors and Coincident Ground Speed or Indicated Airspeed Due to Maneuvers 92

Figure 111. Maneuver Induced Cumulative Load Factor Comparision by Mission Type 93

Figure 113. Maximum and Minimum Incremental Load Factors and Coincident Ground Speed or Indicated Airspeed Due to Maneuver and Change of State 95

Figure 114. Change of State Induced Cumulative Negative Load Factor Comparision by Mission Type 96

NOMENCLATURE

c.g.	center of gravity
DFDR	Digital Flight Data Recorder
g	gravity constant, 32.17 ft/s^2
GPS	global positioning system
GW	gross weight (pounds)
KCAS	calibrated airspeed, knots
KIAS	indicated airspeed, knots
KTAS	true airspeed, knots
Mcdc	number of Cruise-Descent-Cruise phase series per mission
Min	minutes
MQH	number of Climb-Descent phase series per mission
MSL	mean sea level, altitude (ft)
nm	nautical mile
N_{PHASES}	number of phases per mission
NTSB	National Transportation Safety Board
n_z	vertical load factor (g)
PN	phase number
RMS	root mean square
RPM	revolutions per minute
s	seconds
SM	number of stationary phases per mission
SP	short period mode
STD	standard deviation
USFS	United States Forest Service
V_{NE}	velocity, never exceed (knots)
WSU	Wichita State University
Δnz	incremental load factor (g)
ΔV_{NE}	KIAS above V_{NE}, (knots)

CHAPTER 1

INTRODUCTION

A. Background

The U.S. Forest Service (USFS) has long used converted military and civilian aircraft to combat forest fires. These aircraft would perform various functions, primarily the dropping of water or fire retardant chemicals in fire zones; after being stripped and retrofitted with the equipment required for aerial firefighting. While it has been known that the flight loads during a firefighting mission are more severe [1] than what the aircraft was originally designed for, no major health-and-usage-monitoring programs were in place to study the effects of the increased loads on the retrofitted aircraft. Following the catastrophic in-flight failures of two USFS heavy air tankers, the National Transportation Safety Board (NTSB) issued Recommendation A-04-29 [2], stating that the USFS should: *"Develop maintenance and inspection programs for the aircraft that are used in firefighting operations that take into account and are based on the magnitude of maneuver loads and the level of turbulence in the firefighting environment and the effect of these factors on remaining operation life."*

As a result of this recommendation, the Federal Aviation Administration (FAA) and the USFS have executed several programs, one of which is the implementation of digital flight data recorders (DFDRs) on various USFS aircraft, and storing this data in a central repository. Wichita State University (WSU) had previously been supported by the FAA to study the loads environment of a Beech BE-1900D commuter aircraft [3]. WSU was called upon again to study new sets of data taken from heavy air tanker aircraft and a general use helicopter – a Bell Model 205A-1, and perform similar analysis to that which was done on the Beech BE-1900D. In this thesis , results are presented from the exploratory study of the operation conditions of the 205A-1 helicopter while in the service of the USFS.

B. Literature Review

For fixed-wing aircraft, the operational loads and airframe usage characteristics of firefighting aircraft are well studied. In 1974, the National Aeronautic and Space Administration (NASA), using airspeed, loads, and altitude data from a pair of Douglas DC-6Bs, detailed the first complete characterization of flight loads for aerial firefighting aircraft. [1] The report showed that maneuver load factors of magnitude between 2.0 and 2.4 g's occurred 1000 times more often than the DC-6B's commercial counterparts. Further research, taking into account the mission profile and

size of aircraft, was performed in 2005 by Hall [4]. This marked the development of a comprehensive load spectrum for fixed-wing firefighting aircraft, and was the basis upon which previous WSU research was based [5].

For rotary-wing aircraft used in firefighting roles, literature is void of any research into the aircraft usage and operational loads. However, studies not directly related to helicopters repurposed for aerial firefighting have been performed. In 1973, the US Army [6] initiated a study to present comprehensive operation usage data of Army helicopters in a combat environment. Three Bell UH-1H, the military version of the Model 205A-1, were outfitted with flight data recorders, leading to analysis and understanding of the helicopter's usage and flight loads spectrum. In 1974, Arcidiacono [7] presented a study discussing the effect of gusts on a helicopters airframe in terms of flight loading. The study showed that unlike fixed-wing aircraft, a helicopter had a natural damping tendency towards gusts, and that the magnitude and frequency were less than those of a fixed-wing.

Data gathered by the USFS in 2009 has been analyzed in this thesis, in an attempt to fill the void that exists in the study of operational usage and conditions of a helicopter in a firefighting role. Flight data was used to generate statistics on the number and type of missions performed by the helicopter, general usage, and the frequency and magnitude of flight loads encountered during missions. The flight loads were compared to the results found in the Army [6] study, and usage results were compared to limits set forth in the flight manual [9] to determine if the helicopter was being used outside the scope of the original design.

C. Thesis Structure

The methods used to analyze the flight data, determining missions and mission phase, and load disturbance identification and classification are presented in Chapter 2. The results and discussion for aircraft usage for each mission type and mission phase, as well as the results of the flight loads analysis are presented in Chapter 3. The results and discussions are summarized in Chapter 4. Conclusions based on the results are discussed in Chapter 5 and recommendations are given in Chapter 6. The Appendices present gust and maneuver flight load data collected for Reference 6.

CHAPTER 2

METHODS OF ANALYSIS

A. Aircraft Analyzed

A Bell Model 205A-1 helicopter was used for the present study. An onboard DFDR recorded a number of parameters, and with some post-processing, 25 channels of data were made available for further analysis. The helicopter planform and some characteristics are given in Figure 1 and Table 1.

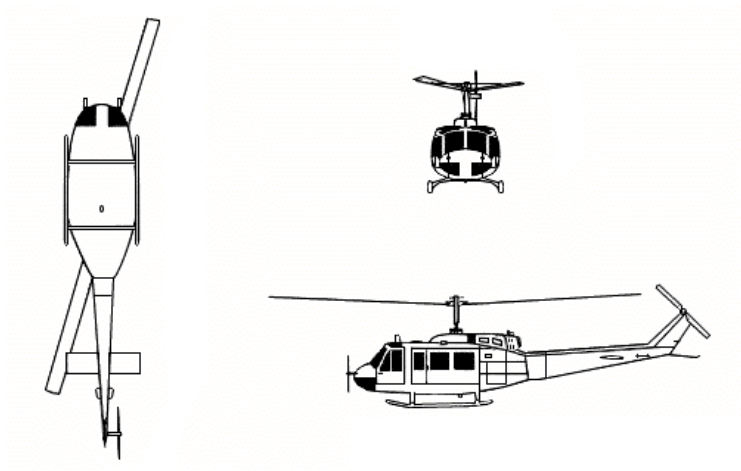

Figure 1. Model 205A-1 Planform

(http://commons.wikimedia.org/wiki/File:Bell_UH-1_IROQUOIS.png)

Table 1. Model 205A-1 Characteristics

	Model 205A-1 [6]
Rotor Diameter (ft)	48
Rotor Solidity	0.0464
Engine	Lycoming T53-13A
Design Gross Weight (lbs)	9,500
Empty Weight (lbs)	4,920
Rated Power (shp)	1,250
100% Rotor Speed (rpm)	324
Max Airspeed (knots)	120

The Bell Model 205A-1 helicopter is the commercial utility version of the Bell UH-1H "Iroquois." The 205A-1 uses the UH-1H's standard Lycoming T53-13A engine, derated from 1,400 shp to 1,250 shp, while retaining all other standard characteristics. The helicopter was designed as a rapid conversion aircraft, capable of performing numerous roles. Mission capabilities include air freight, flying crane, rescue, and passenger roles [8]. The helicopter

is also equipped with an external cargo suspension unit, allowing the external carrying of cargo or equipment. When the suspension unit is being used, maximum design gross weight increases to 10,500 lb [9].

B. Available Flight Data

The helicopter was equipped with an Appareo Systems data recorder capable of producing 30 channels of data at a constant rate. Although data was measured at 256 Hz, the recording was made at a fixed rate of 8 Hz. For this installation, only channels 3-25 were utilized, recording the parameters as shown in Table 2. The DFDR is contained within a single package, and to increase ease of installation it was placed in the nose of the helicopter. Once the data was retrieved from the DFDR, it was stored in the HBM-nCode library.

Table 2. Data Collected by the Appareo Systems Data Recorder

Channel	Parameter	Units
3	Latitude	Degrees
4	MSL Elevation	Feet
5	Longitude	Degrees
6	Pitch	Degrees
7	Roll	Degrees
8	Ground Speed	Knots
9	Vertical Speed	Feet per Minute
10	Heading	Degrees
11	Pitch Rate	Degrees per Second
12	Roll Rate	Degrees per Second
13	Yaw Rate	Degrees per Second
14	Longitudinal Acceleration	g
15	Lateral Acceleration	g
16	Normal Acceleration	g
17	True Airspeed	Knots
18	Equivalent Airspeed	Knots
19	Indicated Airspeed	Knots
20	Course Direction	Degrees
21	Pitot Pressure	Inches of Mercury
22	Static Pressure	Inches of Mercury
23	Outside Air Temperature	Degrees Celsius
24	Horizontal Accuracy	Millimeter
25	Vertical Accuracy	Millimeter

C. Flight Data Files and Data Handling

Prior to uploading into the HBM-nCode library, Appareo Systems trims the beginning and end of the data files to remove excess data. Raw data in the HBM-nCode library, and downloaded by WSU, are in the comma-separated-variable (CSV) format. These files were opened in Microsoft Excel during initial review, allowing for a more user friendly, fixed-width column format. Within the file, headers define each column. Elapsed time is given in seconds and starts on the first line of data and not at the start of the mission. An excerpt of a standard CSV data file, as viewed in Excel is presented in Figure 2.

	A	B	C	D	E	F	G	H	I	J	K
1	#HEADER										
2	#CHANTITLE										
3	Chan1										
4	#TITLES										
5	Index	Time	1:bay_doc	2:discrete	3:latitude	4:elevatio	5:longituc	6:pitch	7:roll	8:speed	9:vertical_
6	#UNITS										
7			discrete	discretes_	degrees	feet	degrees	degrees	degrees	knots	feet_per_
8	#KEYWORDS										
9	Index	Time	1:bay_doc	2:discrete	3:latitude	4:elevatio	5:longituc	6:pitch	7:roll	8:speed	9:vertical_
10	#DATATYPES										
11	HUGE	DOUBLE	FLOAT	FLOAT	FLOAT	FLOAT	FLOAT	FLOAT	FLOAT	FLOAT	FLOAT
12	#DATA										
13	1	0	0	0	46.3765	1390.26	-117.02	-0.4981	-0.0399	0	0
14	2	0.125	0	0	46.3765	1390.26	-117.02	-0.4981	-0.0399	0	0
15	3	0.25	0	0	46.3765	1390.26	-117.02	-0.4674	-0.0432	0.0001	0
16	4	0.375	0	0	46.3765	1390.26	-117.02	-0.4674	-0.0432	0.0001	0
17	5	0.5	0	0	46.3765	1390.26	-117.02	-0.5228	0.0378	0.0001	0
18	6	0.625	0	0	46.3765	1390.26	-117.02	-0.5228	0.0378	0.0001	0
19	7	0.75	0	0	46.3765	1390.26	-117.02	-0.5821	-0.0466	0.0001	0
20	8	0.875	0	0	46.3765	1390.26	-117.02	-0.5821	-0.0466	0.0001	0
21	9	1	0	0	46.3765	1390.26	-117.02	-0.6132	0.024	0.0002	0

Figure 2. Excerpt of Standard CSV Data File

Modification of the original CSV was not required for the development of primary analysis programming, as the language used was capable of reading and separating the values into their needed variable matrices.

D. Aircraft Usage

While fixed-wing firefighting aircraft generally perform a single mission type, the helicopter has is required to perform a number of mission types, ranging from common to exotic. Given the variance in performance and usage required for different mission types, it was important to identify the mission flown for each data file. Supplemental pilot reports, supplied by the helicopter operator, indicated that the helicopter was flown in seven types of missions during its 2009 fire season. It was later found that the seven listed by the operator encompassed all missions flown by the helicopter. The mission types are listed below.

- Bucket: The helicopter was used as an aerial firefighter. A bucket was suspended beneath the aircraft, filled, usually at a body of water near the fire, and then discharged over the fire zone while the helicopter was in motion.
- Ferry: The helicopter was flown from an initial position to a destination that was not the origin, with or without cargo or passengers.
- Passenger: The helicopter was flown from its home base to several other operation bases, usually carrying passengers or other internal cargo.
- Reconnaissance: The helicopter was flown over a predetermined area with only the crew, used to scout out fire zones.
- Helitorch: The helicopter was equipped with a tank, filled with gelatinized fuel, which supplied a steady stream of fire to the ground. Several burn runs and tank refills could occur per mission.
- Longline: The helicopter was flown from its home base to several other operation bases with a load suspended under the belly. The load was not dropped, but was rather delivered to the ground while hovering.
- Rappel: The helicopter was used to transport rappelling firefighters to a fire zone. The aircraft would hover over its drop point allowing 2-3 firefighters to rappel down. There could be more than one rappelling group per mission.

Because of the variation in missions performed, it was necessary to separate the data files into the specific phases of flight. This also provided more detailed insight into the usage of the helicopter, and allowed for a method of identifying the mission types being performed. This was important in that the supplemental pilot reports were not available for all data files and, when they were present, were not always reliable for mission identification. It was found that the flights had ten types of phases, seven universal and three mission-specific phases, as described below.

- Stationary: The helicopter was on the ground with the engine running.
- Start of Flight: The helicopter was transitioning from a stationary or hover phase to a climbing phase.
- Climb: The helicopter was flown with increasing velocity and altitude, in that the rate of climb or the acceleration was positive and non-zero.
- Cruise: The helicopter was flown with relatively constant velocity and altitude.
- Descent: The helicopter was flown while decelerating or descending.
- Start of Landing: The helicopter was transitioning from a descent phase to a stationary or hover phase.

- Hover: The aircraft velocity was small; however, the normal acceleration indicated that the aircraft was not on the ground.
- Fill (Bucket Only): The helicopter was in a specialized hover phase in which the under-slung bucket was being filled.
- Drop (Bucket Only): The helicopter was dropping the contents of the bucket over the fire zone while in motion.
- Burn (Helitorch Only): The aircraft was in a specialized low-speed hover phase in which the torch was deployed.

1. Phase Separation and Identification

Because this was an exploratory study, it was deemed necessary to adequately separate and identify the flight phases to provide initial insight into the helicopter's usage. Near the start of the study, several key elements in determining the phases became apparent, most notably ground speed and the variation in heading. Using these aspects of the flight data, crude phase separation could be performed, in that stationary, climb, cruise, and descent could be determined. However, feedback from the operators suggested that the climb, descent, and stationary phases were hiding two important transitory phases, specifically the start of climb and start of landing. It is in these phases that the helicopter was subjected to additional vertical loads and was no longer on the ground and yet is not truly in a climb or coming out of a descent. Given this fact, four more phase separation parameters were introduced for further refinement of the phases.

Phase separation relied primarily on the changes of key parameters. When determining these variations, the percent difference in magnitude over a one-second range was found and compared with the rolling root-mean-square (RMS) over a 12.5-second range. Since climb and descent were the same in nature except for the sign in the rate of change in ground speed, acceleration an deceleration were used to separate them. The parameters used for phase separation criteria and their percent changes are listed in Table 3.

Table 3. Flight Phase Separation Criteria

Phase	Heading Variation (%)	Roll Rate Variation (%)	Pitch Variation (%)	Ground Speed Variation (%)	Pitch (deg)	Ground Speed (knots)	Slope of Ground Speed
Start of Flight	> 0.50	> 2	> 15	NA	NA	< 6	NA
Climb	NA	NA	NA	> 1	NA	> 6	> 0
Cruise	NA	NA	NA	< 0.55	NA	> 10	NA
Descent	NA	NA	NA	> 2	> 1	> 5	< 0
Start of Landing	> 0.45	> 2	NA	NA	NA	< 5	NA
Stationary	< 0.5	< 2	NA	NA	NA	< 1	NA

Hover, fill, drop, and burn phases are not listed in Table 3 because of the specialized nature of the phases, and had to be handled separately. In determining when the helicopter was in a hover, phases that had been previously identified as stationary had to be re-examined. It was noted that when the helicopter was on the ground the difference between the maximum and minimum n_z was fairly small, and that when the aircraft was in hover, this difference increased. It was also noted that for hovers of shorter duration, less than 12.5 seconds, this difference was less than that of hovers lasting longer than 12.5 seconds. To account for this, two parameters were determined. Based upon the duration of the phase in question, and the difference between maximum and minimum n_z, it was possible to determine if the helicopter was in hover. These criteria are shown in Table 4.

Table 4. Hover Identification Criteria

New Phase Type	Previous Phase Classification	Phase Length (s)	n_z Difference
Hover	Stationary	> 12.5	> 0.175
Hover	Stationary	< 12.5	> 0.1

It was difficult to separate the fill and drop phases. Usually, these occurred when the helicopter performed a specific series of phases: descent, start of landing, climb; or descent, start of flight, climb. If one of these series was present, then the average ground speed was determined at the start of landing phase or start of climb phase. If the average speed was less than 7.5 knots, the start of landing phase or start of flight phase was reclassified as a fill. If the average speed was greater than 7.5 knots, the start of landing phase or start of flight phase was reclassified as a drop. This speed differential was determined based upon the logic that, for the fill phase, the aircraft had slowed down to such a pace as to allow the bucket to be gently dipped into the body of water without sudden forces on the bucket cable, the cargo hook, or the underside of the helicopter itself. The magnitude of the average speed limit was found by examining a host of representative files, and testing against a larger group.

Similar to fill and drop classification, burn identification required recognizing when a certain series of events occurred. However, unlike the fill and drop classification, a simple reclassification of a phase could not be done because the burn phase was generally buried within another phase type. Therefore, further steps were needed to successfully determine if a burn had occurred. Figure 3 shows how a burn and the climb out of burn phases were introduced into the phase record; the top table represents the phase record before the burn is considered, and the bottom represents the record once the burn has been included. The Separation Index was the point at which the phase begins in the data. The Phase Index is an account of the phases occurring within a mission, and is a simple number showing when a phase occurs in relation to other phases. If the phase series, as displayed in the top table of Figure 3 occurred, the average ground speed of Cruise-B was determined. If the average speed of Cruise-B was less than 28 knots, a burn phase and new climb phase was introduced into the series. To determine the new Separation Index points, it was found when the ground speed in Descent-A fell below 18 knots. Once within the burn phase, the Separation Index for the end of the burn, and the beginning of the new climb phase, was found when the ground speed exceeded 20 knots. With those two points determined, burn phase introduction was complete.

Separation Index	a-3	a-2	a-1	a	a+1	a+2	a+n
Phase Index	i-3	i-2	i-1	i	i+1	i+2	i+n
Phase Type	Cruise-A	Descent-A	Cruise-B	Descent-B	…	…	…

BECOMES

Separation Index	a-3	a-2	New Sep.	New Sep.	a-1	a	a+n
Phase Index	i-3	i-2	i-1	i	i+1	i+2	i+n
Phase Type	Cruise-A	Descent-A	Burn	Climb	Cruise-B	Descent-B	…

Figure 3. Burn Phase Introduction Logic

After all of the phases that occurred within a flight data file were identified, it was possible to identify the mission.

2. Mission Identification

As previously stated, operator-supplied supplemental reports allowed for the identification of some missions prior to any data analysis. While only a handful of missions had such reports, it was possible to use these as a test bed for determining if criteria created to identify missions were accurate. These marked missions also allowed for the

direct comparison of data between the missions of the same type, giving further insight into common characteristics that could be used to identify missions.

The first mission identified was also the most basic, a ferry mission. This mission was one in which the helicopter was simply flown from one base to another. In terms of phases, a ferry mission had two stationary, and a single start of flight, climb, cruise, descent, and start of landing, as displayed in Figure 4.

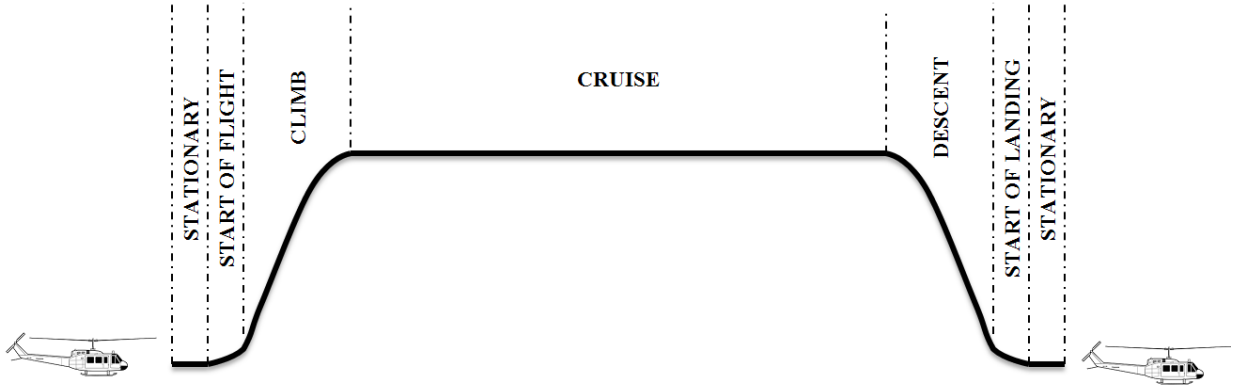

Figure 4. Helicopter Ferry Mission Profile

It followed naturally that, in terms of phase progression, passenger, longline, recon, and rappel missions were several ferry missions performed in sequence, but each having its own subtle characteristics. For bucket and helitorch, their complexities, at least in comparison with the more basic mission types, rendered them more easily recognizable. A sample of the initial section of a bucket mission phase profile is displayed in Figure 5.

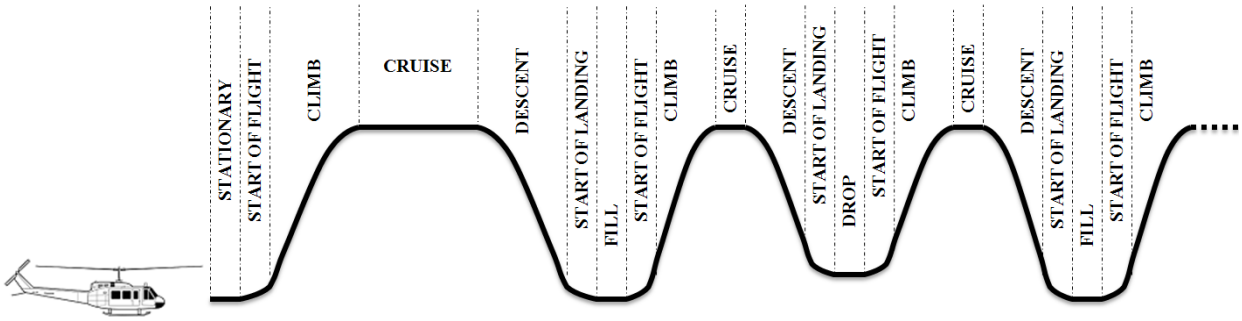

Figure 5. Helicopter Initial Bucket Mission Profile

Once the flights were examined, and mission defining characteristics were determined, it was found that seven indicators were useful is determining the mission type. The seven indicators were:

1. Mission score, given by

$$Score = \frac{\sum PN + (SM - 2) - (Mcdc * 4.5)}{N_{PHASES} + (SM - 2) + (MQH * 2) - Mcdc} \tag{1}$$

2. Number of phases in the flight,
3. Number of times the helicopter returned to its launch point,
4. Number of stationary phases,
5. Number of hover phases,
6. Phase density, defined as the ratio of the number of phases to the length of the data, and
7. Number of cruise-descent-cruise phase sequences.

Limiting values for these indicators were determined by trial-and-error and are presented in Table 5.

Table 5. Mission Classification Criteria

Mission	Mission Score	Number of Phases	Returns to Launch Point	Number of Stationary Phases	Number of Hover Phases	Phase Density	Number of Cruise-Descent-Cruise Phase Series
Bucket	NA	> 50	< 5	NA	≥ 9	< 850	NA
Ferry	= 2.486	= 7	= 0	= 2	= 0	NA	NA
Passenger	NA	NA	NA	NA	< 5	> 850	< 5
Recon	NA	NA	NA	NA	<2	> 700	≥ 5
Helitorch	NA	> 50	≥ 5	NA	NA	NA	NA
Longline	NA	NA	NA	NA	≥ 5	NA	< 5
Rappel	< 2.4	< 65	NA	≤ 3	2 ≤ H < 5	NA	NA

While results were being compared to the classifications given in the supplemental pilot reports, it was noticed that for multiple flights, identical information was being listed in the latter. To help ensure proper classification, the latitude and longitude data, given by the GPS, was uploaded into Google™ Earth, which plotted the flight path data onto the three-dimensional map. A sample flight track of a bucket mission in Google™ Earth is shown in Figure 6. It is clear from the flight path that the helicopter was flown repeatedly from a body of water to some fixed location, presumably where the fire was located.

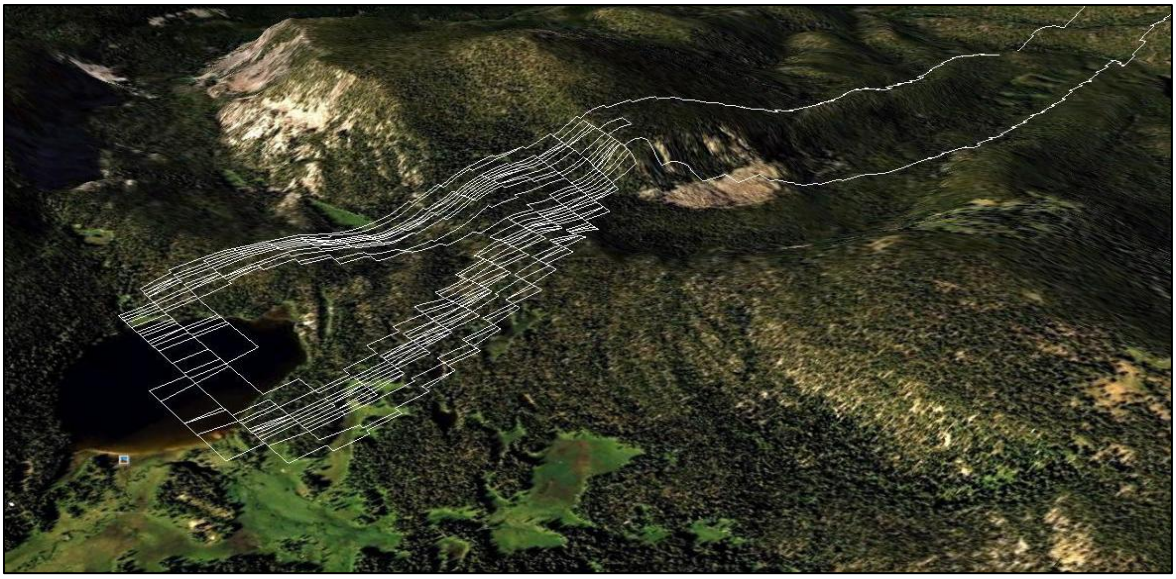

Figure 6. Helicopter Flight Track in Google™ Earth

3. Phase Separation and Mission Identification Program Architecture

Because of the volume of data and the number of characteristics that were being analyzed for phase separation and classification, as well as mission identification, a MATLAB code was written to handle all final analysis. A subroutine was developed to read the flight CSV file directly, extracting the data and inserting them into individual matrices. This separation allowed for ease of data management and indexing for other subroutines. Once data matrices were created, the initial phase separation subroutine was activated. Within this subroutine the variation of key elements and then determining the RMS of that variation occurred. With the needed data in hand, the subroutine separated the six basic phases: start of flight, climb, cruise, descent, start of landing, and stationary. A phase list was generated, which also included the time into the file when one phase transitioned to another. The subroutine then identified when a hover would occur, using the previous discussed logic. In order to ensure the fidelity of the phase list, the subroutine would then perform two "clean-up" operations. The first was the identification of "quick-hops," a phase series in which the helicopter performed a climb then immediately transitioned into a descent without an intermediate cruise. It also eliminated cases when a climb was transitioning directly into a start of landing, which is a highly improbable situation. For such cases, examination of the files usually showed a descent occurring before the start of landing, so it was added to the phase list. The other clean-up operation was the elimination of repeating phases, such as the phase list showing two cruises occurring in succession. The subroutine combined the

two repeating phases into a single phase, enabling more accurate counts of the number of phases occurring during a mission.

When developing the initial phase separation it was found that ferry, passenger, recon, longline, and rappel missions could have their phases separated easily. However, the complex nature of buckets and helitorch missions produced muddled and inaccurate phase separation. To counteract this, separate phase identification subroutines were designed specifically for each of these two missions. If a mission was initially identified as a bucket, a subroutine would be used to clear the previously defined phase list. Then, using the same criteria for the six basic phases, it would redefine the phase list. However, unlike the initial phase separation, extra coding was introduced to allow for the insertion of the missed drop and fill phases. Code similar to the bucket separation was developed for the helitorch, using the algorithm for burn recognition rather than drop/fill recognition. A flowchart showing the initial phase separation and bucket and helitorch subroutines is displayed in Figure 7.

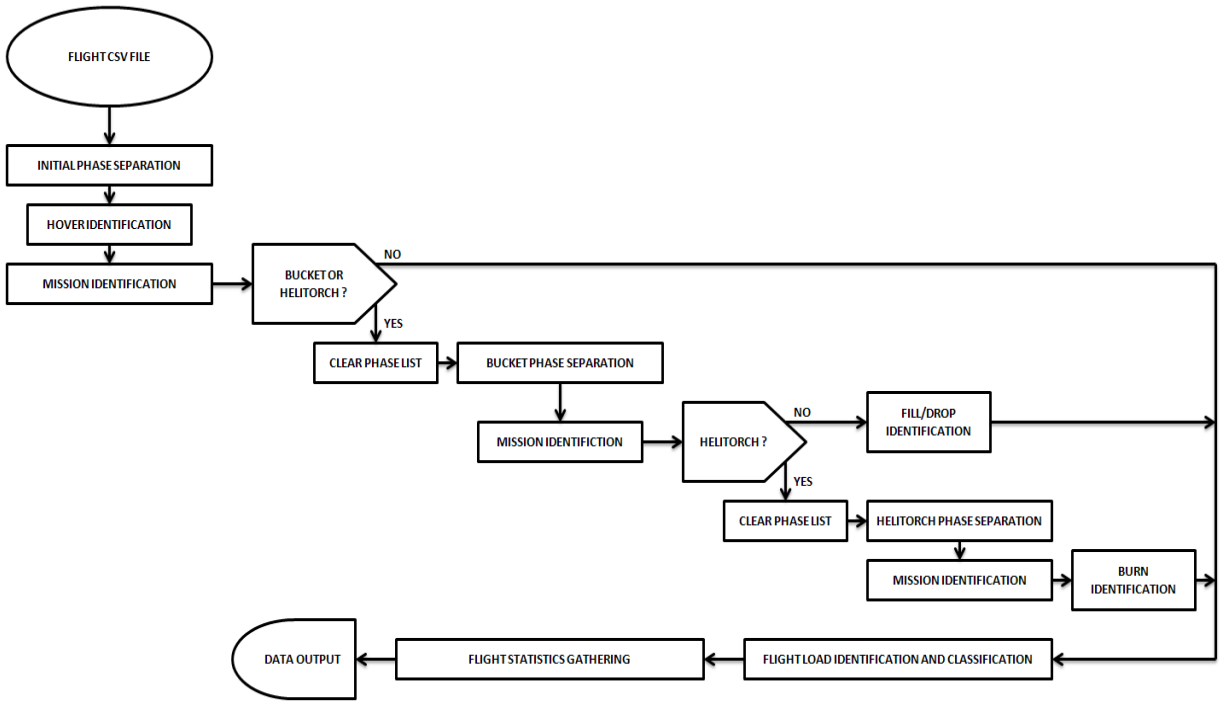

Figure 7. Data Analysis Program Architecture

Once phase separation and mission identification were completed, the main program would call subroutines that would identify and classify flight load n_z via criteria discussed in the next section. Once all analysis was complete, flight usage and flight load statistics were gathered and outputted.

E. Flight Loads

1. Normal Load Identification

Along with mission and phase usage data, the flight loads experienced by the helicopter are important for understanding the structural fatigue during its life in firefighting service. In Reference 6, flight loads of importance were defined by incremental normal load factors that were beyond ±0.2 g, significantly larger than ±0.05 g used in fixed-wing studies [5]. The increased width of the dead band was to remove the accelerations associated with the airframe vibrations that are naturally present in helicopters and are generally on the order of ±0.05-0.1 g [10]. For the present investigation, the accelerometers were placed near the nose of the helicopter, which further increased the effect of the inherent vibrations. For this reason, the dead band was widened further to ±0.3 g. This increase of 0.1 g was based on the visual examination of the data.

When counting occurrences of the loads, the "Peak-Between-Means" [11] method was used. In this method, the load of interest is the maximum or minimum value that occurs when the incremental load factor is outside of the dead band. The time between crossing the mean (in this study 1 g) was used to determine the duration of the flight load disturbance. This allowed for an estimation of the duration of a disturbance, since, in theory, the n_z should remain at 1 g during steady flight. Figure 8 shows a graphical representation of the "Peak-Between-Means" method.

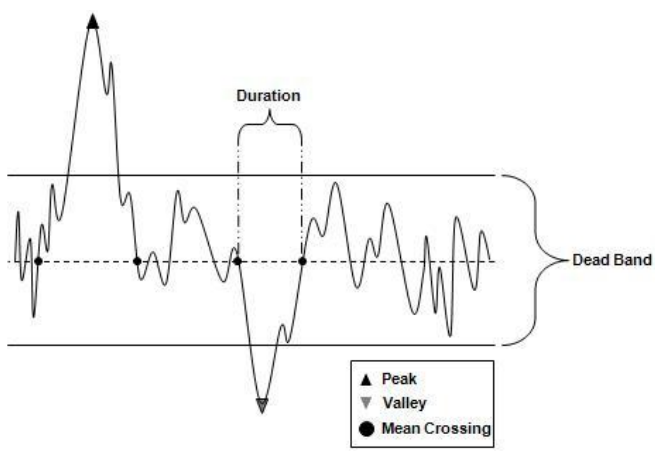

Figure 8. Peak-Between-Means and Time-Between-Means Logic

2. Normal Load Classification

With fixed-wing aircraft, using the duration of the disturbance is one method of classifying normal loads into gust induced and those caused by maneuvers. In the "two-second-rule," [3] loads lasting less than two seconds are attributed to gusts and those lasting longer are assumed to be caused by maneuvers. This method, while suitable for fixed-wing aircraft, had no basis for application to rotorcraft. Another duration-based approach was to compare the

load duration to the short-period [12]. This method was explored but ultimately rejected due to the perceived artificial shortening of load durations as a result of accelerometer placement. As the classification of normal loads was a key element in this study, a new method was devised.

Classification via visual analysis of data traces had been used in a previous US Army study involving a Bell UH-1H helicopter [6] in which the normal loads were categorized into gusts and maneuvers. Specifically, *"An n_z peak was coded as being gust-induced if the airspeed trace had a jagged pattern and the n_z peak had a short duration and an exponential decay. All other peaks were coded as maneuvers."* The data trace used in Reference 6 was not available, so quantitative definitions of "jagged pattern" and "short duration" could not be determined. During the exploration of duration-based methods of classification in the present study, normal loads were being visually classified based on their magnitude as well as the behavior of roll and pitch angles over the duration of the load. The visual-neurological "black box" that was being used to classify peaks was put into a quantitative form so that the logic could be programmed.

Three discrete sets of events were observed within flights. In the first set, the recorded load factor was accompanied with large variations in the pitch or the roll angles. These were defined as maneuver induced loads. In the second type, while a load factor was recorded, the pitch and the roll angles remained fairly constant. Furthermore, the load occurred as a solitary event, in that it was not immediately preceded or followed by another load. These were defined as gust induced loads. A third set was when the pitch and the roll angles were fairly constant, yet several load variations were closely grouped. One possibility was that these were induced by the extended presence of turbulence. However, further investigation showed that these load groups occurred consistently as the helicopter was transitioning from one flight phase to another, such as from cruise to descent. This behavior suggested that these loads occurred as the result of some pilot input, and as such, they were defined as change of state induced loads. For classification, changes of state induced loads were handled separately from maneuvers, though by classical definition, change of states are maneuvers.

Because variations in pitch or roll angles were relative to previously occurring angles, it was decided to use the pitch and roll rates. In order to define thresholds for the roll and the pitch rates, their averages and standard deviations were found during climb, cruise, and descent phases of 108 missions. The threshold for a large roll and pitch rate were set as the mean plus or minus one standard deviation. These limits were set arbitrarily and should be investigated further. The actual values used in the process are shown in Table 6.

Table 6. Normal Load Factor Classification Criteria

Disturbance Classification	Roll Rate (deg/sec)	Pitch Rate (deg/sec)	Time Between Extrema (sec)
Maneuver	-3.42 > RR > 3.37	-1.22 > PR >2.12	NA
Gust	-3.42 < RR < 3.37	-1.22 < PR < 2.12	> 7.5
Change of State	-3.42 < RR < 3.37	-1.22 < PR < 2.12	< 7.5

To test this new method of classification, results obtained were compared to a 1974 NASA study which had analyzed the gust alleviation factor inherent in helicopters due to rotor dynamics [7]. In Reference 7, the authors stated that: *"The conclusive finding in each of these [flight measurement] programs was that normal loads attributed to gust encounters were of much lesser magnitude and frequency than maneuver loads. Further, when the total load factor experience was statistically examined for each aircraft, the loads directly attributed to gust encounters were found to be only a small percentage of the total experience."* When compared to these findings, which covered 1477 flight hours, it was found that the method proposed in this study produced similar results.

F. Aircraft Usage Statistics

To examine the helicopter usage, statistics were gathered and categorized for individual missions and each of the phases. Distance traveled was determined by integration of the ground speed.

In those cases where speed was of interest, ground speed was used rather than true airspeed due to pitot-static tube interference from rotor downdraft. When operating under 30 knots the pressure reading, and therefore airspeed, would be inaccurate. Often zero airspeed was recorded while ground speed and change in position data indicated the helicopter was moving.

Because the sensor package did not record rotor RPM, engine torque, collective or cyclic positions, etc, comparisons to limitations by the manufacturer, stated in the flight manual [9], were somewhat restricted. However, it was possible to compare the airspeed to the provided V_{NE}, which was given in knots calibrated airspeed (KCAS) [9]. Calibrated airspeed was not included in the data files, however, according to airspeed system calibration charts in the flight manual, the difference between it and indicated remained less than ±2 knots. For missions not equipped with external cargo the formula for V_{NE} for weights up to 7,500 pounds was given by Eq. (2), derived from data given in the flight manual. For every 1,000 pounds above 7,500 pounds up to 9,500 pounds, V_{NE} would have to be reduced by 5 knots. With external cargo attached, a fixed V_{NE} of 80 KCAS is set for all weight ranges up to 10,500 pounds.

$$V_{NE} = \frac{MSL - 4 \cdot 10^4}{-3.333 \cdot 10^2} \quad \text{KCAS} \tag{2}$$

When comparing maximum airspeed to V_{NE}, a 10% margin was allowed. This ensured that airspeeds recorded as exceeding V_{NE} were not due to instrument error or other factors. In every case, when V_{NE} was exceeded, the duration was noted and the maximum value was stored as one incident.

Extracted data used in plotting results is shown in Table 7, while data presented in tables is given in Table 8.

Table 7. Extracted Usage Data Used for Graphical Presentation

Flight Type	Extracted Data	Coincident Data
Mission and Phase	Max Altitude (ft)	Indicated Airspeed (knots)
	Max KIAS (knots)	Altitude (ft)
	Max Altitude (ft)	Distance (nm)
	Max Duration (s)	Distance (nm)
Mission Only	Normal Distribution	Duration (s)
	Normal Distribution	Distance (nm)
	Normal Distribution	Min -Δn_z (g)
	Normal Distribution	Max +Δn_z (g)
	Max $\pm\Delta n_z$ (g)	Indicated Airspeed (knots)
	Max Pitch (deg)	Indicated Airspeed (knots)
	Min Pitch (deg)	Indicated Airspeed (knots)
	Max Roll (deg)	Indicated Airspeed (knots)
	Min Roll (deg)	Indicated Airspeed (knots)
Overall	Cumulative Frequency Distribution	Δn_z (g)

Table 8. Extracted Usage Data for Tabular Presentation

Flight Type	Mission and Phase	Mission Only	
Extracted Data	Average Duration (s)	Average Number of Stationaries	Average Exceedance Duration (s)
	Max Duration (s)	Average Number of Start of Flight	Average ΔV_{NE} (kts)
	Average Distance (nm)	Average Number of Climbs	ΔV_{NE} Standard Deviation (kts)
	Max Distance (nm)	Average Number of Cruises	Max ΔV_{NE} (kts)
	Max Altitude (ft)	Average Number of Descents	-
	Max KIAS (knots)	Average Number of Start of Landings	-
	-	Average Number of Hovers	-
	-	Average Number of Fills	-
	-	Average Number of Drops	-
	-	Average Number of Burns	-

CHAPTER 3

RESULTS AND DISCUSSION

A. Available Data

A total of 299 flight files from the 2009 fire season were available. Of the original 299 files, 282 files were considered to have usable data. Most of the rejected 17 files were very short and appeared not to contain flight data. The remaining data files totaled 263.46 hours, covering 15,989 nm. Data extracted from these files included mission type and phase composition, and relevant information such as altitude, airspeed, duration, pitch angles, and roll angles.

B. Aircraft Usage

1. Mission Usage Results

In the following sections, the results are given separated by the mission type during which the statistics were obtained. The initial table presents some performance usage data, along with the number of missions of that type and the average number of each flight phase. The third table presents data concerning the exceedance of V_{NE}. Eight plots are then displayed, showing key flight data along with coincident information, and the normal distributions of flight duration and flight distance for that mission type. For maximum airspeed and coincident MLS altitude, the bolded line indicates the V_{NE} airspeed.

a. Bucket Mission Usage Data

The overall usage statistics for bucket missions are given in Table 9. From this table, it can be seen that the average bucket mission lasted less than two hours, with the maximum length being less than three hours. With a total of 31, bucket missions accounted for 11% of total missions in the database, indicating that this helicopter had only a limited role in actual firefighting operations. However, in a firefighting role, the helicopter was used for many drops during a single mission. As indicated in Table 9, this resulted in an average of 30 drops in an average mission length of less than two hours. It should be noticed that the average number of fills and drops is not equal; this is due to the average ground speed threshold established in the bucket identification subroutine. While accurate for the majority of cases, instances of incorrect fill or drop classification may occur, thus resulting in the differing average. Based on an average bucket size used for firefighting operations, each drop would entail delivering 450 gallons of water to a fire zone, or a total of approximately 13,500 gallons of water in an average mission.

Table 9. Bucket Mission Usage Statistics and Average Mission Profile

Mission	Bucket		
Average Duration (s)	6194.46	Missions Performed	31
Max Duration (s)	9791.75	Stationary	3.06
Average Distance (nm)	77.47	Hover	0.16
Max Distance (nm)	137.2346	Start of Flight	2.23
Max Altitude (ft)	11031.90	Climb	64.26
Max KIAS (knots)	117.66	Cruise	14.94
		Descent	53.68
		Start of Landing	2.16
		Fill	30.48
		Drop	29.35

Information pertaining to the apparent exceedance of V_{NE} is presented in Table 10. It is quite obvious from this data that there were numerous exceedances of the V_{NE} + 10% during bucket missions. The reader is reminded that since there was a load suspended underneath the helicopter, the limit V_{NE} of 80 KCAS (88 knots with the +10% addition) was applied. Despite the frequency, the magnitude of the exceedance averaged only 1.48 knots with a standard deviation of 2.57 knots. A point of concern was the nearly 30 knot maximum ΔV_{NE}, equal to 118 KIAS, that was found in one of the missions. Ten others had a V_{MAX} greater than 100 KIAS. Based on the results shown in Figure 9, only two missions had maximum airspeeds of less than 80 knots, with most being greater than 90 knots. This would suggest that in all likelihood, the bucket apparatus was not attached to the helicopter when it was flown at that maximum airspeed. Because there was no sensor on the helicopter hook (i.e. switch or load cell) it could not be determined when a load was slung beneath the helicopter. Therefore, the 80 KCAS was applied throughout the entire mission, leaving some uncertainty in the actual number and magnitude of exceedances.

Table 10. Bucket Mission V_{NE} Exceedance Statistics

Mission	Number of Exceedances	Average Duration (s)	Average ΔV_{NE} (knots)	StdDev ΔV_{NE} (knots)	Max ΔV_{NE} (knots)
Bucket	2548	4.92	1.48	2.57	29.66

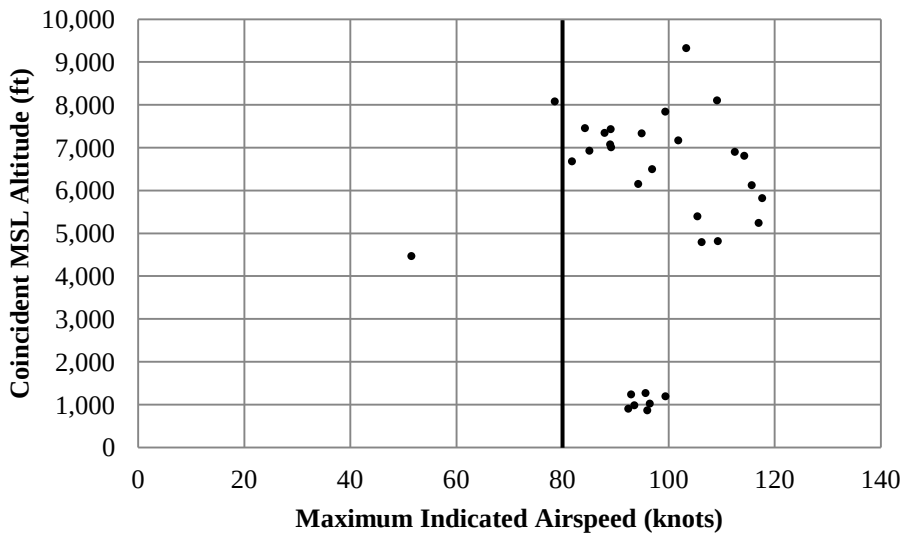

Figure 9. Maximum Indicated Airspeed and Coincident MSL Altitude for Bucket Missions

As can be seen in Figure 10, the maximum MSL altitude the helicopter reached during bucket missions was less than 12,000 ft, well below the 20,000-ft ceiling, as indicated in the flight manual. Most bucket missions were flown between 8,000 and 10,000 ft, with a smaller group occurring at less than 2,000 ft. The variation in the maximum altitudes was in all likelihood due to local terrain elevation. It is plausible that the same data in terms of altitude above ground level (AGL) would show much less variation in maximum altitude.

There was no clear correlation between maximum MSL altitude and the coincident distance flown, as shown in Figure 11. Given the variation of terrain elevation and the highly repetitive nature of the mission, the maximum altitude could have occurred shortly after take-off if traveling to a fire zone which lay at a lower elevation, somewhere in the middle if the fire zone was at a higher elevation, or near the end of the mission if landing at a secondary operations base that was at a higher elevation than either the primary operations base or the fire zones.

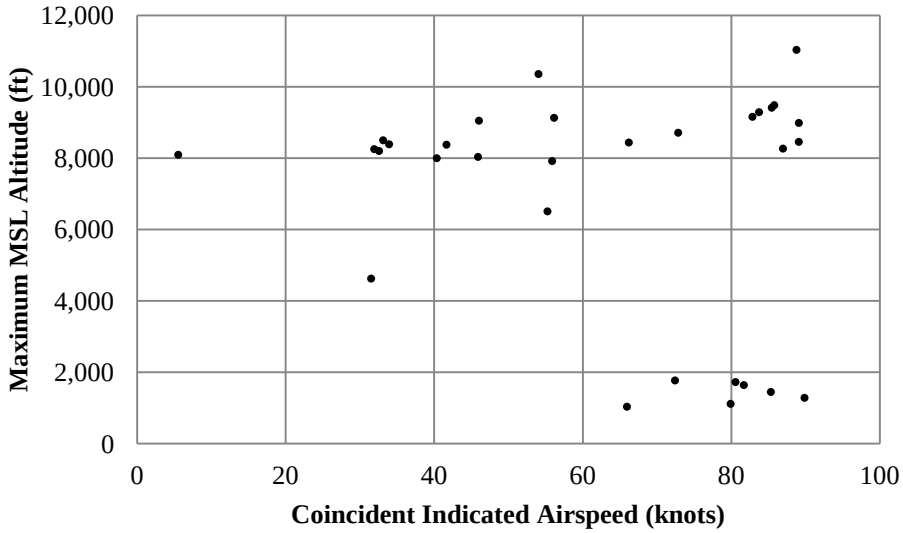

Figure 10. Maximum MSL Altitude and Coincident Indicated Airspeed for Bucket Missions

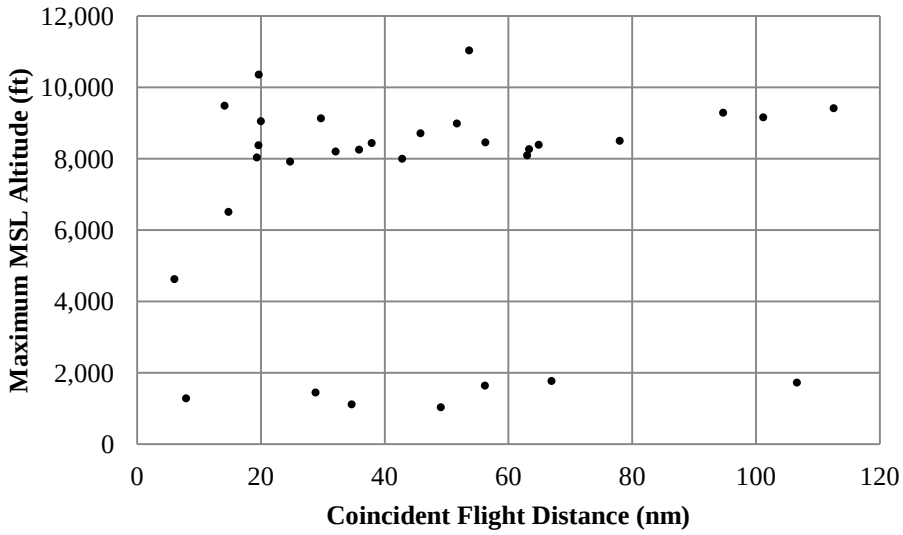

Figure 11. Maximum MSL Altitude and Coincident Flight Distance for Bucket Missions

Figure 12 shows the maximum flight duration and coincident flight distance for the bucket missions. Comparing these results with those from other missions, such as passenger or ferry missions, little correlation between duration and distance is observed for the bucket missions. Much better correlation was present in all other missions, except for the longline. Compared to other missions, the buckets have a larger number of hovers (fills and drops being a specialized form of hover) which increase duration without much associated flight distance. This is further highlighted in the normal distributions shown in Figure 13 and Figure 14. It is obvious from the results shown in these

figures that average flight time for these missions was less than two hours, yet covering a total distance of only 80 nautical miles.

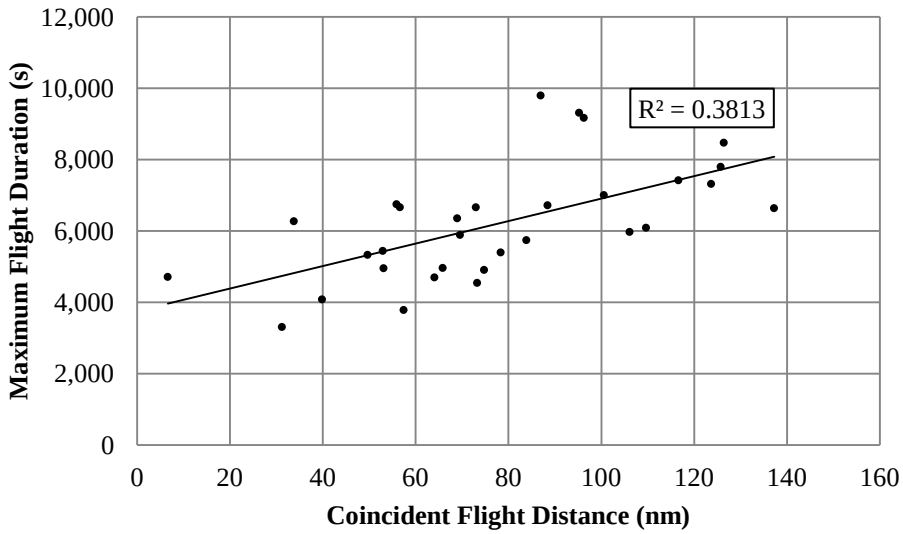

Figure 12. Maximum Flight Duration and Coincident Flight Distance for Bucket Missions

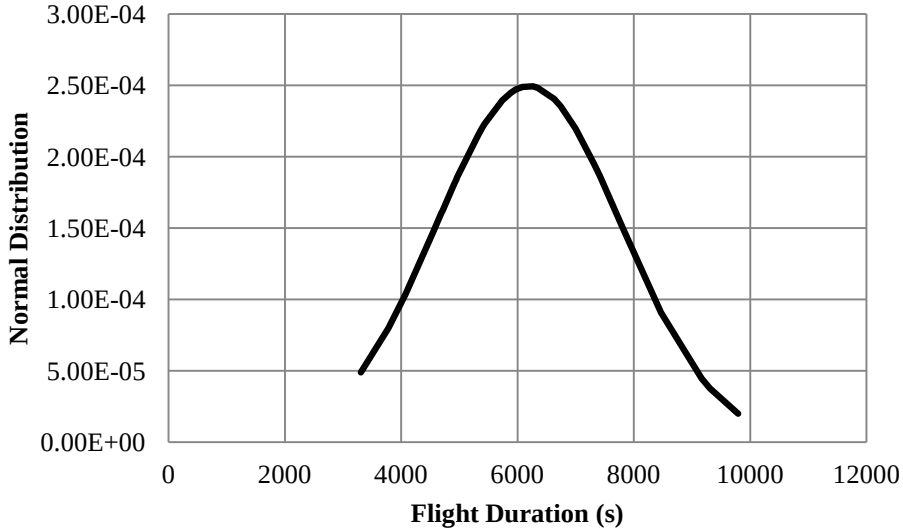

Figure 13. Normal Probability Distribution of Flight Duration for Bucket Missions

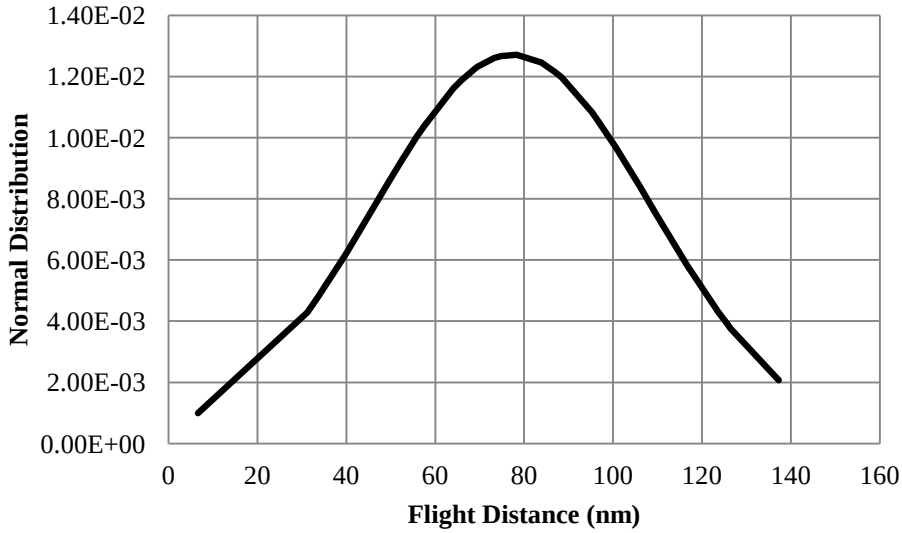

Figure 14. Normal Probability Distribution of Flight Distance for Bucket Missions

The majority of maximum pitch angles during bucket missions occurred at zero airspeed, as shown in Figure 15. This suggests that the maximum pitching up occurred just before landing when the aircraft pitched up to cease forward movement. Conversely, the minimum pitch angles occurred during forward flight. Given that a helicopter has to pitch forward naturally during forward flight to gain airspeed, this was not surprising. The large negative pitch angles (-15 to -25 deg) were most likely resulting for the increased payload of a full bucket, requiring a larger pitch angle for adequate acceleration. Both the maximum and minimum roll angles occurred with approximately the same magnitude (20-50 deg), and were spread across the full ranges of airspeeds, as shown in Figure 16.

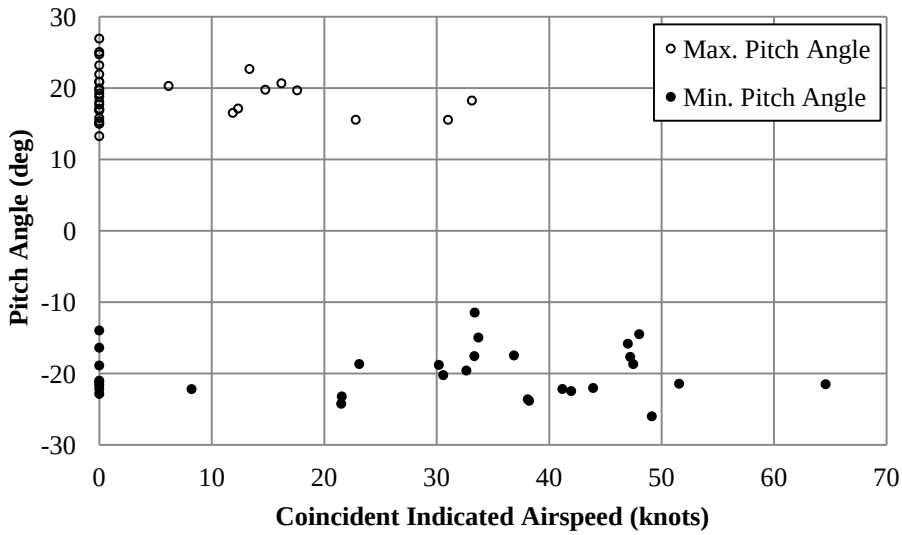

Figure 15. Maximum and Minimum Pitch Angle and Coincident Indicated Airspeed for Bucket Missions

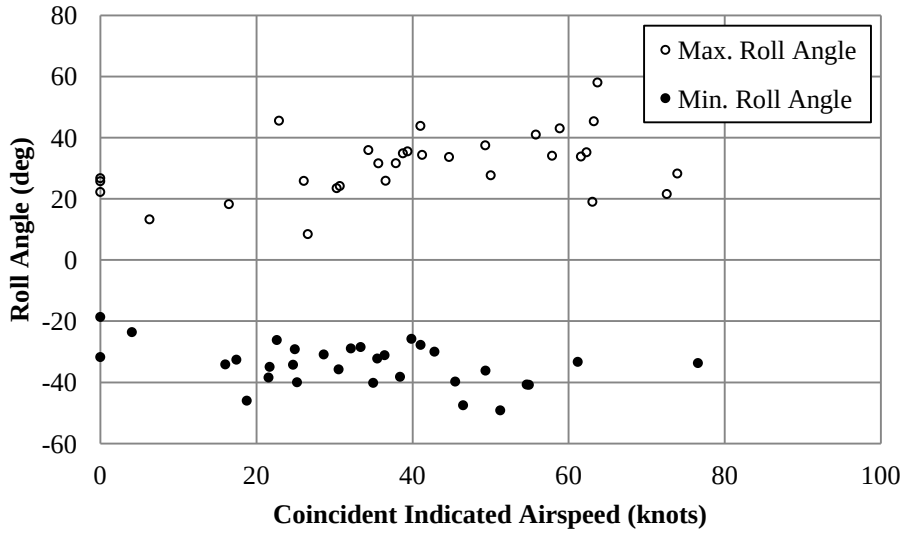

Figure 16. Maximum and Minimum Roll Angle and Coincident Indicated Airspeed for Bucket Missions

b. Ferry Mission Usage Data

Ferry usage data is presented in Table 11, showing an average and maximum durations of 45 minutes and over two hours, respectively. There was also a wide range of distances covered in ferry missions. While the average was 67 nm, the distances traveled were as far as 244 nm. This is a characteristic of the ferry missions as the helicopter is flown from one operations base to another, whether the second base is near the original fire zone, or in another state. Because of the basic nature of the ferry mission, they all have exactly two stationary phases, a single start of flight, climb, cruise, descent, and start of landing, and no hovers; as shown in Table 11. At a total of 74 operations, ferry missions accounted for 26% of all flights analyzed, making it the 2nd most common mission performed.

While examining the maximum airspeed, it was noted that the V_{NE} was exceeded a total 3,992 times. This accounted for nearly 40% of total airspeed exceedances. Since there was no external cargo involved, V_{NE} was based entirely on altitude. In general, the magnitude of average exceedances was rather small.

Table 11. Ferry Mission Usage Statistics and Average Mission Profile

Mission	Ferry		
Average Duration (s)	2678.89	Missions Performed	74
Max Duration (s)	8019.63	Stationary	2
Average Distance (nm)	67.4	Hover	0
Max Distance (nm)	244.57	Start of Flight	1
Max Altitude (ft)	11169.6	Climb	1
Max KIAS (knots)	128.39	Cruise	1
		Descent	1
		Start of Landing	1

Table 12. Ferry Mission V_{NE} Exceedance Statistics

Mission	Number of Exceedances	Average Duration (s)	Average ΔV_{NE} (knots)	StdDev ΔV_{NE} (knots)	Max ΔV_{NE} (knots)
Ferry	3992	3.12	1.26	1.89	25.30

The helicopter was not flown higher than 12,000 ft during ferry missions, as shown in Figure 17 . Three instance of maximum MSL altitude occurred at zero indicated airspeed. This indicated that the flight started or ended at the high elevation base. In the flight manual the highest allowable airspeed is set at 120 KCAS. The flight manual also states that the difference between calibrated and indicated airspeed is less than ±2 knots. Therefore, the calibrated and indicated airspeeds were assumed to be the same. Included in the 3,992 exceedances, there were six instances in which the airspeed exceeded 120 knots, with the maximum being 128 KIAS, as shown in Figure 18. Maximum Indicated Airspeed and Coincident MSL Altitude However, all of these cases occurred at relatively low altitudes and remained within the 10% margin of V_{NE}.

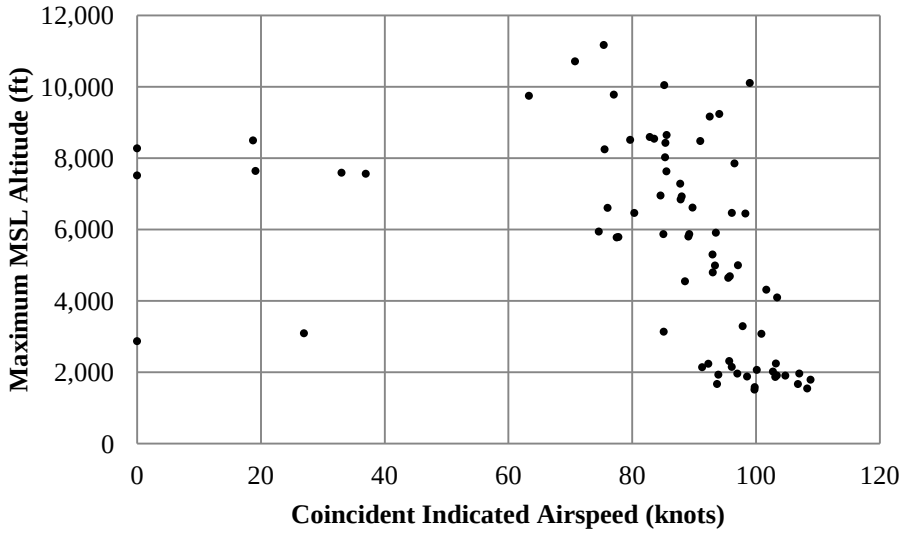

Figure 17. Maximum MSL Altitude and Coincident Indicated Airspeed for Ferry Missions

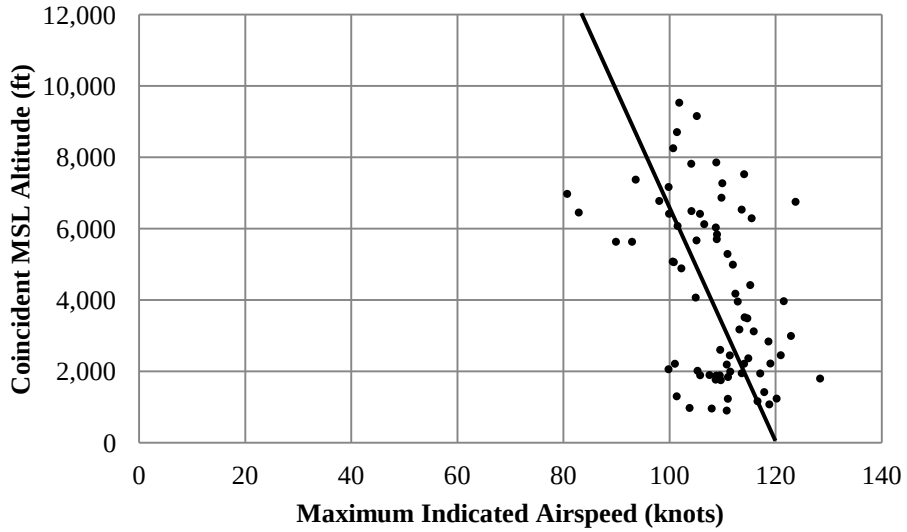

Figure 18. Maximum Indicated Airspeed and Coincident MSL Altitude for Ferry Missions

Figure 19 shows the maximum MSL altitude and coincident flight distance. The results shown in this figure suggest that for the majority of ferry missions there was little correlation between maximum MSL altitude and distance into flight. As can be seen in Figure 20, there is very good correlation between the duration and the distance traveled. Given the simplicity of the mission, with no hovers and only two stationaries, this correlation was expected.

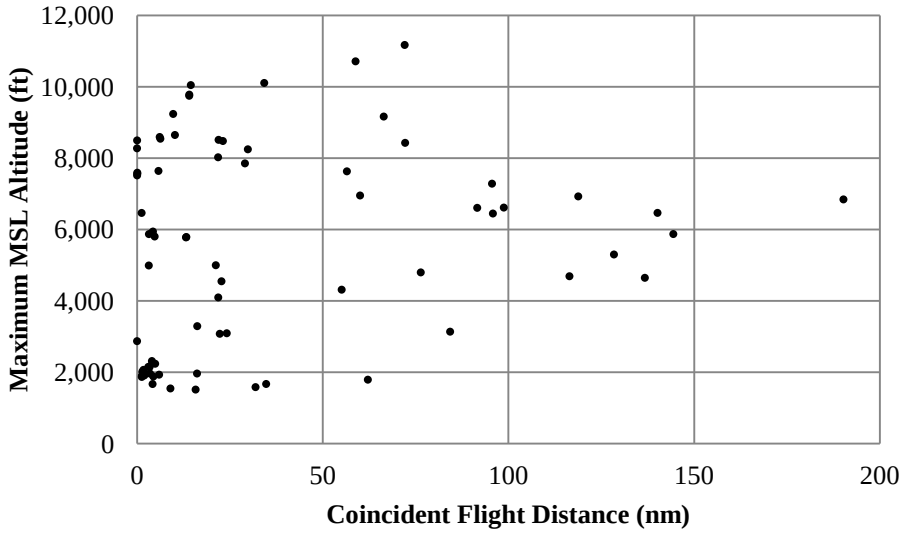

Figure 19. Maximum MSL Altitude and Coincident Flight Distance for Ferry Missions

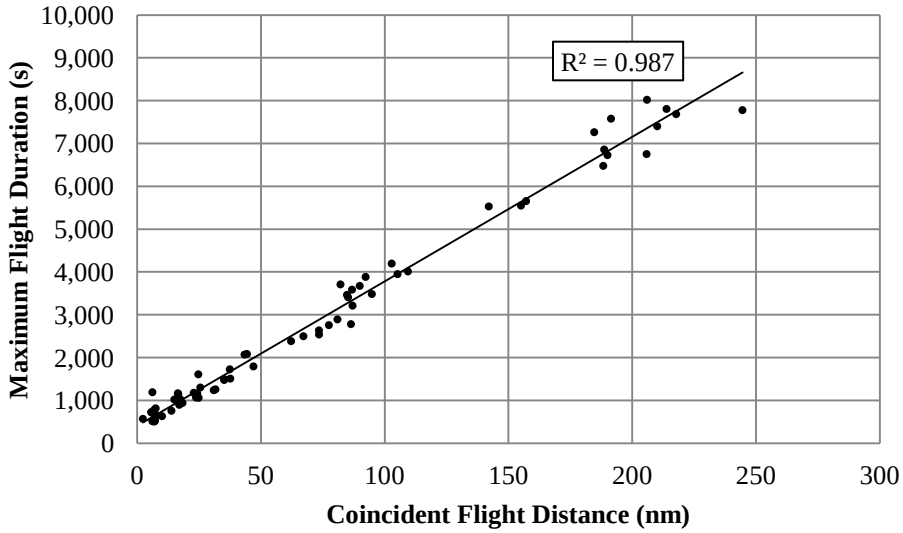

Figure 20. Maximum Flight Duration and Coincident Flight Distance for Ferry Missions

Normal probability distribution of the flight duration and distance are shown in Figure 21 and Figure 22. These results show average flight duration of approximately 45 minutes, and average distance traveled of 67 nautical miles, as discussed earlier. Also, the close similarity between the shapes of these two curves is consistent with correlation between these two parameters, shown in Figure 20

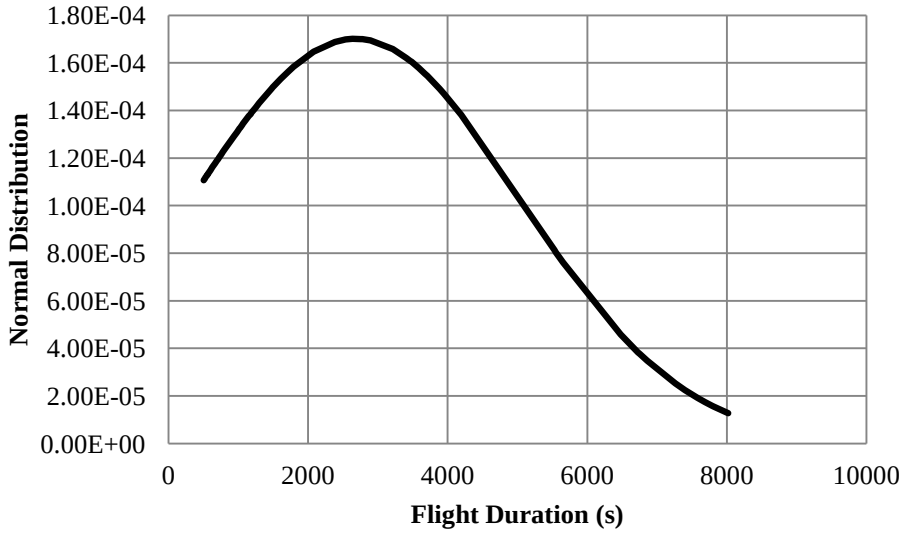

Figure 21. Normal Probability Distribution of Flight Duration for Ferry Missions

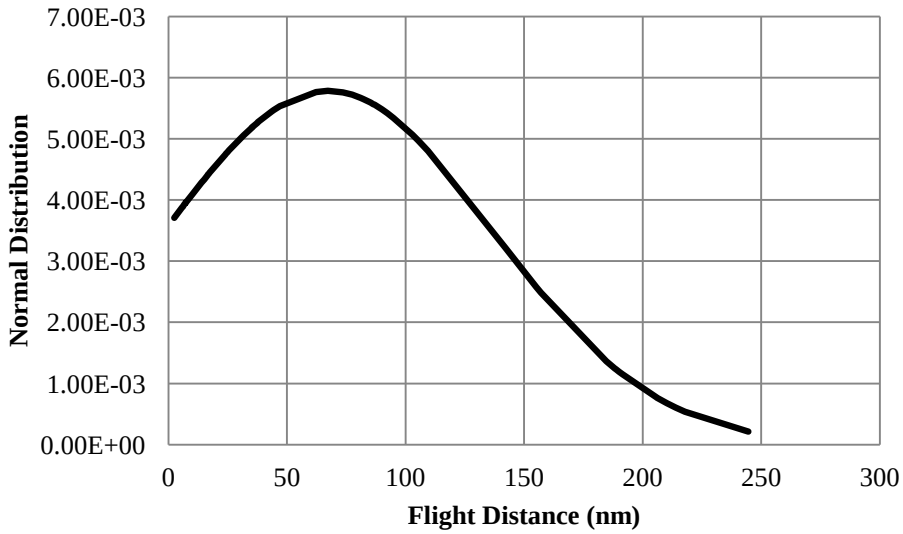

Figure 22. Normal Probability Distribution of Flight Distance for Ferry Missions

Figure 23and Figures 24 show the maximum and minimum pitch angles and coincident indicated airspeeds. Much like in the bucket missions, the maximum pitch angle occurred at zero indicated airspeed, further suggesting this occurs at an approach to landing. However, in this case, the magnitudes were much smaller. It can also be seen that minimum pitch angles occurred across all airspeeds, while maximum pitch angles occurred at less than 45 KIAS. The roll angles ranged from -50 to 45 deg, scattered across all airspeed ranges, suggesting that there was no particular mission section that promoted a large roll angle.

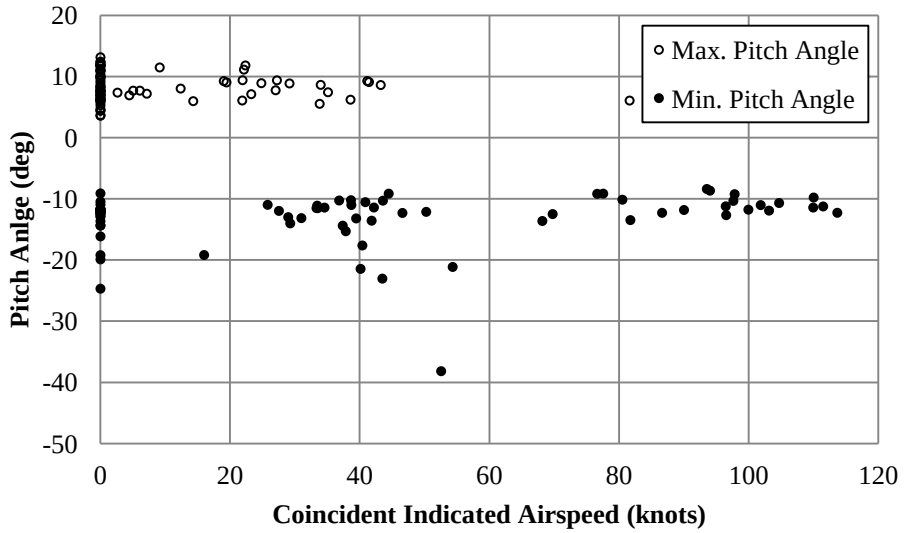

Figure 23. Maximum and Minimum Pitch Angle and Coincident Indicated Airspeed for Ferry Missions

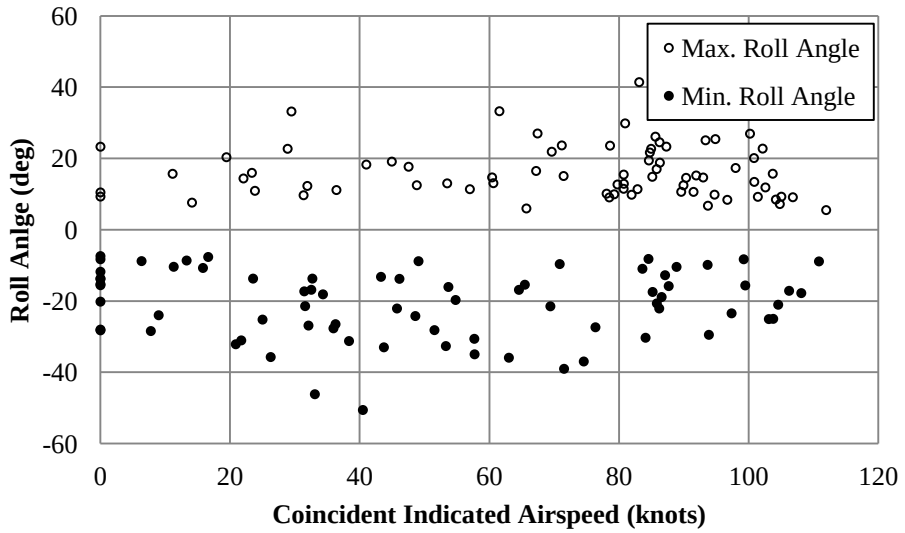

Figure 24. Maximum Roll Angle and Coincident Indicated Airspeed for Ferry Missions

c. Passenger Mission Usage Statistics

Similar to ferry missions, passenger missions had a large array of durations and distances. Average duration was 47 minutes and the longest mission lasted 2.5 hours. Average distance was 55 nm and the farthest distance traveled was 237.5 nm. While the statistics of the passenger mission are very similar to those of the ferry, the reader is reminded that the former could be considered to be two or more short ferry missions tacked on to one another in succession. One example would be launching from an initial operations base, carrying supplies to a secondary base,

then passengers to a tertiary one, etc. Unlike a ferry mission, however, a passenger mission could include hover phases; though uncommon (a passenger mission averaged 0.53 hovers per mission as shown in Table 13), as a large number of hovers would result in the mission being classified as a longline, as per Table 4.

Table 13. Passenger Mission Usage Statistics and Average Mission Profile

Mission	Passenger		
Average Duration (s)	2823.01	Missions Performed	88
Max Duration (s)	9295.25	Stationary	2.75
Average Distance (nm)	55.04	Hover	0.53
Max Distance (nm)	237.55	Start of Flight	1.88
Max Altitude (ft)	10743.20	Climb	2.34
Max KIAS (knots)	129.88	Cruise	2.82
		Descent	2.90
		Start of Landing	1.90

Airspeed exceedance results are summarized in Table 14. Passenger missions analyzed here showed 1,976 cases of exceeding V_{NE}, which accounted for 20% of total exceedances. Similar to ferry cases, there were eight instances of maximum indicated airspeed being above 120 knots, exceeding it by nearly 10 knots. But again, in every case, the airspeed remained within the 10% margin of V_{NE}.

Table 14. Passenger Mission V_{NE} Exceedance Statistics

Mission	Number of Exceedances	Average Duration (s)	Average ΔV_{NE} (knots)	StdDev ΔV_{NE} (knots)	Max ΔV_{NE} (knots)
Passenger	1976	4.09	1.47	2.40	31.06

Figure 25 indicates that the majority of passenger missions had maximum MSL altitude within 1,000-5,000 ft and 8,000-10,000 ft altitude bands. As indicated in Figure 26, the majority of maximum indicated airspeeds were greater than 100 knots, while at altitude less than 4,000 ft. At altitude greater than 6,000 ft, V_{NE} via Eq. (2) is 102 knots, and many of the maximum airspeeds exceeded this value.

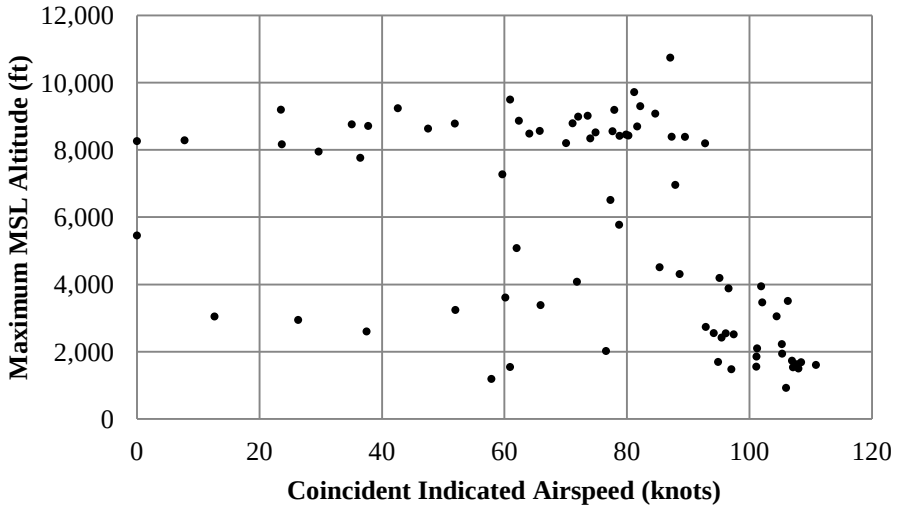

Figure 25. Maximum MSL Altitude and Coincident Indicated Airspeed for Passenger Missions

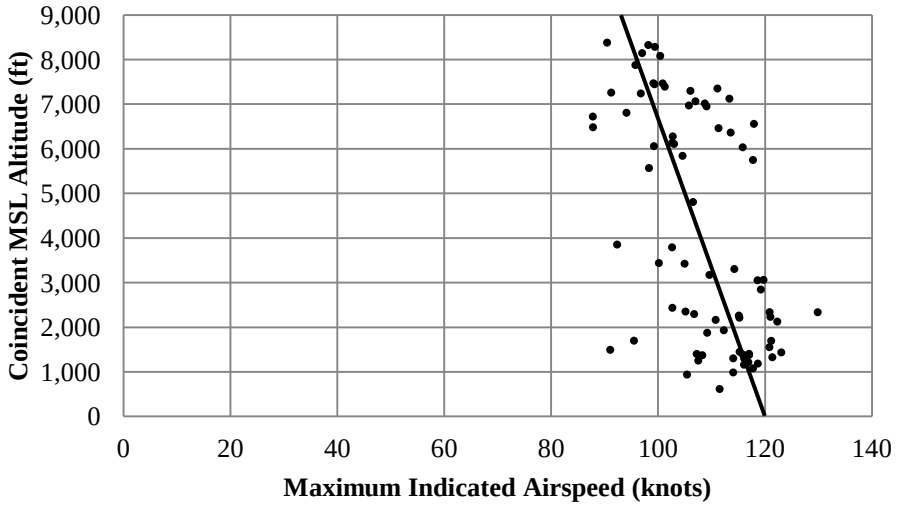

Figure 26. Maximum Indicated Airspeed and Coincident MSL Altitude for Passenger Missions

Figure 27 shows that the majority of passenger missions had maximum MSL altitude attained within the first 50 nm, and all but three attained maximum MSL altitude within the first 100nm. Figure 28 shows that all but three of the passenger missions were shorter than 130 nm, and within that range, two sets of missions are identifiable. Flights shorter than 75 nm showed a high correlation between the distance and time traveled. This indicated little time in stationary phases or hover. The second group, between 75 and 135 nm, showed less correlation between the two parameters, indicating longer stationary and a higher number of hover phases.

Normal probability distributions of flight duration and distance are shown in Figure 29 and Figure 30. The information conveyed here is consistent with that presented in Table 13. The average mission duration was approximately 45 minutes, while the average distance spanned 55 nm.

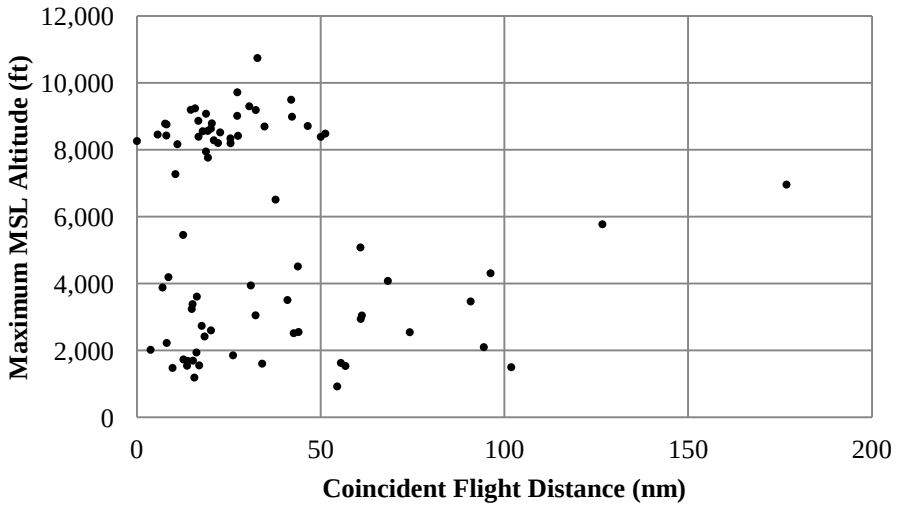

Figure 27. Maximum MSL Altitude and Coincident Flight Distance for Passenger Missions

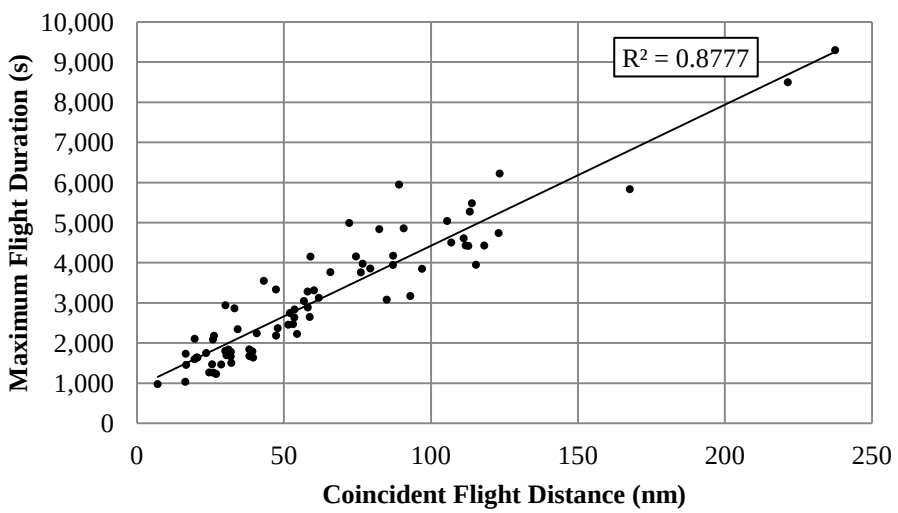

Figure 28. Maximum Flight Duration and Coincident Flight Distance for Passenger Missions

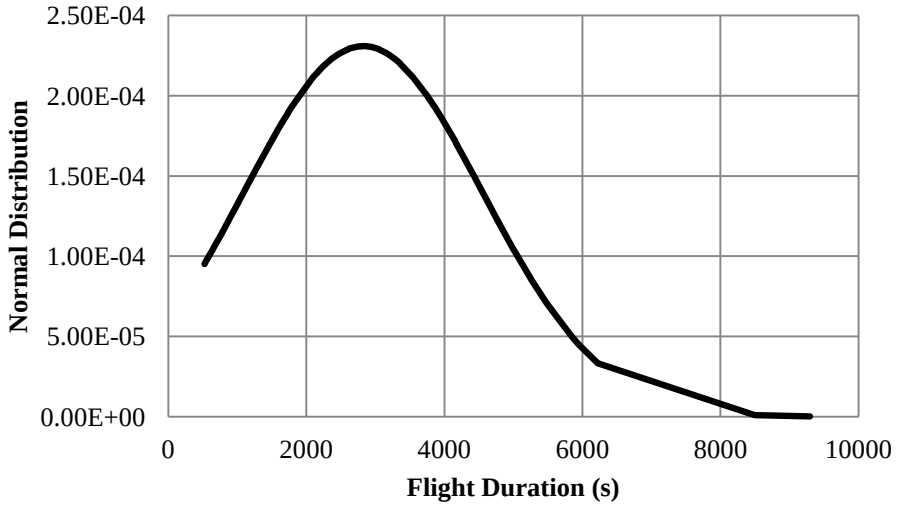

Figure 29. Normal Probability Distribution of Flight Duration for Passenger Missions

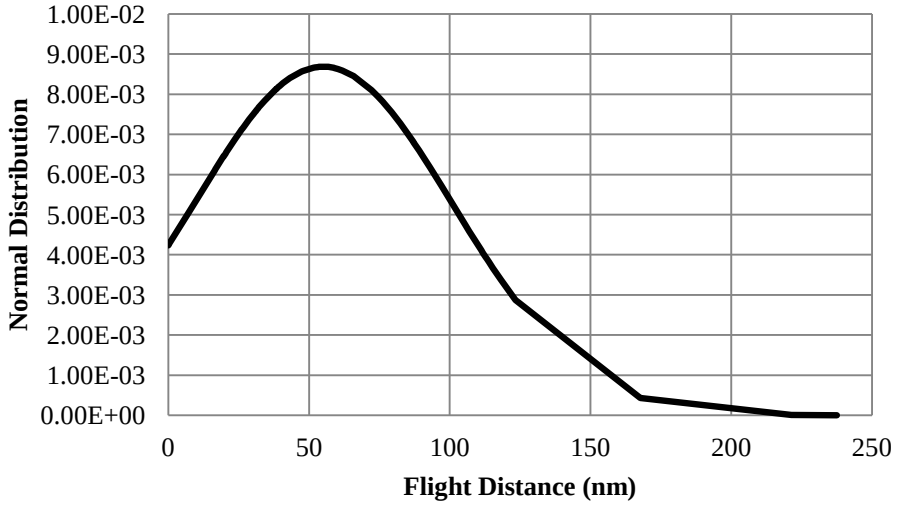

Figure 30. Normal Probability Distribution of Flight Distance for Passenger Missions

Maximum and minimum values of pitch angle are shown in Figure 31. Figure 31 indicates that maximum pitch mostly occurred shortly prior to landing, though there were a larger percentage of instances at airspeeds greater than zero. Minimum pitch angles were more consistent with bucket missions. Figure 32 show a broad array of roll angles and coincident airspeed, indicating no particular correlation between the two. It is noteworthy that roll angles in excess of 50 degrees were recorded. It is currently unknown what would have precipitated the need for such extreme roll angles during such a simple mission profile.

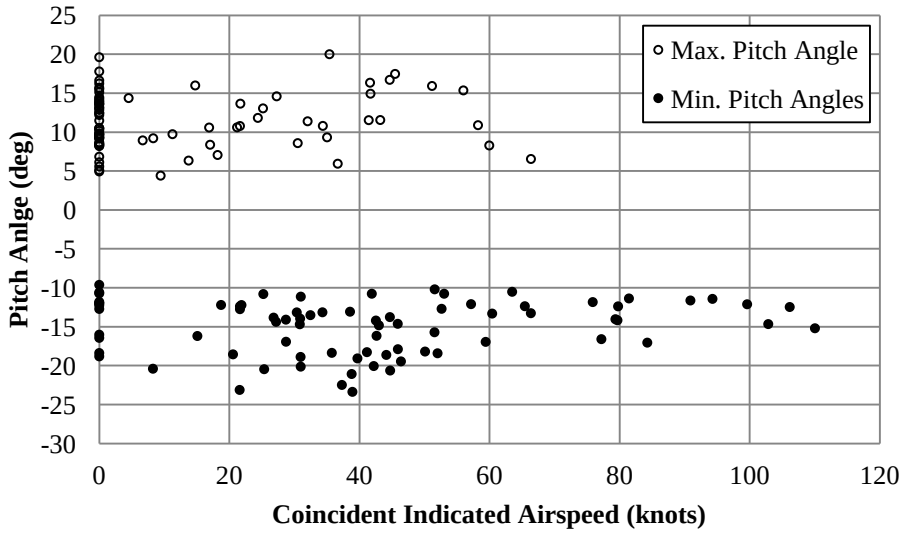

Figure 31. Maximum and Minimum Pitch Angle and Coincident Indicated Airspeed for Passenger Missions

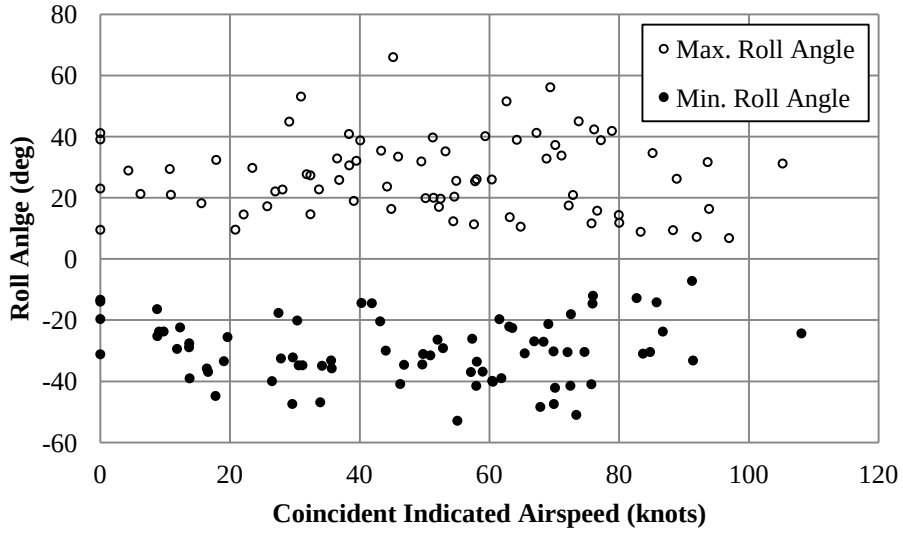

Figure 32. Maximum Roll Angle and Coincident Indicated Airspeed for Passenger Missions

d. Reconnaissance Mission Usage Statistics

Reconnaissance missions had an average duration of 46 minutes, and a maximum of over 2 hours; almost identically to ferry (45 minutes and 2.2 hour) and passenger missions (47 minutes and 2.6 hour). This suggests similar airframe usage in all three missions. One of the primary characteristics that defined a reconnaissance mission was the number of cruise-descent-cruise phase series that occurred during the mission. This becomes evident when one

examines the average number of climbs, cruises, and descents. In reconnaissance missions there are a larger number of cruises and descents than climbs, as seen in Table 15. This suggests that when performing a reconnaissance mission, an operator would cruise to a location, descend into the area, and then cruise again to scout it. The climbs out of the cruises were so gradual that they did not meet the phase separation criteria for a climb phase. This resulted in the average number of cruises and descents to be over three times that of the climb phases.

Table 15. Reconnaissance Mission Usage Statistics and Average Mission Profile

Mission	Recon		
Average Duration (s)	2746.57	Missions Performed	21
Max Duration (s)	7896.38	Stationary	2.67
Average Distance (nm)	43.18	Hover	0.67
Max Distance (nm)	119.26	Start of Flight	1.76
Max Altitude (ft)	9973.8	Climb	2.43
Max KIAS (knots)	119.29	Cruise	7.81
		Descent	8.24
		Start of Landing	1.86

Incidents of exceeding V_{NE} are shown in Table 16. At 205 cases, exceedances during reconnaissance missions accounted for less than 2% of total, and had the lowest maximum ΔV_{NE} of all the mission types. This is most likely due to the nature of the reconnaissance mission. As the name suggests, the point of a reconnaissance mission is to gather data about an area and this is most effectively done at slower speed, thus leading to fewer opportunities to exceed V_{NE}.

Table 16. Reconnaissance Mission V_{NE} Exceedance Statistics

Mission	Number of Exceedances	Average Duration (s)	Average ΔV_{NE} (knots)	StdDev ΔV_{NE} (knots)	Max ΔV_{NE} (knots)
Recon	205	4.01	1.14	1.99	14.86

Much like the passenger mission, Figure 33 displayed altitude stratification, suggesting two distinct terrain elevation profiles. Though, unlike passenger missions, the lower elevation profile resulted in a maximum altitude of

less than 2,000 ft. If these missions were being performed in similar geographical locations, it would suggest that reconnaissance missions were flown very close to the ground. Given that reconnaissance is being performed, having low AGL altitude near the target area would provide for more accurate visual inspection of the area.

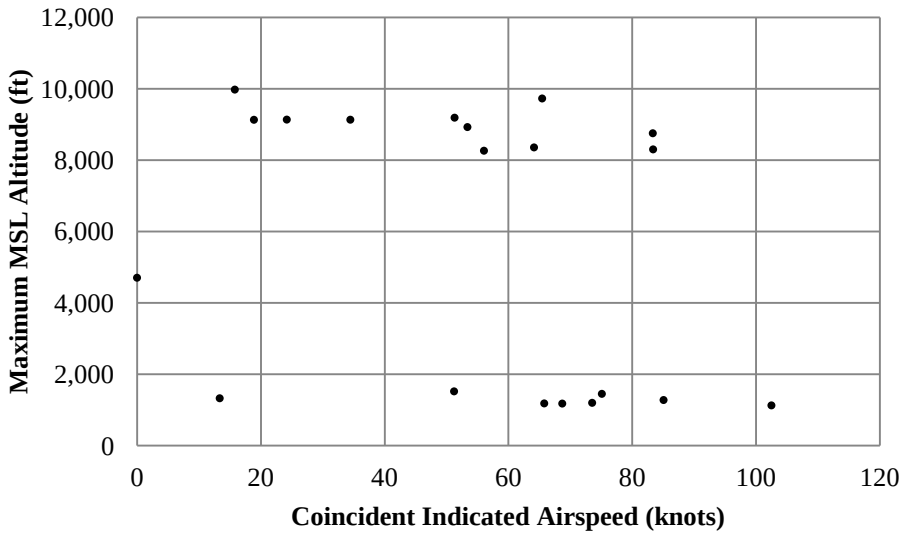

Figure 33. Maximum MSL Altitude and Coincident Indicated Airspeed for Reconnaissance Missions

Figure 34 shows the maximum indicated airspeed and coincident altitude. Again, it is clear from this figure that flights could be placed into two distinct groups depending on the altitude. This behavior was also present when examining the maximum altitude and the coincident flight distance, shown in Figure 35.

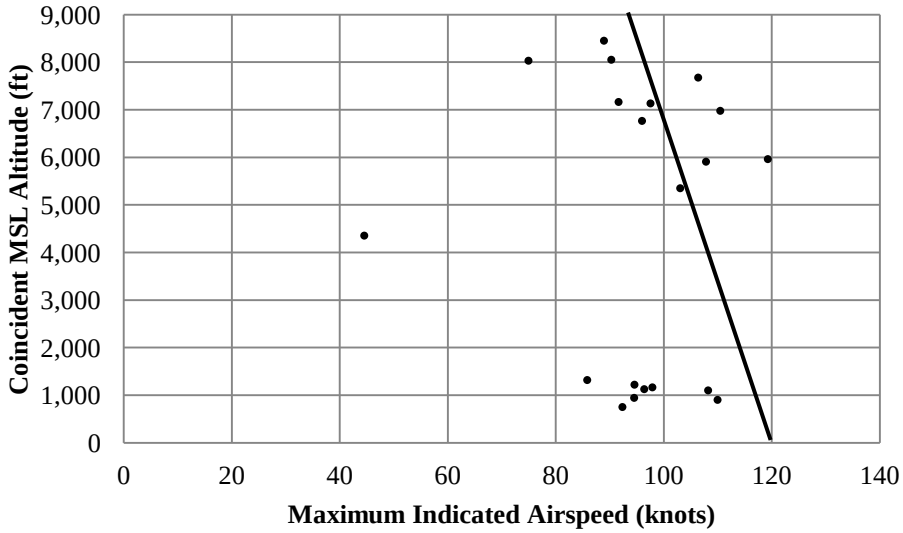

Figure 34. Maximum Indicated Airspeed and Coincident MSL Altitude for Reconnaissance Missions

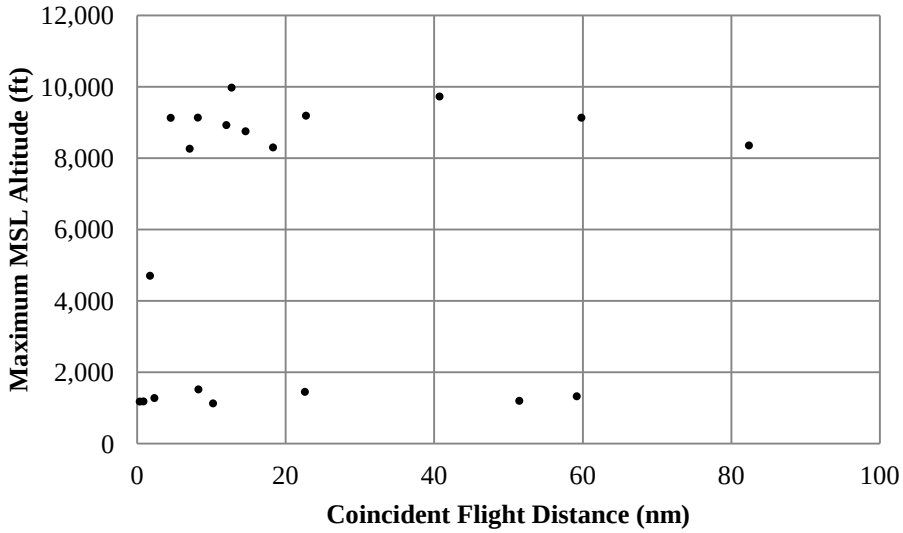

Figure 35. Maximum MSL Altitude and Coincident Flight Distance for Reconnaissance Missions

While a limited number of stationary and hover phases are being performed during a reconnaissance mission, the correlation between duration and distance was less than that of a ferry mission (R^2=.987); and was more on par with a passenger mission (R^2=.877). This increased deviation is most likely, again, due to the mission profile of a reconnaissance, requiring lower average speeds to properly scout a target area.

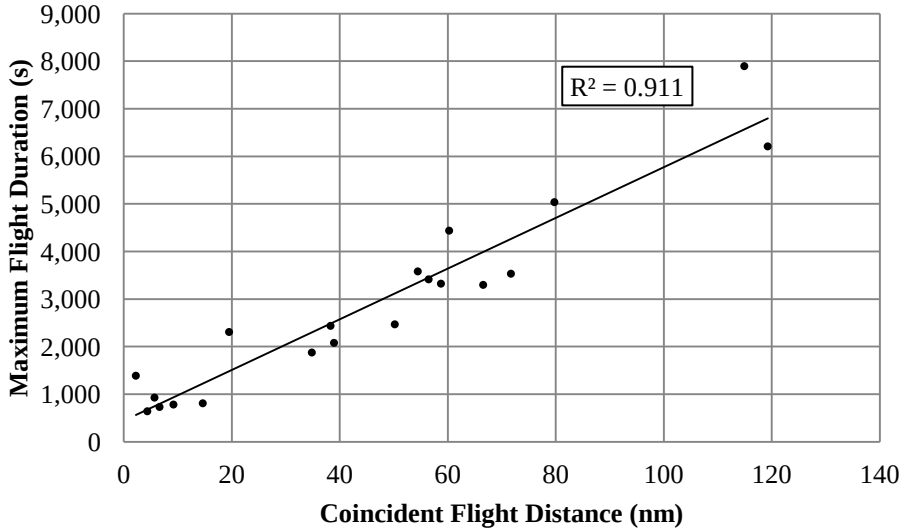

Figure 36. Maximum Flight Duration and Coincident Flight Distance for Reconnaissance Missions

Normal probability distributions of flight duration and flight distance are shown in Figures 43 and 44. These results show an average duration and distance of 45 minutes and 43 nm, respectively. Also, a relatively large standard deviation can be observed for both parameters.

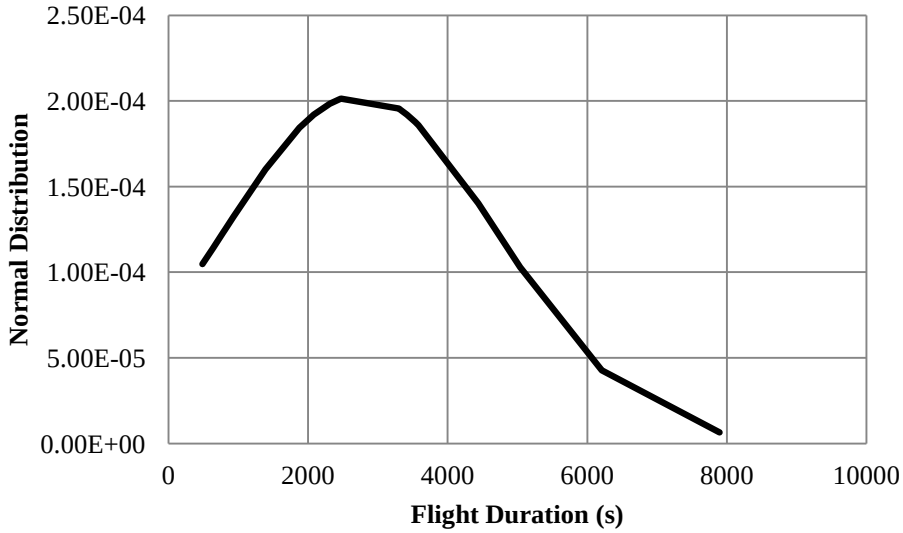

Figure 37. Normal Probability Distribution of Flight Duration for Reconnaissance Missions

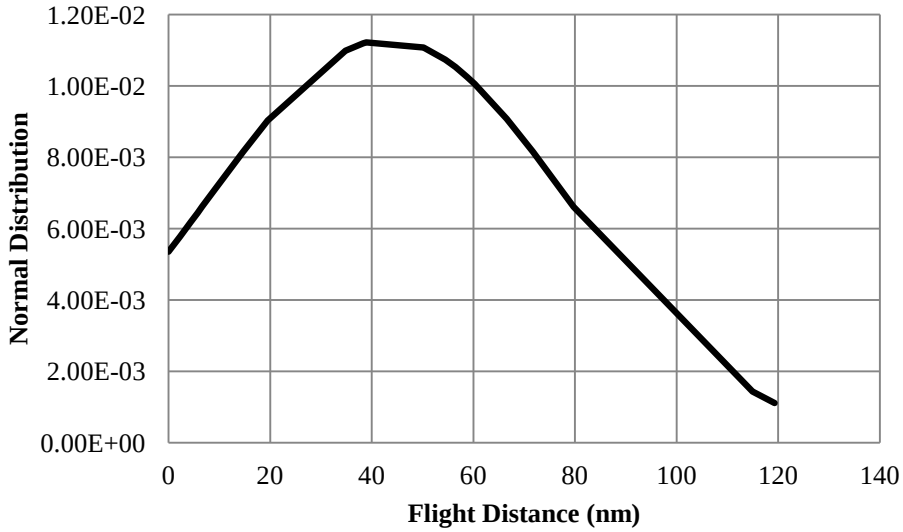

Figure 38. Normal Probability Distribution of Flight Distance for Reconnaissance Missions

In most other missions, the majority of maximum pitch angles occurred at zero airspeed. However, in the case of reconnaissance missions, only 33% of maximum pitch angles corresponded to zero indicated airspeed. If reconnaissance missions were indeed flown very close to the ground, then such a flight path would require an increased number of pitch-up during forward flight to avoid obstacles or gain altitude, which is substantiated by the results shown in Figure 39. Only three cases of maximum negative pitch angle were observed at zero airspeed.

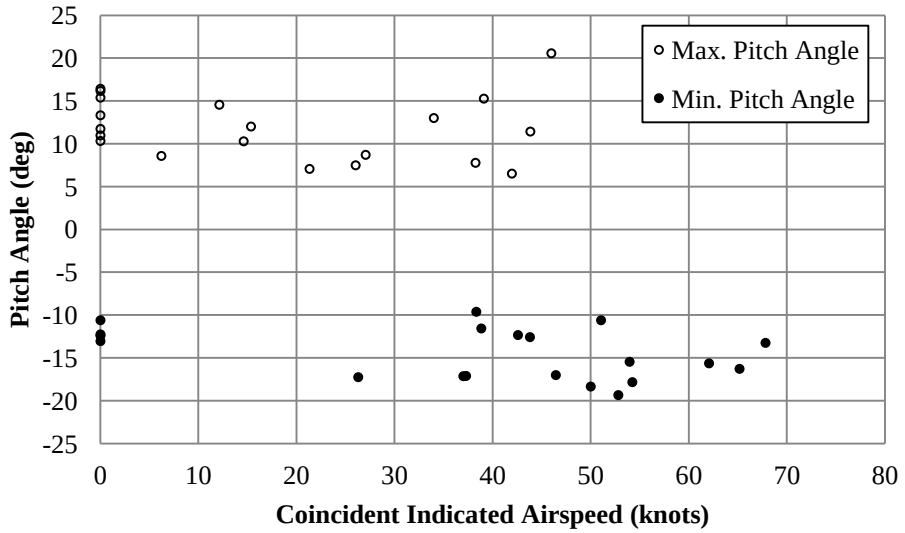

Figure 39. Maximum and Minimum Pitch Angle and Coincident Indicated Airspeed for Reconnaissance Missions

Like most missions, the maximum and minimum roll angles occurred across a broad spectrum of magnitudes and airspeeds, as shown in Figure 40. The magnitudes of the angles and the coincident airspeeds at which they occurred were similar to those of other missions, further suggesting that specific missions did not display characteristic roll angle behavior.

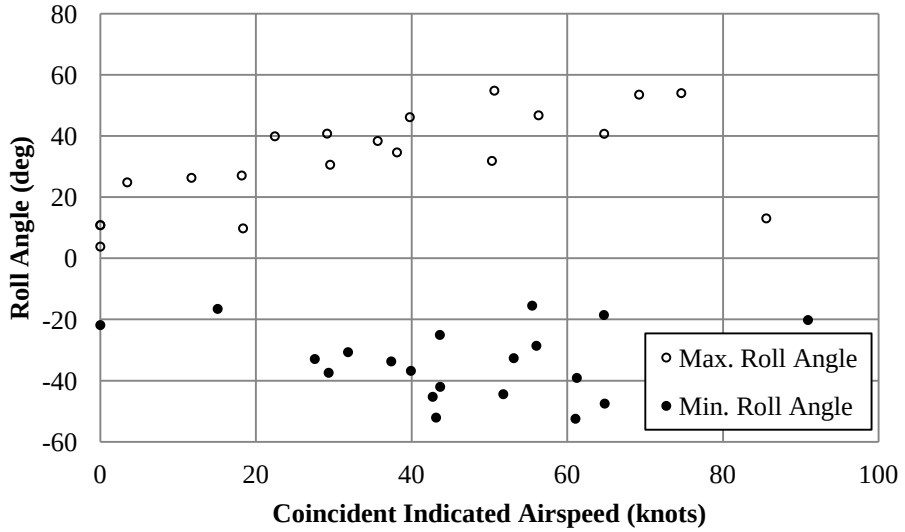

Figure 40. Maximum Roll Angle and Coincident Indicated Airspeed for Reconnaissance Missions

e. Helitorch Mission Usage Statistics

Only nine helitorch missions could be identified among the recorded flight files. Therefore, the results shown here pertaining to these missions are not statistically correct due to the very limited amount of data available. For the identified helitorch missions, as seen in Table 17, the average duration of a mission, at 2.2 hours, was greater than the maximum duration of reconnaissance, longline, and rappel missions. The maximum duration was 3.72 hours, lasting 37% longer than the maximum of the bucket mission, which was next longest. The primary objective of a helitorch mission is the burn phase. However, this is also the most difficult phase to separate using an automated process because there is a large variation in how the burn phase is flown. Given this difficulty, the possibility arises that some burn phases were missed, thus reducing the average number of burns shown in Table 17.

Table 17. Helitorch Mission Usage Statistics and Average Mission Profile

Mission	Helitorch		
Average Duration (s)	7998.44	Missions Performed	9
Max Duration (s)	13420.00	Stationary	6.33
Average Distance (nm)	69.07	Hover	15.00
Max Distance (nm)	154.07	Start of Flight	5.44
Max Altitude (ft)	10012.80	Climb	22.78
Max KIAS (knots)	103.51	Cruise	20.89
		Descent	29.44
		Start of Landing	6.44
		Burn	1.33

As helitorches are external cargo missions, a V_{NE} of 80 knots is applied for the mission. The helitorch missions had the fewest number of V_{NE} exceedances, and the lowest average ΔV_{NE}, as shown in Table 18. This reduction in exceedances is most likely due to the nature of the apparatus attached to the belly, a part of which is a large container in which gelatinized fuel is held. This gelatinized fuel is funneled to an ignition and delivery point

from which the ignited fuel is dropped to a pre-designated point to burn vegetation. Given the inherently dangerous nature of the apparatus, it is possible extra care was most likely given in terms of maximum velocity attained during flight.

Table 18. Helitorch Mission V_{NE} Exceedance Statistics

Mission	Number of Exceedances	Average Duration (s)	Average ΔV_{NE} (knots)	StdDev ΔV_{NE} (knots)	Max ΔV_{NE} (knots)
Helitorch	158	4.66	1.05	2.07	15.51

Figure 41 shows the maximum MSL altitude and the coincident indicated airspeed for the nine helitorch missions. Figure 42 displays maximum indicated airspeed at the coincident MSL altitude. It is clear from these figures that the recorded helitorch missions occurred at two elevation levels.

As can be seen in Figure 43, all but two missions had the maximum MSL altitude occur within the first 10 nm of the mission start. Given that the average distance of a helitorch mission is 69 nm, this suggests that the maximum altitude is obtained in the initial cruise phase of the mission.

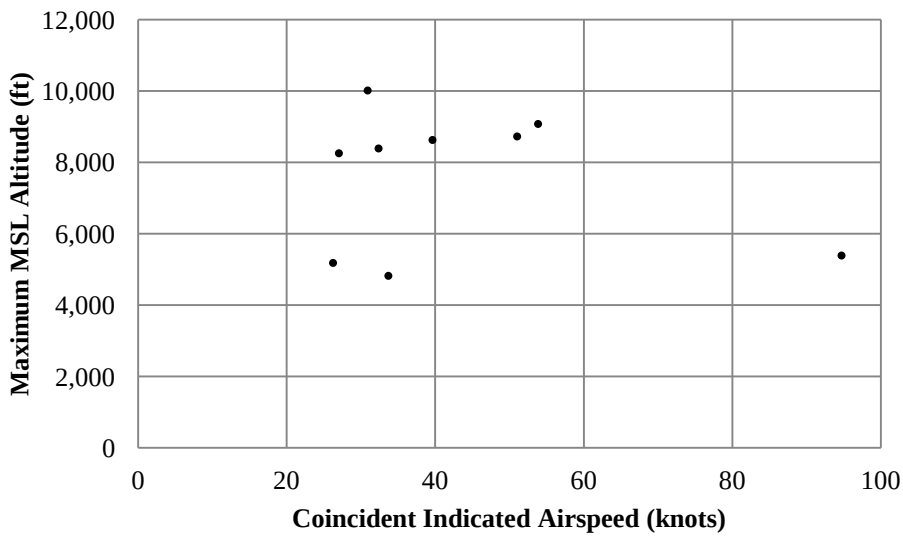

Figure 41. Maximum MSL Altitude and Coincident Indicated Airspeed for Helitorch Missions

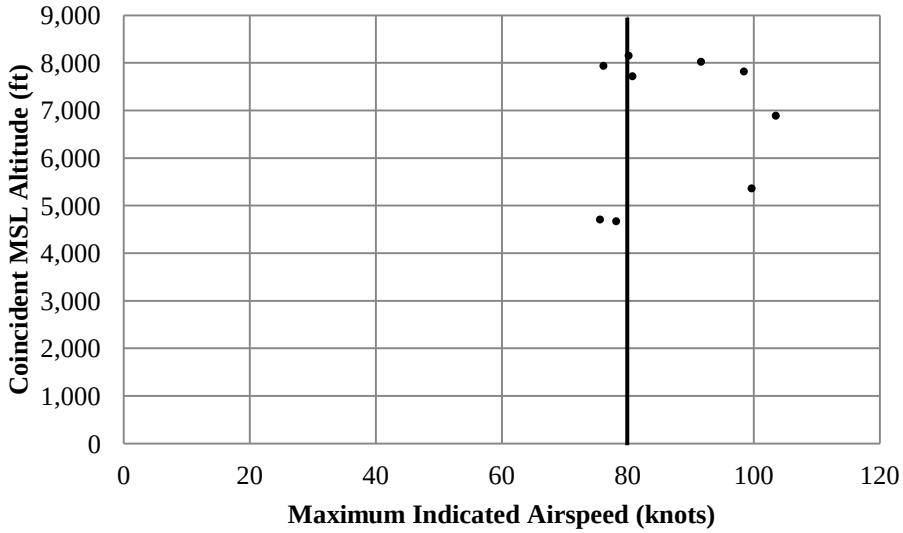

Figure 42. Maximum Indicated Airspeed and Coincident MSL Altitude for Helitorch Missions

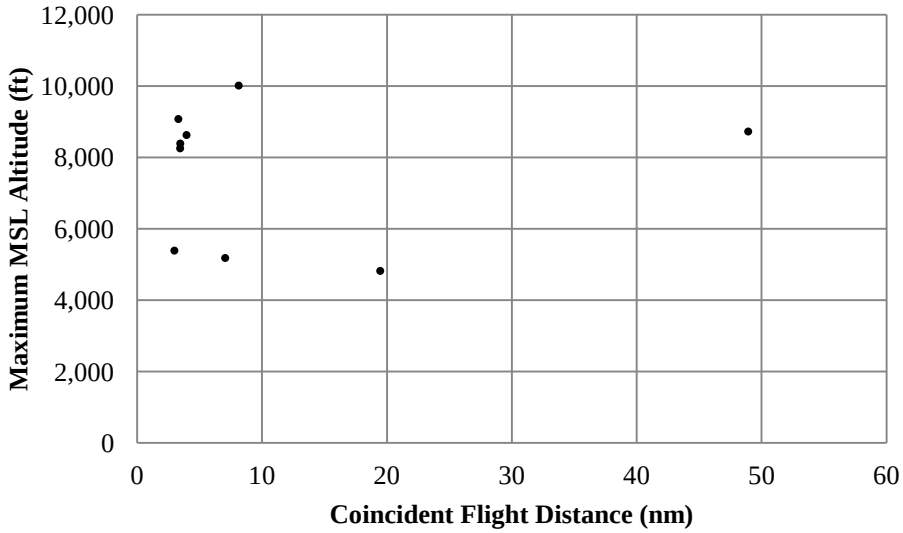

Figure 43. Maximum MSL Altitude and Coincident Flight Distance for Helitorch Missions

As can be seen in Figure 44, there were two sets of helitorch missions, the majority lasting on average 7,000 seconds at a distance of 50 nm, and two around 12,000 seconds and 150 nm. These high duration missions suggest that there were two instances in which the helicopter was required to fly to a burn target that was at a greater distance than what was usually required. Given the special equipment that is needed to perform a helitorch mission, such as gelatinizing the fuel, the helicopter would most likely have a single operational base that would serve as the primary helitorch refilling station. Thus if a target location was at a greater distance, the helicopter would fly from the primary operation base that held the helitorch equipment, rather than a closer operations base, necessitating high flight

distances. Also, the longer missions could be indicative of when the aircraft landed and refueled multiple times during the same mission, thus extending the overall duration and distance of the mission.

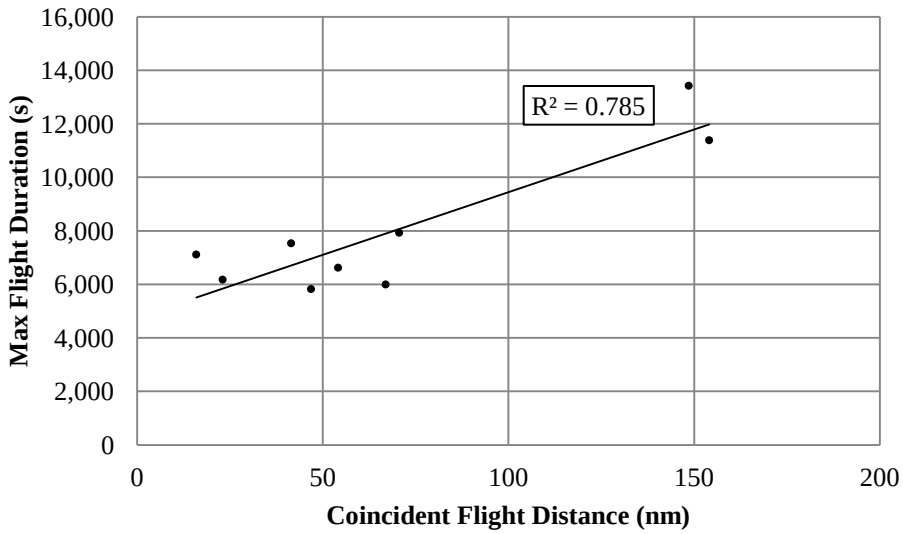

Figure 44. Maximum Flight Duration and Coincident Flight Distance for Helitorch Missions

Figure 45 and Figure 46 show the normal probability distribution for flight duration and flight distance for helitorch missions. These figures show an average duration of 8000 seconds and average distance of 70 nm, respectively. Of note is the linear portion of the two figures, which is due to the limited number of helitorch missions recorded and the presence of two sets of missions which differed greatly from the average overall distance and duration, as discussed previously.

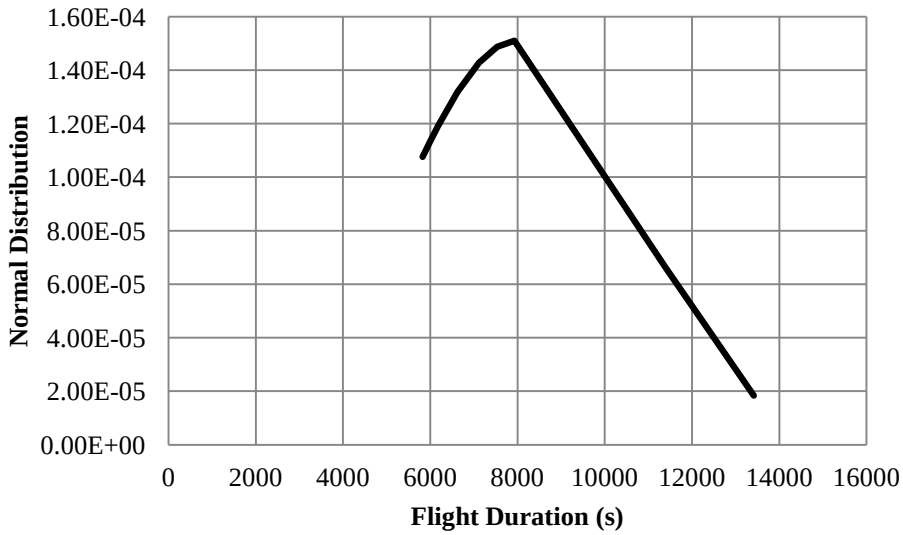

Figure 45. Normal Probability Distribution of Flight Duration for Helitorch Missions

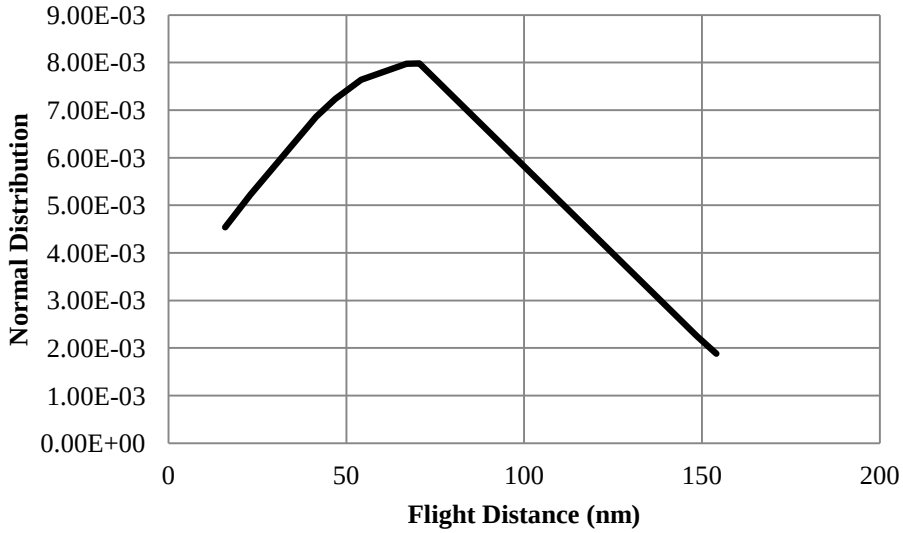

Figure 46. Normal Probability Distribution of Flight Distance for Helitorch Missions

While most missions had a majority of maximum pitch at zero airspeed, there were always instances of maximum pitch occurring at some airspeeds greater than zero. Helitorch missions, however, had no instances of maximum pitch angles occurring at airspeeds greater than zero, and all remained in a band between 15 to 20 deg. Similarly, the minimum pitch angles remained between -14 to -20 deg. Maximum and minimum roll angles show no specific trends in magnitude or coincident airspeed for helitorch missions.

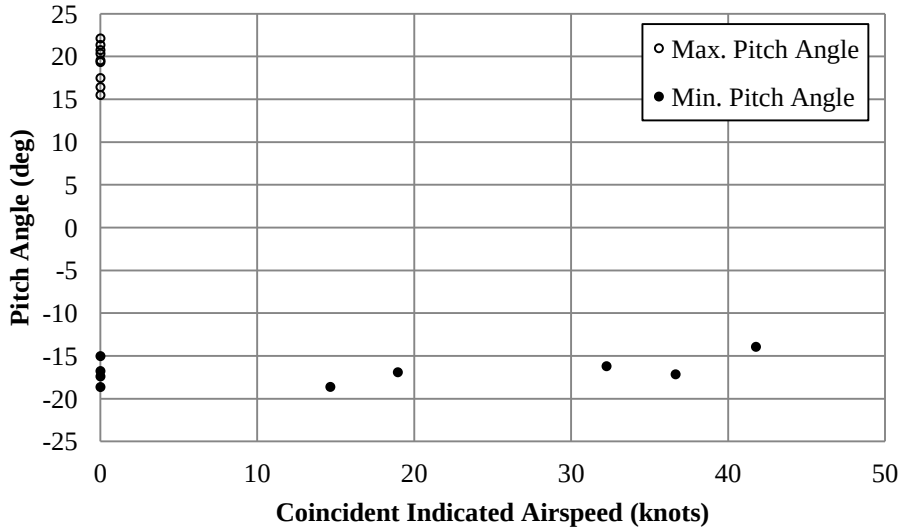

Figure 47. Maximum and Minimum Pitch Angle and Coincident Indicated Airspeed for Helitorch Missions

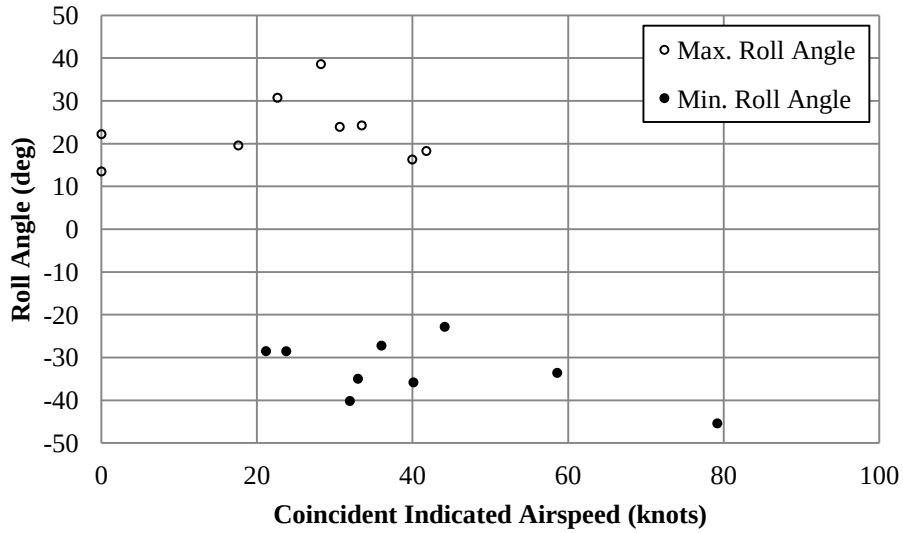

Figure 48. Maximum and Minimum Roll Angle and Coincident Indicated Airspeed for Helitorch Missions

f. Longline Mission Usage Statistics

Longline missions had an average duration of 63 minutes and a maximum of approximately 2 hours. Unlike many missions which had maximum altitudes of nearly 12,000 ft, Table 19 shows that longline missions remained at altitudes less than 9,000 ft. Longline missions, in essence, are passenger missions that have a large number (5 or more) of hover phases. This distinction is made since cargo is attached to the external hook and delivered to the drop site via a hover phase. As can be seen in Table 19, longline missions had an average of six hovers per mission, suggesting that an average longline mission had six deliveries or extractions performed during a mission. Including the number of stationaries, the average longline mission performed nine deliveries or extractions, approximately 3 times as many as a passenger mission.

When a helicopter is performing a longline mission and has external cargo attached, the V_{NE} of 80 KCAS has to be applied, independent of the altitude. However, as can be seen in Table 19, stationary phases did occur, which would suggest that an external cargo was not always attached to the helicopter. However, with the current flight data provided, it was not possible to make the distinction of when external cargo was connected to the helicopter. As a result the V_{NE} of 80 KCAS was applied for the entire mission. This is the root cause of why longline missions showed, not including the number of V_{NE} exceedances, the highest magnitudes for V_{NE} exceedance statistics. Only ferry and passenger missions (i.e. internal cargo missions), had maximum airspeeds exceeding 120 knots. Therefore, the

maximum KIAS of 126 knots for longline missions further substantiates that external cargo was not always connected throughout these flights. Also, like ferry and passenger missions, this maximum was within the 10% margin.

Table 19. Longline Mission Usage Statistics and Average Mission Profile

Mission	Longline		
Average Duration (s)	3781.32	Missions Performed	26
Max Duration (s)	7467.75	Stationary	3.62
Average Distance (nm)	43.045	Hover	6
Max Distance (nm)	134.73	Start of Flight	3.27
Max Altitude (ft)	8971.96	Climb	10.85
Max KIAS (knots)	125.95	Cruise	5.69
		Descent	8.5
		Start of Landing	3.58

Table 20. Longline Mission V_{NE} Exceedance Statistics

Mission	Number of Exceedances	Average Duration (s)	Average ΔV_{NE} (knots)	StdDev ΔV_{NE} (knots)	Max ΔV_{NE} (knots)
Longline	1125.00	14.12	1.96	4.59	37.95

In previous missions, there was stratification of the maximum MSL altitude. Longline missions do not show a similar trend, rather maximum MSL altitudes are spread throughout the altitude ranges, as shown in Figure 49. Figure 51 shows there was little correlation of maximum MSL altitude to distance flown.

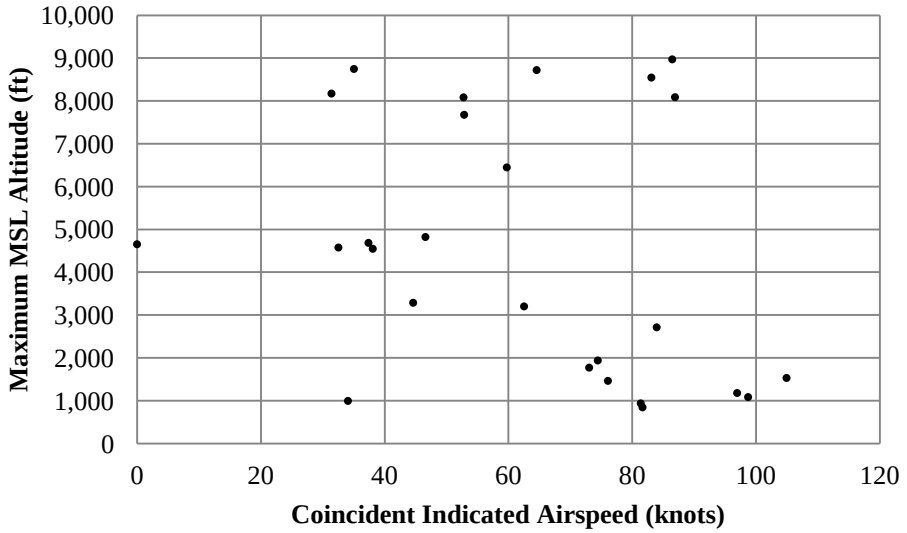

Figure 49. Maximum MSL Altitude and Coincident Indicated Airspeed for Longline Missions

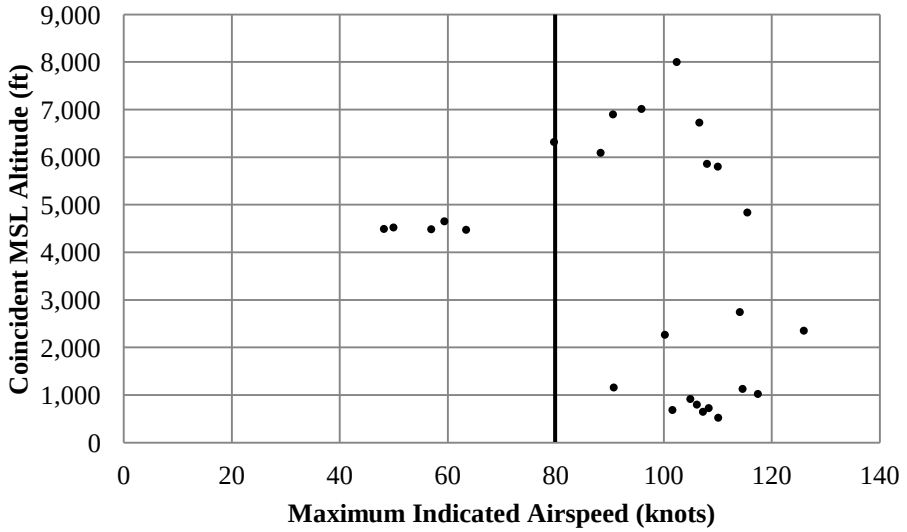

Figure 50. Maximum Indicated Airspeed and Coincident MSL Altitude for Longline Missions

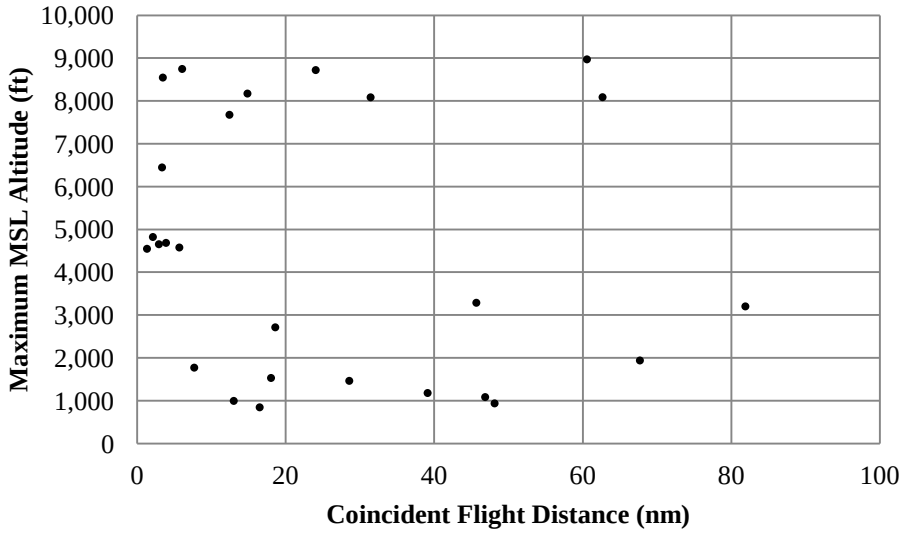

Figure 51. Maximum MSL Altitude and Coincident Flight Distance for Longline Missions

There also was very little correlation between flight duration and distance for longline missions, as shown in Figure 52. This was due to the amount of time spent in stationary and hover phases. Since the duration of the stationary and hover phases was not consistent throughout all longline missions, distance and duration cannot be correlated

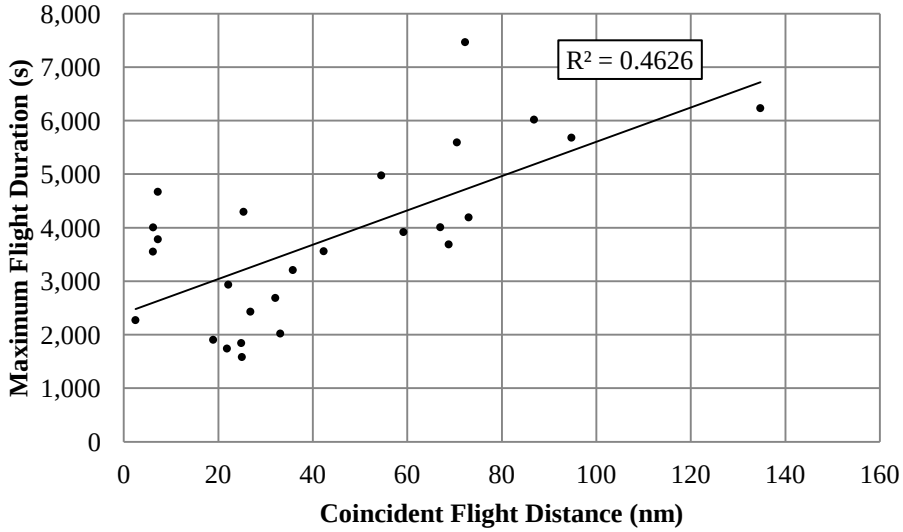

Figure 52. Maximum Flight Duration and Coincident Flight Distance for Longline Missions

Figure 53 and Figure 54 show the normal probability distribution for flight duration and flight distance for longline missions.

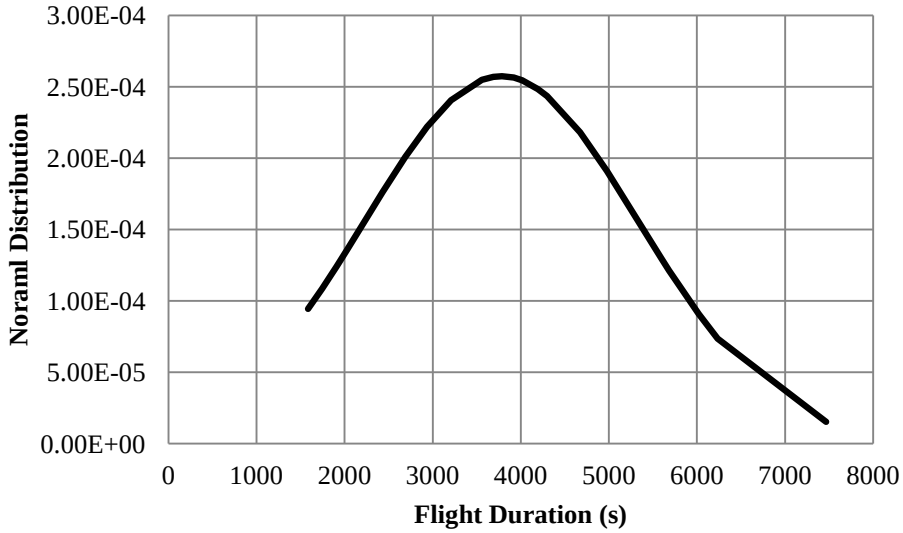

Figure 53. Normal Probability Distribution of Flight Duration for Longline Missions

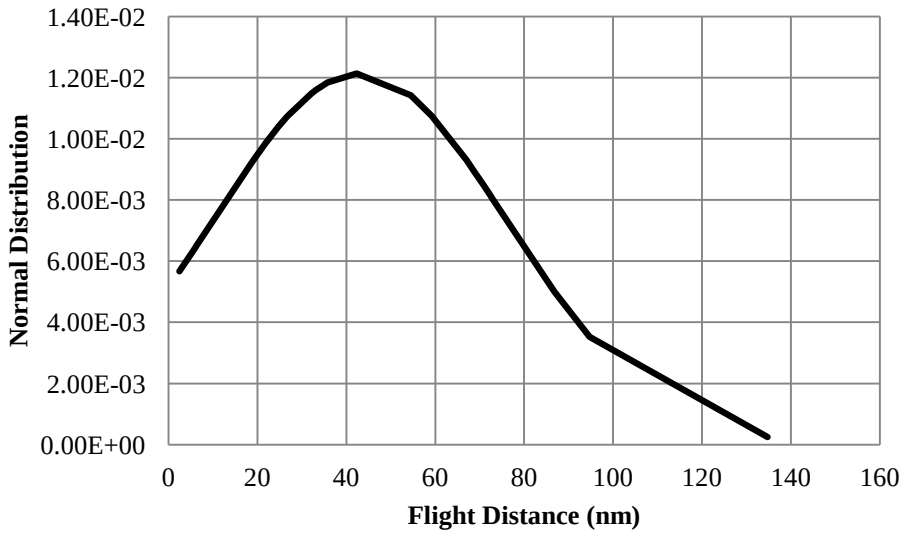

Figure 54. Normal Probability Distribution of Flight Distance for Longline Missions

Even though a longline mission has extra cargo slung beneath the helicopter, the minimum pitch angles did not appear to be of greater magnitude than those of a passenger mission. The maximum pitch angles, though, did show a greater pitch up magnitude, similar to that of a bucket mission. Like all other missions, the maximum and minimum roll angles were spread across magnitudes and airspeeds, and no special correlation between the roll angles and the longline mission was apparent.

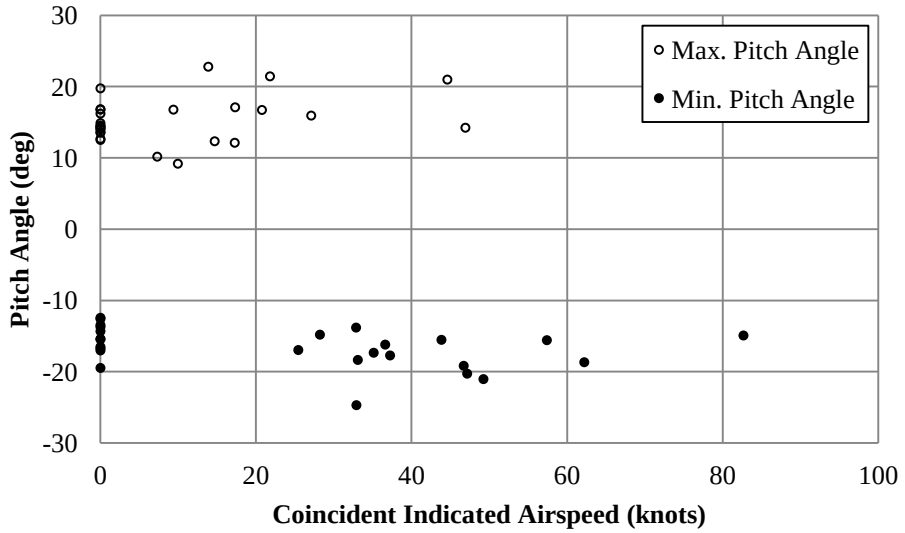

Figure 55. Maximum and Minimum Pitch Angle and Coincident Indicated Airspeed for Longline Missions

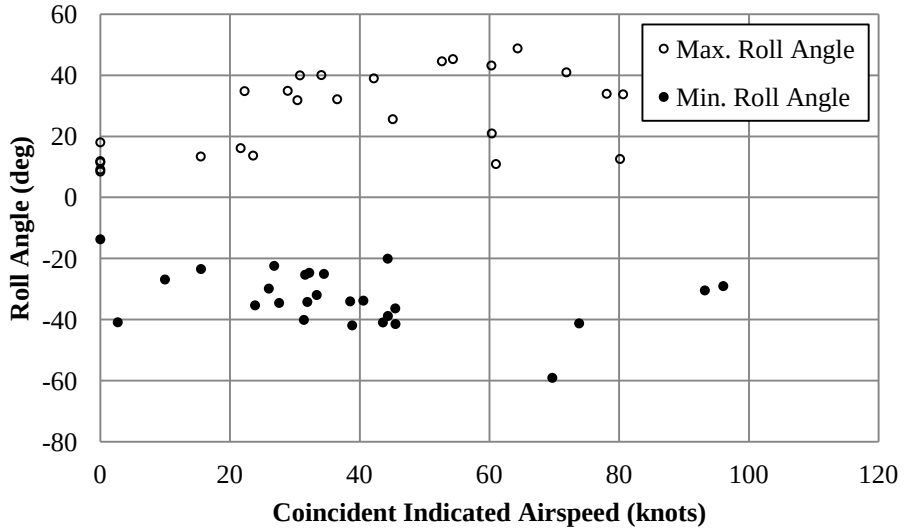

Figure 56. Maximum and Minimum Roll Angle and Coincident Indicated Airspeed for Longline Missions

g. Rappel Mission Usage Statistics

Rappel missions had an average duration of 41 minutes and a maximum duration of less than 2 hours, making rappel missions the quickest missions in both average and maximum duration. Given that the purpose of a rappel mission is to deposit a limited number of firefighters to a fire zone, the brevity of a rappel mission would be expected. It is during hover phases that firefighters would rappel down into a target drop point, and by Table 21, the average

number of rappels was approximately two per mission. The average of nearly three stationaries per mission would suggest that for most of the missions, once the helicopter deployed its initial group of rappelers, it would be flown to an operation base to pick up another set of rappelers.

Table 21. Rappel Mission Usage Statistics

Mission	Rappel		
Average Duration (s)	2478.41	Missions Performed	33
Max Duration (s)	7177.50	Stationary	2.82
Average Distance (nm)	33.58	Hover	2.21
Max Distance (nm)	113.97	Start of Flight	1.94
Max Altitude (ft)	10252	Climb	4.24
Max KIAS (knots)	118.81	Cruise	4.33
		Descent	5
		Start of Landing	2.09

While few exceedances happened during rappel missions, there was still a large maximum ΔV_{NE}, as shown in Table 22. Given that this was an internal cargo mission, the only factor affecting V_{NE} was the altitude at which the helicopter was flying. While the magnitude of an average ΔV_{NE} was low, the average duration of an exceedance was the highest of all internal cargo missions.

Table 22. Rappel Mission V_{NE} Exceedance Statistics

Mission	Number of Exceedances	Average Duration (s)	Average ΔV_{NE} (knots)	StdDev ΔV_{NE} (knots)	Max ΔV_{NE} (knots)
Rappel	292	11.48	1.74	3.39	26.07

Stratification of the altitudes was shown to occur in several of the mission types, though usually only showing two layers. Rappel missions had three distinct maximum altitude bands, as shown in Figure 57: less than 2,000 ft, between 4,000-6,000 ft, and higher than 8,000 ft. Figure 58 shows that there were five rappel missions which had a limited maximum airspeed of less than 60 KIAS, although there was no indication in the flight data as to the reason for the lower airspeed.

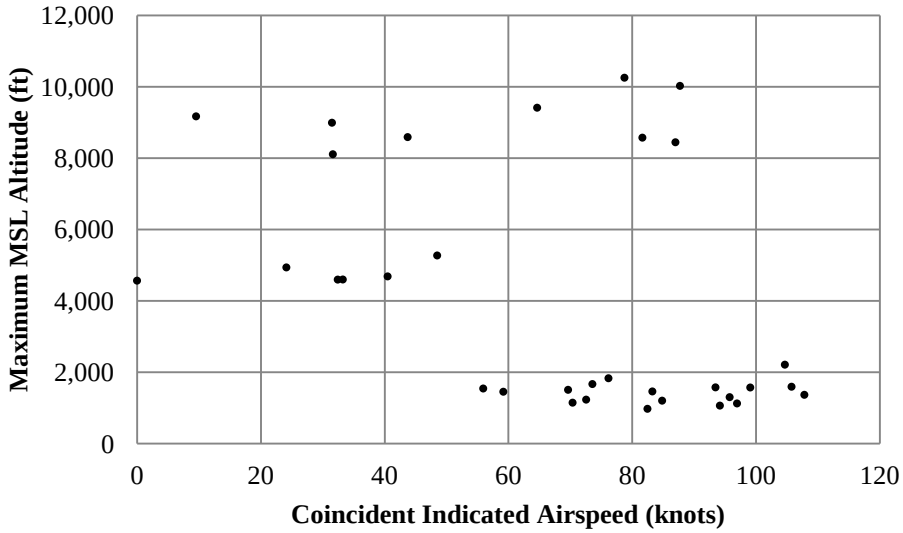

Figure 57. Maximum MSL Altitude and Coincident Indicated Airspeed for Rappel Missions

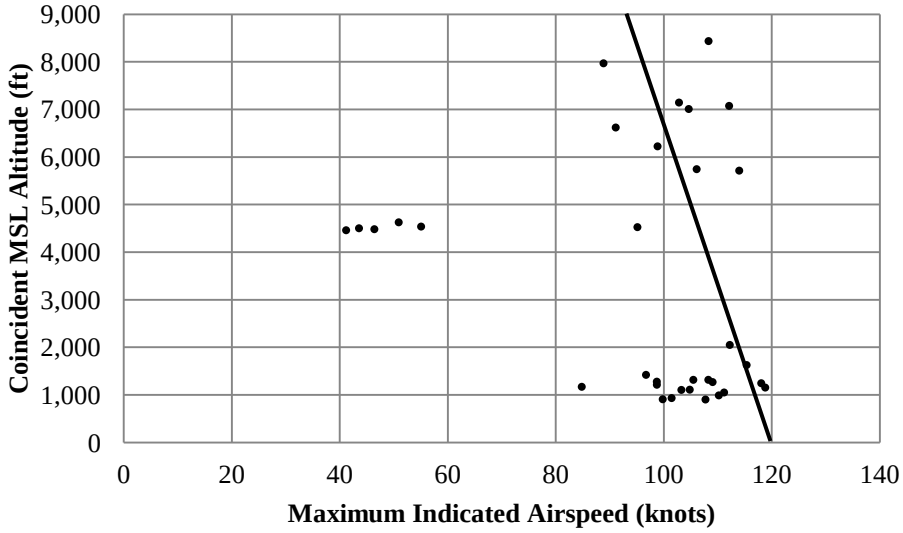

Figure 58. Maximum Indicated Airspeed and Coincident MSL Altitude for Rappel Missions

Figure 59 shows that there was little correlation between maximum MSL altitude and distance into flight. This holds true when comparing the coincident flight distances of Figure 59 and Figure 60, as it can be seen that maximum MSL altitude occurred during any portion of the mission. As can also be seen in Figure 60, there is somewhat limited correlation between duration and distance, yet the correlation was greater than other missions which had an increased number of hovers, such as bucket, helitorch, and longline. Since, during a rappel mission the

helicopter is only at zero airspeed to allow firefighters to rappel for delivery, a higher correlation occurred relative to the other three missions.

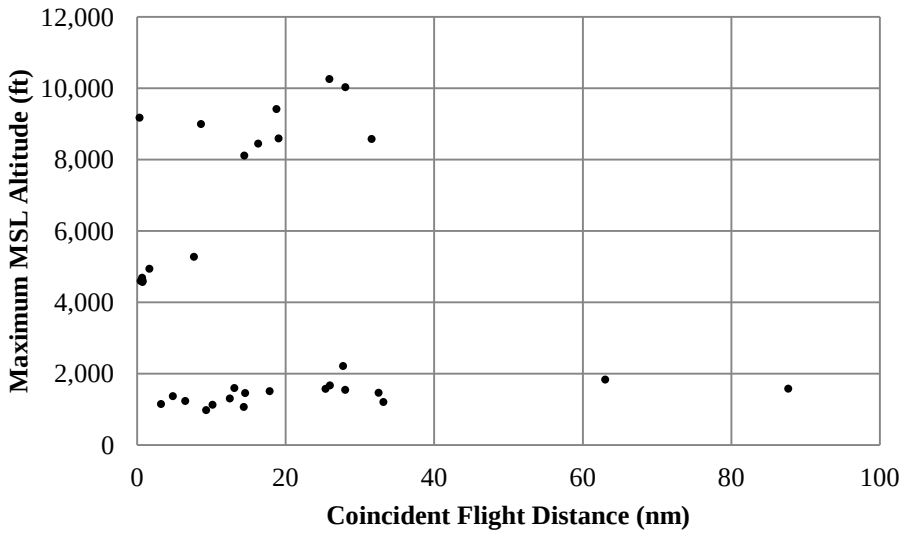

Figure 59. Maximum MSL Altitude and Coincident Flight Distance for Rappel Missions

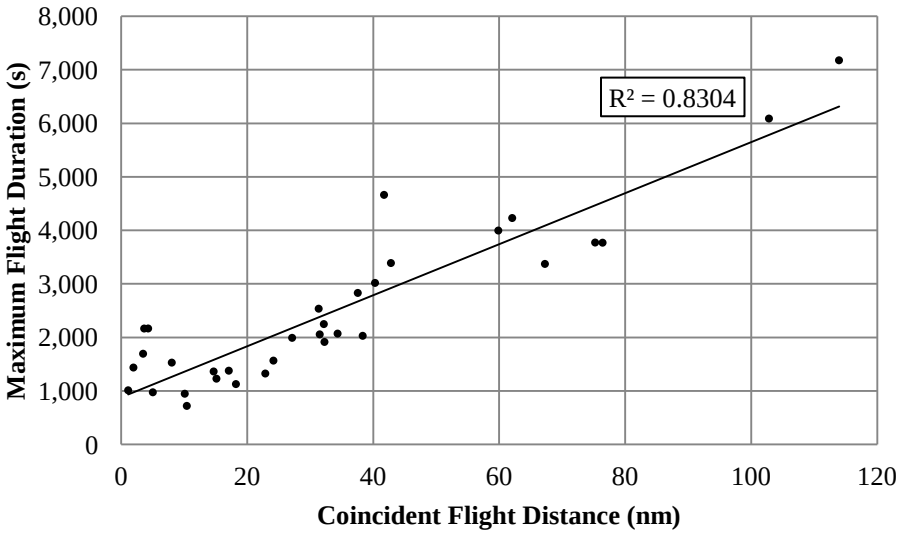

Figure 60. Maximum Flight Duration and Coincident Flight Distance for Rappel Missions

Figure 61 and Figure 62 show the normal distribution of duration and distance for rappel missions.

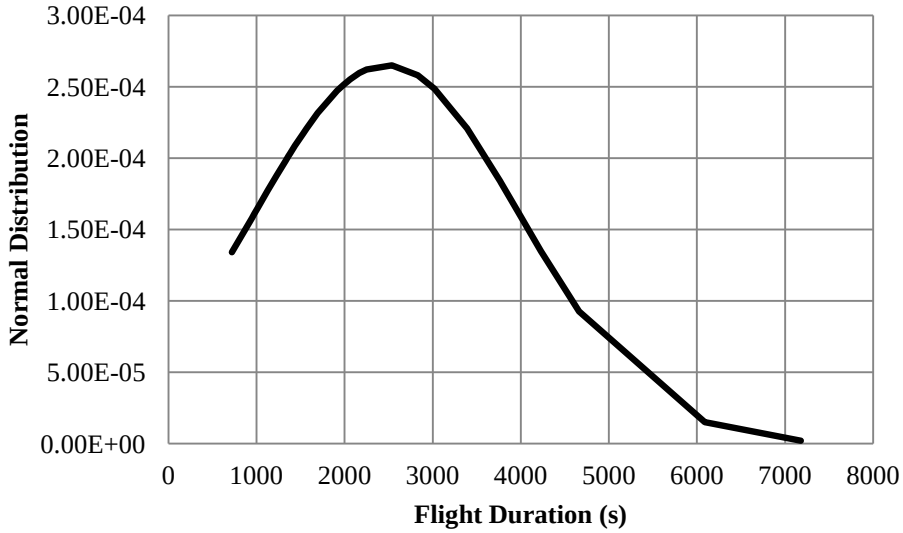

Figure 61. Normal Probability Distribution of Flight Duration for Rappel Missions

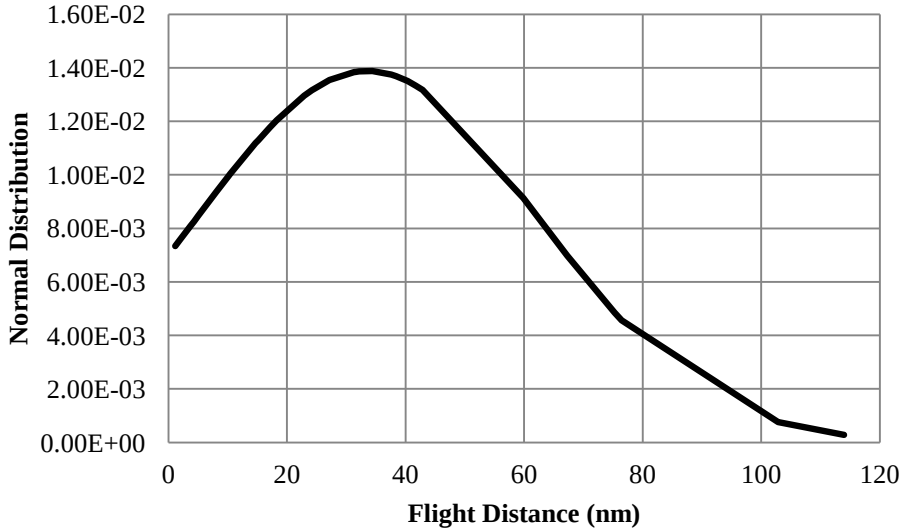

Figure 62. Normal Probability Distribution of Flight Distance for Rappel Missions

As seen in Figure 63 and Figure 64, the maximum and minimum pitch and roll angles during rappel missions has the same trends seen in the previous mission types. Most maximum pitch angles occurred at zero airspeed, and there was no correlation between mission type and maximum and minimum roll angles and coincident KIAS.

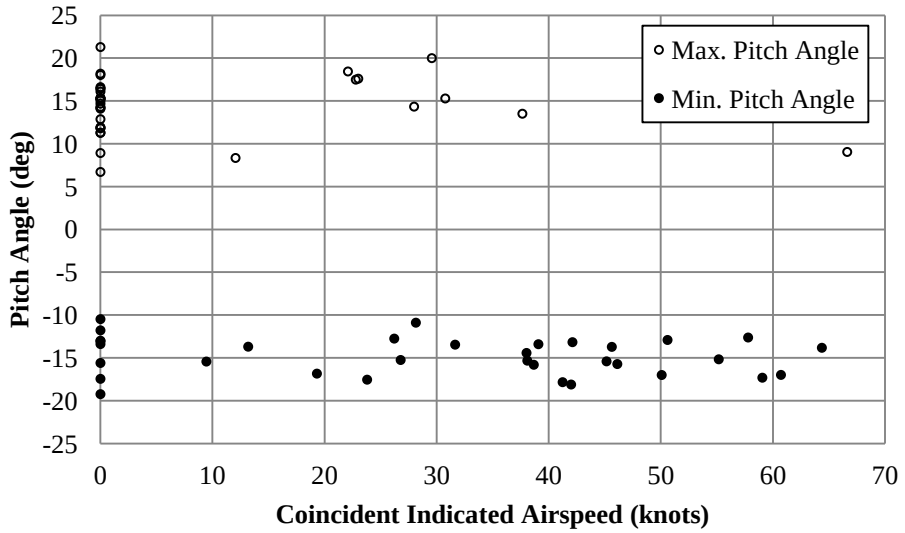

Figure 63. Maximum and Minimum Pitch and Coincident Indicated Airspeed for Rappel Missions

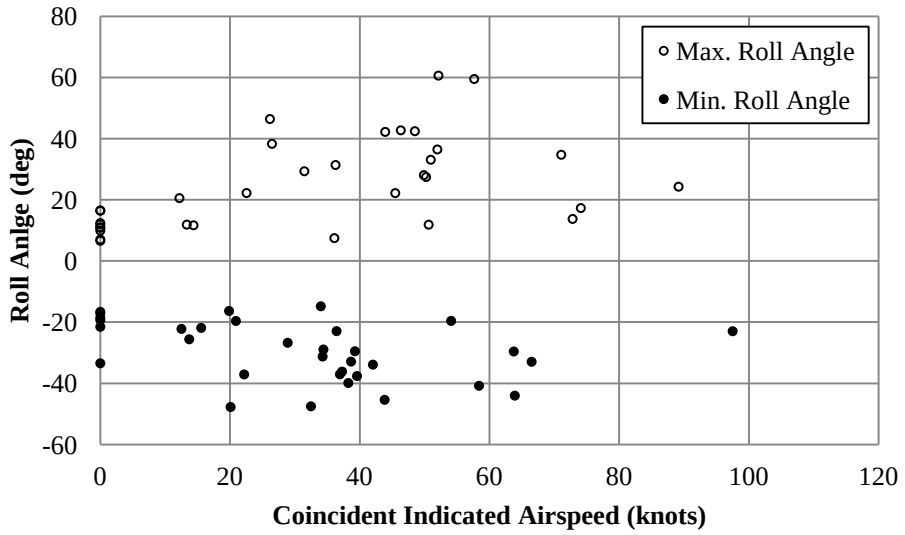

Figure 64. Minimum and Minimum Roll Angle and Coincident Indicated Airspeed for Rappel Missions

2. Phase Usage Results

The following sections discuss the usage statistics during the phase in which they were gathered. The initial table shows average and maximum values of key data sets, while the figures that follow show the maximum of primary data sets and the coincident data occurring at those points. Some figures that have maximum or coincident airspeed have both ground speed and airspeed plotted. This is due to the interference of rotor downwash with the

pitot-static tube at forward velocities less than 30 knots. To help provide more accurate results, ground speed was used for velocities less than 30 knots, while indicated airspeed was used for velocities greater than 30 knots.

a. Stationary Phase Usage Statistics

The average stationary phase lasted 3 minutes with the longest lasting nearly 29 minutes. Because the end of a stationary phase was based on achieving a threshold in certain data, the helicopter could take-off and move prior to the marked end of the stationary phase. Therefore it was possible for stationary phases to have ground speeds greater than zero. Also lending to greater than zero ground speeds is that this parameter is based on GPS data. Drift in GPS data, which was observed in elevation, could have registered as forward flight, thus leading to a maximum ground speed of 12 knots, as seen in Table 23.

Table 23. Usage Statistics of the Stationary Phase

Phase	Average Duration (s)	Max Duration (s)	Average Distance (nm)	Max Distance (nm)	Max Altitude (ft)	Max GS (knots)
Stationary	180.40	1716.75	0.0133	0.18	9029.66	12.00

With Figure 65, it is possible to see the altitude of every landing location. As stated in the mission usage section, altitude stratification was noticed in a number of missions' maximum MSL altitude figures. Figure 65 allows for a clearer observation of this, with four primary levels: less than 2,000 ft, at 4,000 ft, about 6,000 ft, and greater than 7,000 ft.

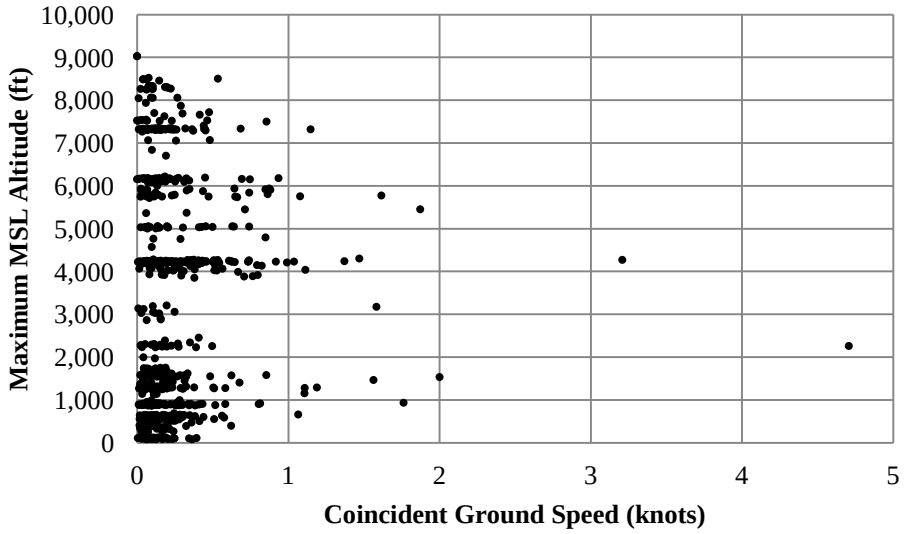

Figure 65. Maximum MSL Altitude and Coincident Ground Speed of the Stationary Phase

Figure 66 would suggest that even when the helicopter was in a stationary phase it was not in fact "stationary." As discussed before, this was due to phase separation program inaccuracy and drift in GPS data. If one were to view Figure 67, it can be seen that the vast majority of stationary phases covered a distance of less than 0.02 nm, or 121 ft. Given this is such a small distance, the inaccuracy or drift is of small consequence in overall analysis of the helicopter's usage during this phase.

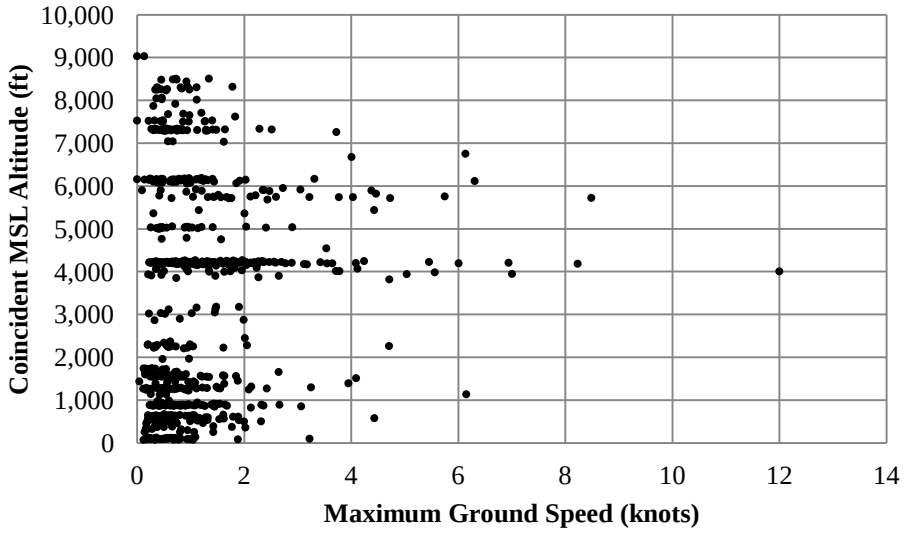

Figure 66. Maximum Ground Speed and Coincident MSL Altitude of the Stationary Phase

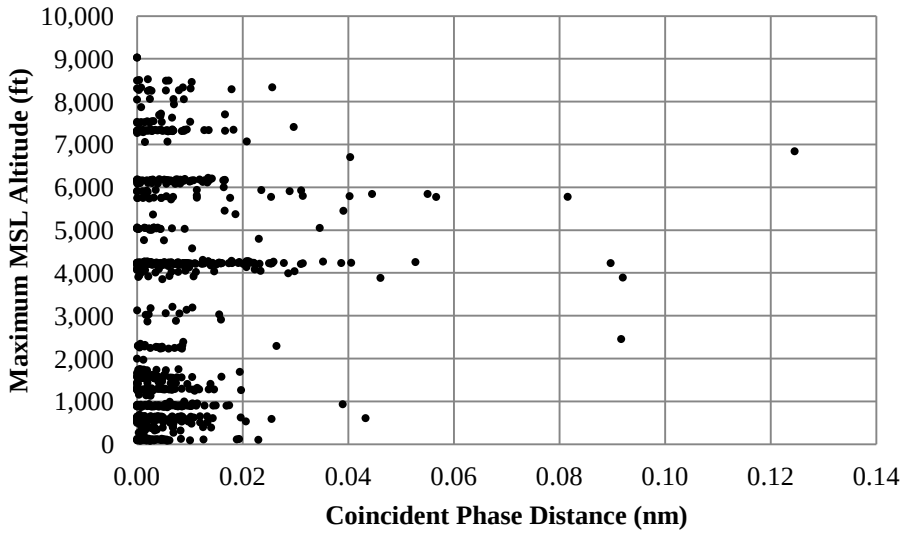

Figure 67. Maximum MSL Altitude and Coincident Phase Distance of the Stationary Phase

There was little correlation between duration and distance for stationary phases. This was not surprising given that the length of time to load cargo or passengers varied for every mission, depending on the weight and amount of cargo and number of passengers. The vast majority of stationary phases lasted less than 400 seconds, or less than 6.7 minutes. This would suggest that for the majority of time, the helicopter did not remain at a landing point longer than was needed.

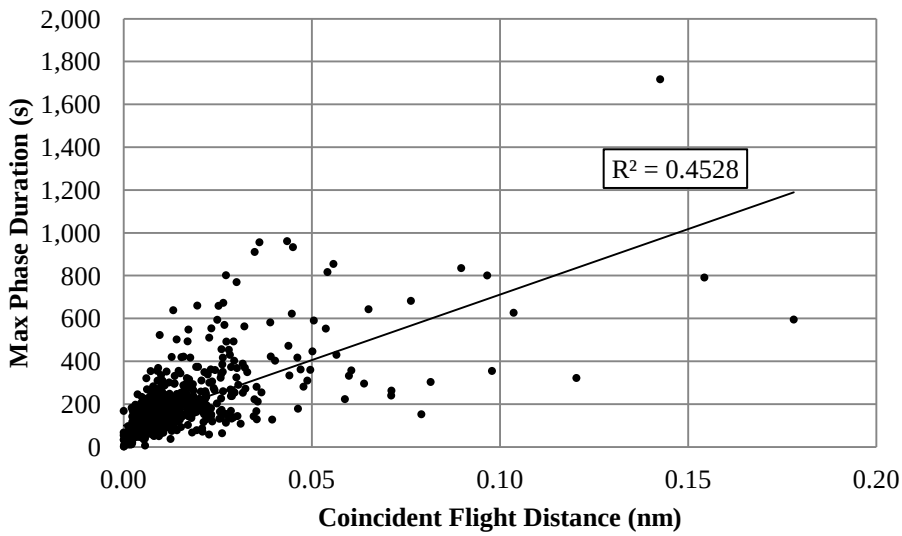

Figure 68. Maximum Phase Duration and Coincident Flight Distance of the Stationary Phase

b. Start of Flight Phase Usage Statistics

The average distance of a start of flight was only 60 ft, with a maximum distance of 243 ft. The reader is reminded that start of flight is a transitory flight phase, covering when the helicopter transitioned from a stationary or hover phase to a climb. As such, it was expected to have a short duration and distance.

Table 24. Usage Statistics of the Start of Flight Phase

Phase	Average Duration (s)	Max Duration (s)	Average Distance (nm)	Max Distance (nm)	Max Altitude (ft)	Max GS (knots)
Start of Flight	17.69	270.50	0.0062	0.04	9029.66	10.79

Table 3 states that one of the identifying factors of a start of flight was a speed less than 6 knots. Therefore it would seem impossible for a start of flight phase to have ground speeds greater than 6 knots as seen in Figure 69 and Figure 70. However, before the phase separation program would mark the end of a start of flight and beginning of

climb, the RMS of variation in ground speed was required to increase beyond 1% and exceed 6 knots. If the helicopter accelerated slowly enough, the program would consider the separation parameters unfulfilled, and the start of flight phase would continue. This is also the reason why the maximum MSL altitude occurs at speeds greater than six knots. Since the altitude was increasing when the flight path transitioned into a climb, at that point the helicopter was at its maximum MSL altitude and maximum ground speed.

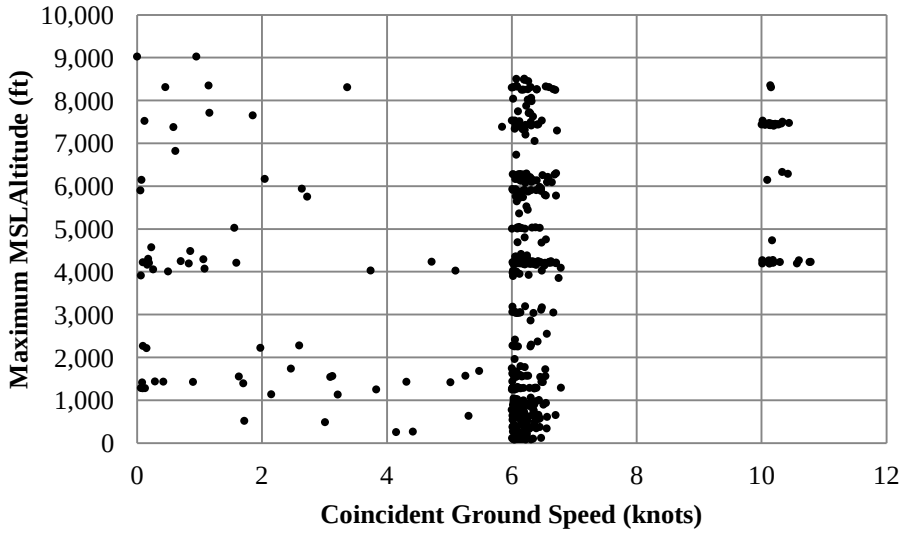

Figure 69. Maximum MSL Altitude and Coincident Ground Speed of the Start of Flight Phase

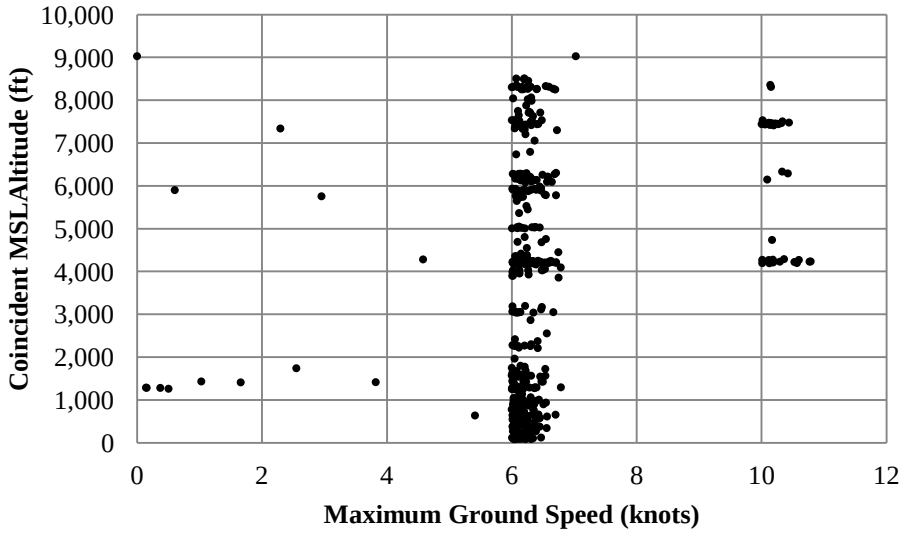

Figure 70. Maximum Ground Speed and Coincident MSL Altitude of the Start of Flight Phase

Figure 71 shows that the majority of start of flight phases had the maximum MSL altitude occur at the overall average phase distance of 0.0062 nm. Also of note is the group of maximum MSL altitude at approximately 7,500 ft covering distances from 0.01 nm to 0.03 nm.

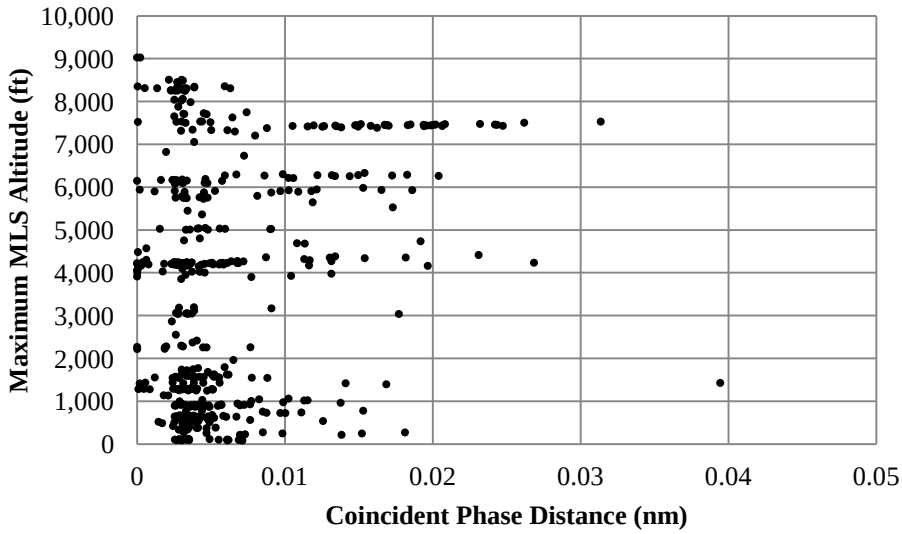

Figure 71. Maximum MSL Altitude and Coincident Phase Distance of the Start of Flight Phase

When viewing Figure 72, there is an anomalous data point during which the duration reaches 270 seconds or 4.5 minutes, and there is no gain in distance. This is most likely the result of beginning a start of flight phase then returning to a stationary phase. The phase separation subroutine would not recognize this, resulting in the long duration. It can also be seen that for the majority of start of flight phases there was good correlation between phase distance and phase duration. The diminished R^2 resulted from the few phases which had extended durations. This would suggest that, when performing this phase, the helicopter was handled consistently by the operator for the majority of start of flight phases.

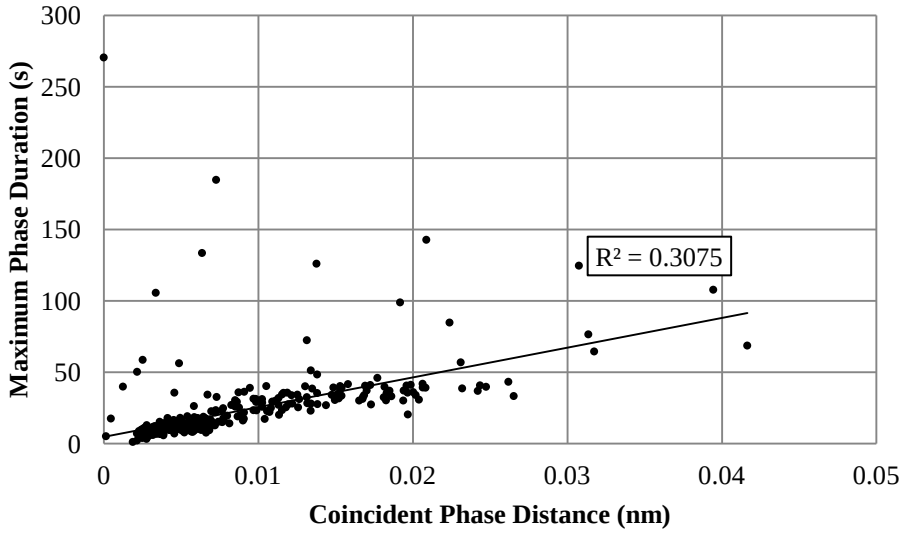

Figure 72. Maximum Phase Duration and Coincident Phase Distance of the Start of Flight Phase

c. Climb Phase Usage Statistics

With an average duration of 31 seconds and distance of 0.39 nm, as shown in Table 25, the helicopter quickly achieved cruise altitude via a climb in most cases. The maximum duration of 6.67 minutes and the maximum distance of 4.34 nm indicate that some climb phases had slower rates of achieving cruise altitude or airspeed.

Table 25. Usage Statistics of the Climb Phase

Phase	Average Duration (s)	Max Duration (s)	Average Distance (nm)	Max Distance (nm)	Max Altitude (ft)	Max KIAS (knots)
Climb	30.95	400.38	0.39	4.34	10354.50	119.41

As can be seen in Figure 73 and Figure 74, coincident airspeed at maximum MSL altitude and maximum airspeed occurred across nearly the entire speed range of this helicopter. The variation in maximum airspeed indicates that the helicopter was required to perform a broad array of flight profiles. Also of note is the series of maximum MSL altitudes at zero airspeed.

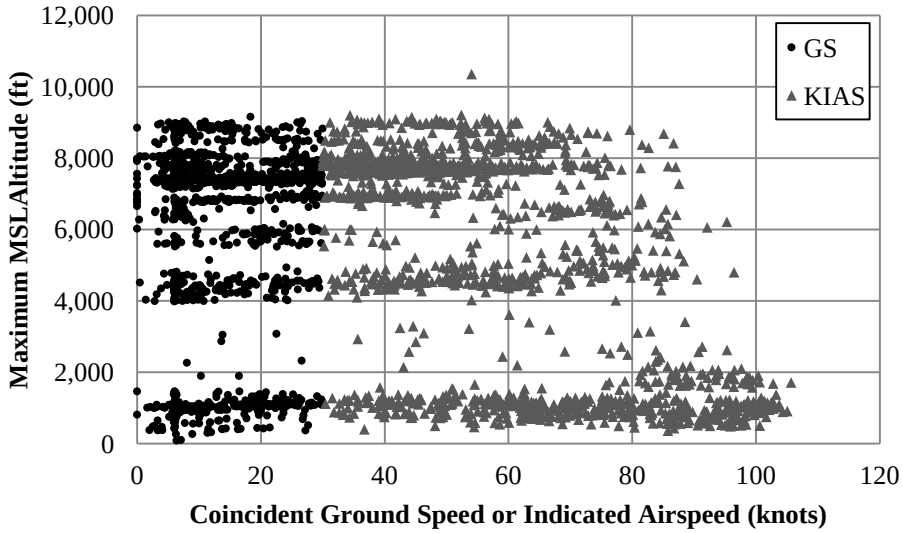

Figure 73. Maximum MSL Altitude and Coincident Ground Speed or Indicated Airspeed of the Climb Phase

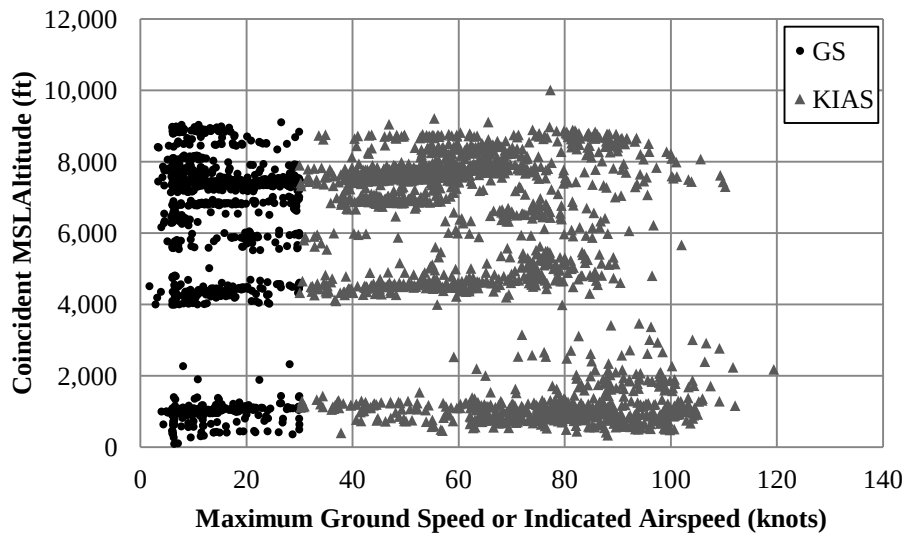

Figure 74. Maximum Ground Speed or Indicated Airspeed of the Climb Phase

As can be seen in Figure 75, there was little correlation between maximum MSL altitude and the distance into phase.

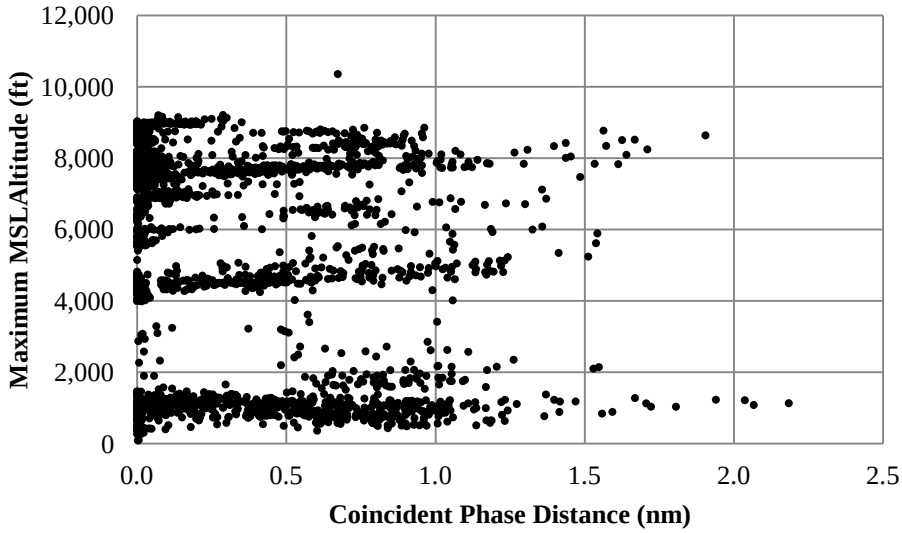

Figure 75. Maximum MSL Altitude and Coincident Phase Distance of the Climb Phase

When viewing Figure 76, it can be seen that there was good correlation between duration and distance for the majority of climb phases, and yet there are some instances that did not follow the trend. At distances from 1.5 nm to 2.5 nm, there was decreased correlation; signifying that climbs between these distances had greater variation in achieving cruise conditions.

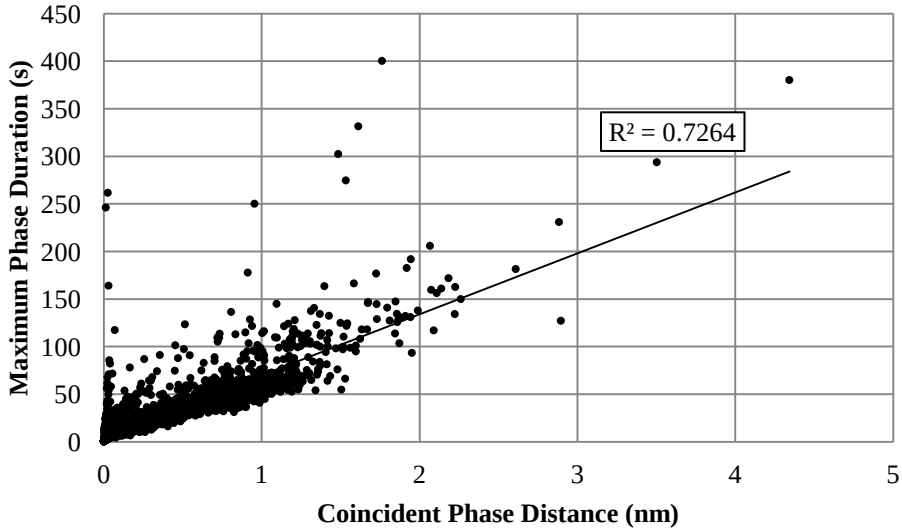

Figure 76. Maximum Phase Duration and Coincident Phase Distance of the Climb Phase

d. Cruise Phase Usage Statistics

While it might seem peculiar that the average distance covered by a cruise phase was 9.4 nm, as shown in Table 26, the reader is reminded that the majority of mission types were flight between nearby operations bases (such as passenger or longline missions) or a specialty mission in which the helicopter cruised to nearby target locations (helitorch, bucket, and rappel). Given the proximity of the target location from the initial operation base, the helicopter would not be required to cover a large distance for the majority of missions, thus resulting in the "low" average distance.

Table 26. Usage Statistics of the Cruise Phase

Phase	Average Duration (s)	Max Duration (s)	Average Distance (nm)	Max Distance (nm)	Max Altitude (ft)	Max KIAS (knots)
Cruise	337.85	7722.63	9.40	243.52	11169.60	129.88

As previously discussed, stratification of altitudes was perceived present in the maximum MSL altitude, which was further refined in the stationary phase analysis, showing four primary altitude levels. With Figure 77, it can be seen that the majority of cruises occurred in two altitude bands with a random smattering of altitudes between the two main levels. This would suggest that the helicopter was flown in cruise at certain MSL altitudes regardless of AGL altitude, generally within a 1,000-1,500 ft band at altitudes of 1,000 ft and 8,000 ft. Of note is single maximum MSL altitude that occurred at zero ground speed. It is currently not known why this would occur during a cruise phase, as such a reduction of velocity should have caused a change in phase. Figure 78 shows that maximum speed covered a wide range. This suggests that the helicopter would not cruise at similar speeds for all cases.

With an average distance of 9.4 nm, Figure 79 shows that there was little correlation between maximum MSL altitude and the distance into the phase. Despite large variation in maximum airspeeds achieved for cruise phases, there was very good correlation of phase duration and phase distance, as shown in Figure 80.

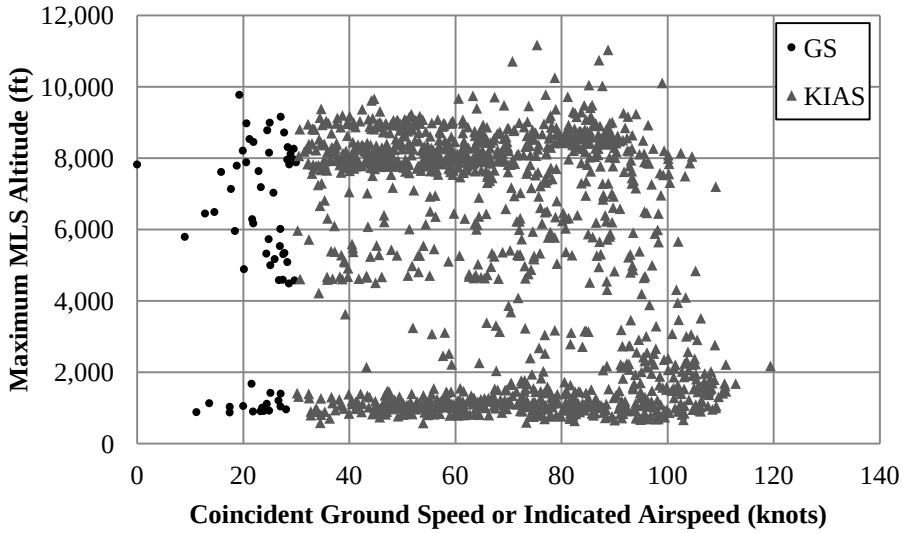

Figure 77. Maximum MSL Altitude and Coincident Ground Speed or Indicated Airspeed of the Cruise Phase

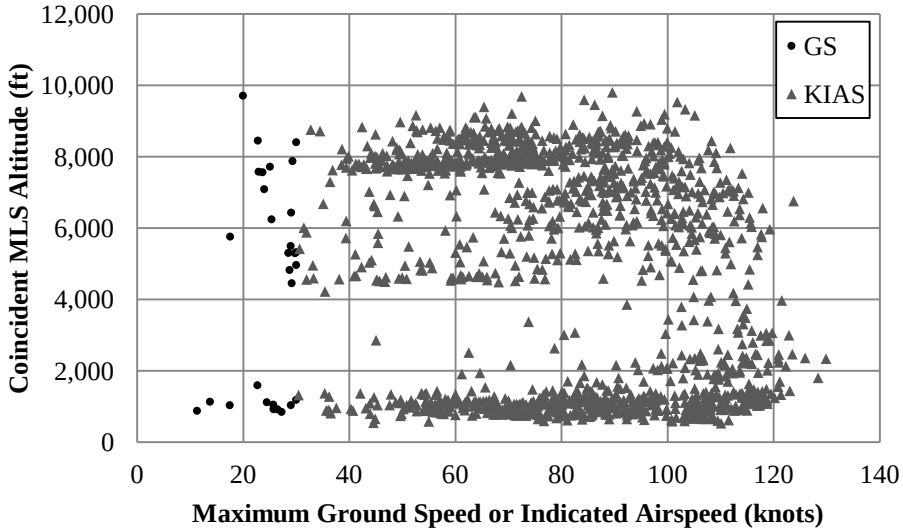

Figure 78. Maximum Ground Speed or Indicated Airspeed and Coincident MSL Altitude of the Cruise Phase

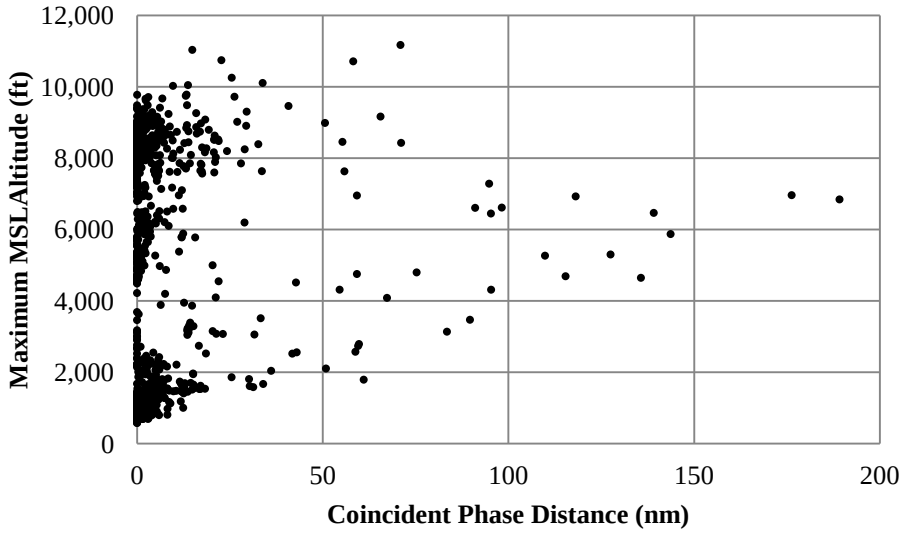

Figure 79. Maximum MSL Altitude and Coincident Phase Distance of the Cruise Phase

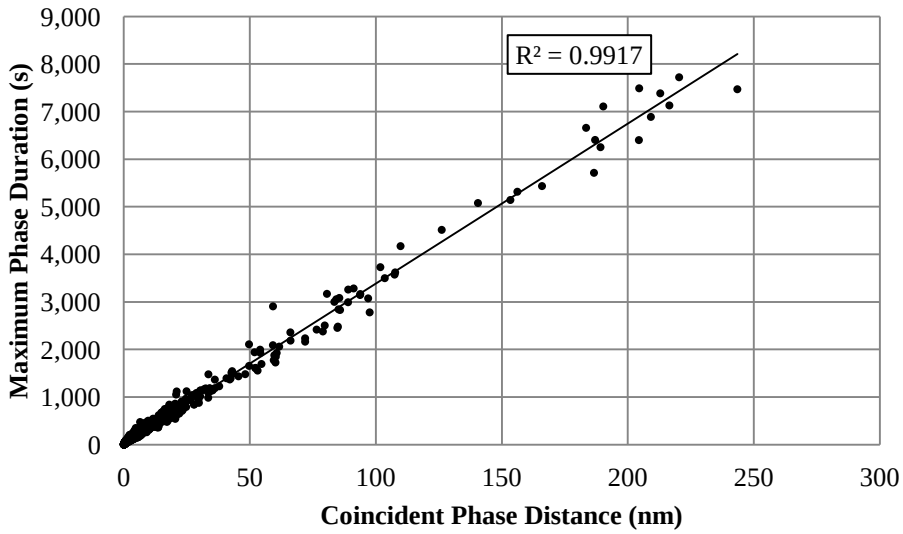

Figure 80. Maximum Phase Duration and Coincident Phase Distance of the Cruise Phase

e. Descent Phase Usage Statistics

Table 27 shows that descent phases had an average duration of 0.717 minutes and a maximum duration of 8 minutes. Descents have statistics similar to climb phases in both duration and distance, which is not surprising given that a descent might be considered to be the inverse of a climb phase; rather than a positive rate of climb, descents have a negative rate of climb.

Table 27. Usage Statistics of the Descent Phase

Phase	Average Duration (s)	Max Duration (s)	Average Distance (nm)	Max Distance (nm)	Max Altitude (ft)	Max KIAS (knots)
Descent	43.66	481.75	0.47	7.56	10012.80	114.01

As stated when discussing the climb phases, there were a handful of instances when the helicopter transitioned from a climb phase to a descent, and at that transition point it had zero forward velocity.

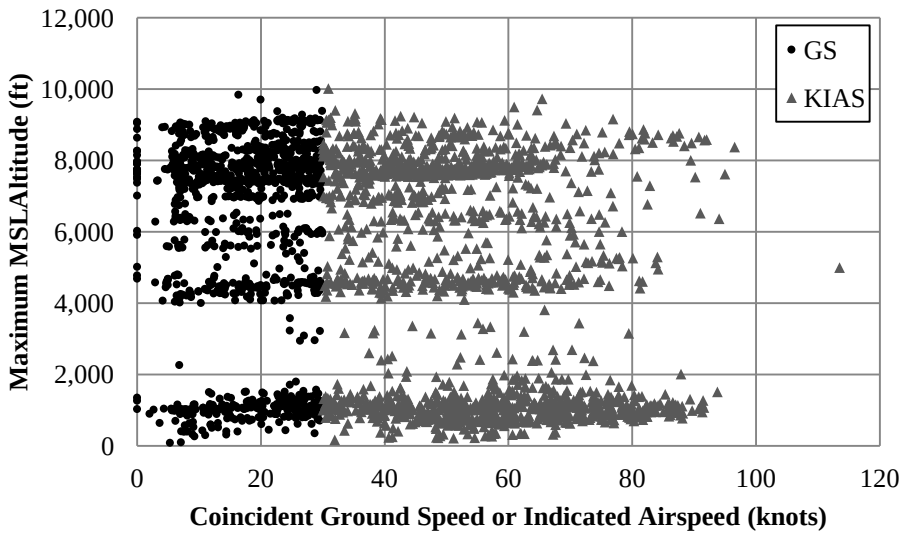

Figure 81. Maximum MSL Altitude and Coincident Ground Speed and Indicated Airspeed of the Descent Phase

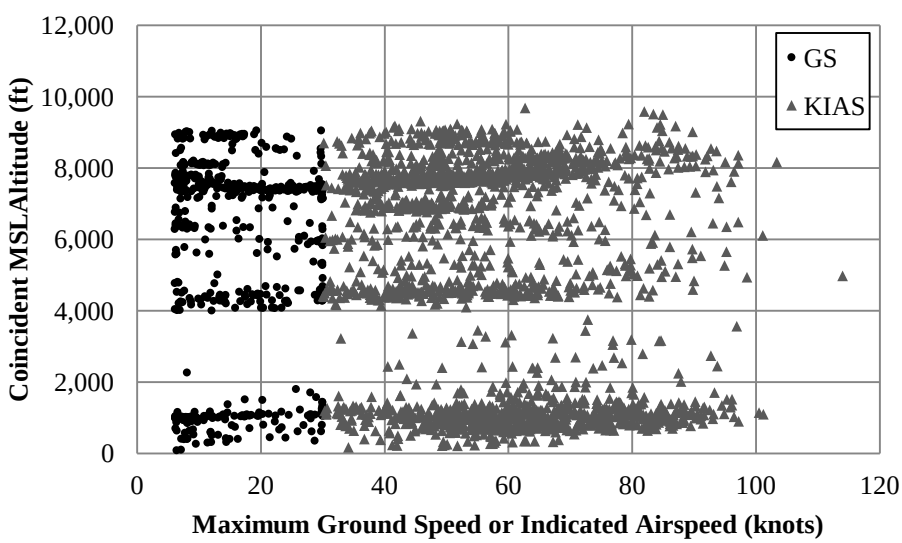

Figure 82. Maximum Ground Speed or Indicated Airspeed and Coincident MSL Altitude of the Descent Phase

For the vast majority of descent phases, the maximum altitude occurred within the first 0.5 nm. This was expected with the basic nature of the descent phase itself. The points of interest, however, were the instances in which maximum altitude was attainted at phase distances greater than 1 nm. This would suggest that the helicopter had begun its descent, but was required to increase its altitude, though not in a manner to cause the program to mark the beginning of a climb phase. There was no particular altitude band during which these commonly occurred, as there were a similar number of instances at 1,000 ft, 5,500 ft, and 8,000 ft.

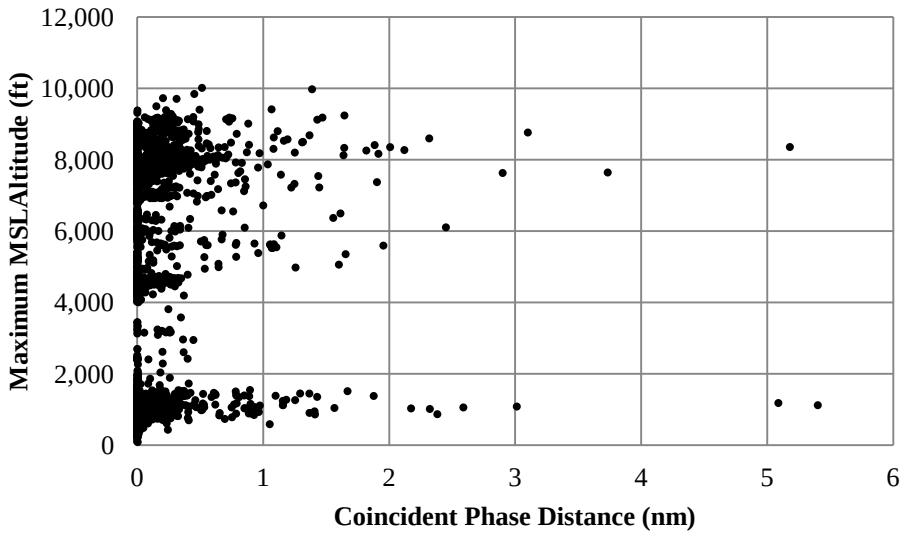

Figure 83. Maximum MSL Altitude and Coincident Phase Distance of the Descent Phase

The correlation between phase duration and phase distance for descents was less than that of climbs. At a coincident phase distance of 1 nm, there was upwards of a 50 second variation in maximum phase duration. This variation was common for distances of 0.25 nm to 1 nm. Figure 84 also shows that the majority of descent phases were less than 100 seconds in duration and 1.5 nm in distance.

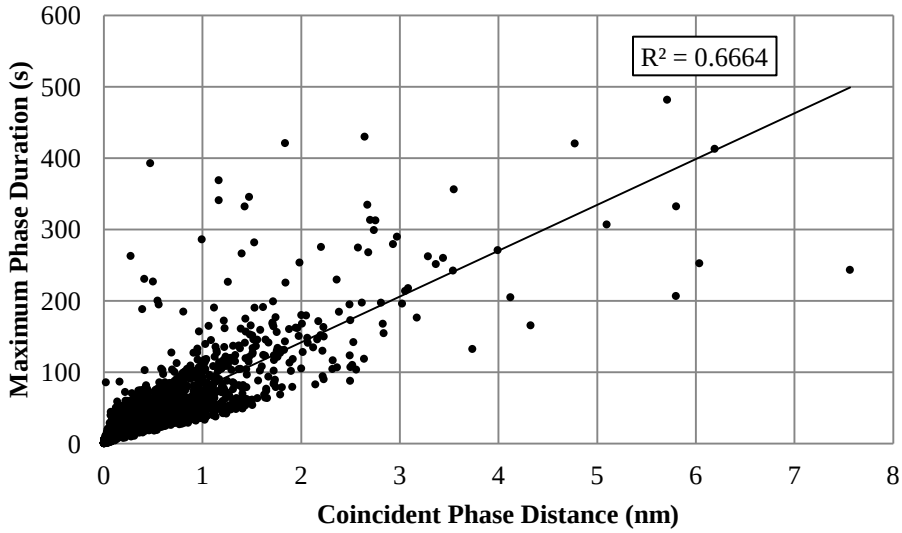

Figure 84. Maximum Phase Duration and Coincident Phase Distance of the Descent Phase

f. Start of Landing Phase Usage Statistics

One might consider a start of landing to be similar to a start of flight phase, since they are both transitory phases. However, viewing the average duration of start of landing in Table 28, it was 2.88 times longer than the start of flight, with the maximum duration being 2.35 times longer. Despite the longer durations, the distances covered during a start of landing were similar to a start of flight, the average being the same and the maximum is 0.02 nm longer. When a helicopter is in the start of landing phase, it is transitioning from a descent phase into a stationary phase; in essence, the helicopter is landing. While the distances covered are not great, there would be an increase in time given that the operator must ensure a proper lining up of the helicopter for a safe touch-down on its designated landing zone. These precautionary measures caused an increase in duration of the start of landing phase.

Table 28. Usage Statistics of the Start of Landing Phase

Phase	Average Duration (s)	Max Duration (s)	Average Distance (nm)	Max Distance (nm)	Max Altitude (ft)	Max GS (knots)
Start of Landing	48.99	468.75	0.0102	0.06	8517.37	10.40

For the most part, the maximum MSL altitude during a start of landing occurred at the point at which the helicopter transitioned from a descent phase to the start of landing. This is shown in Figure 85 by the grouping of maximum MSL markers which occurred at or just below 5 knots. Comparing Figure 85 and Figure 86, it can be

noticed that the vast majority of maximum ground speeds greater than 6 knots occurred at the same airspeeds and altitudes as their counterparts for maximum MSL altitude.

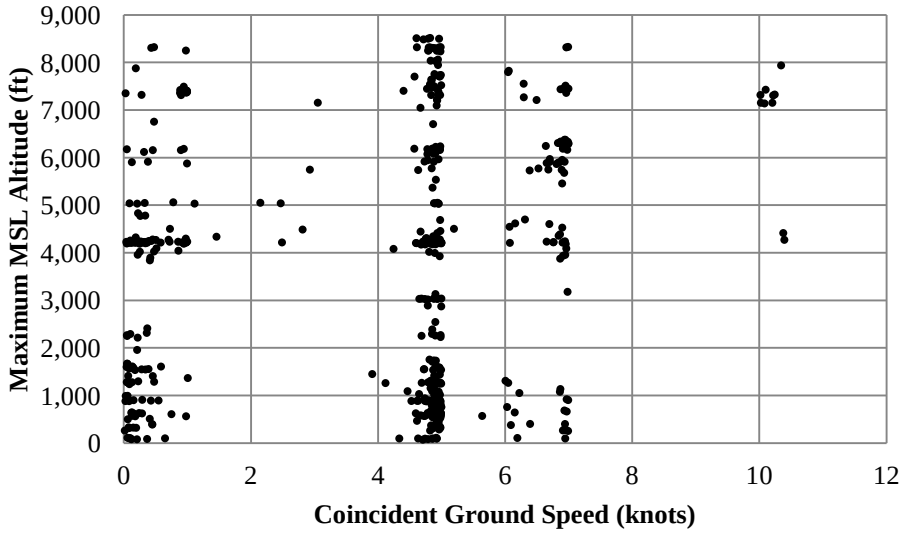

Figure 85. Maximum MSL Altitude and Coincident Ground Speed of the Start of Landing Phase

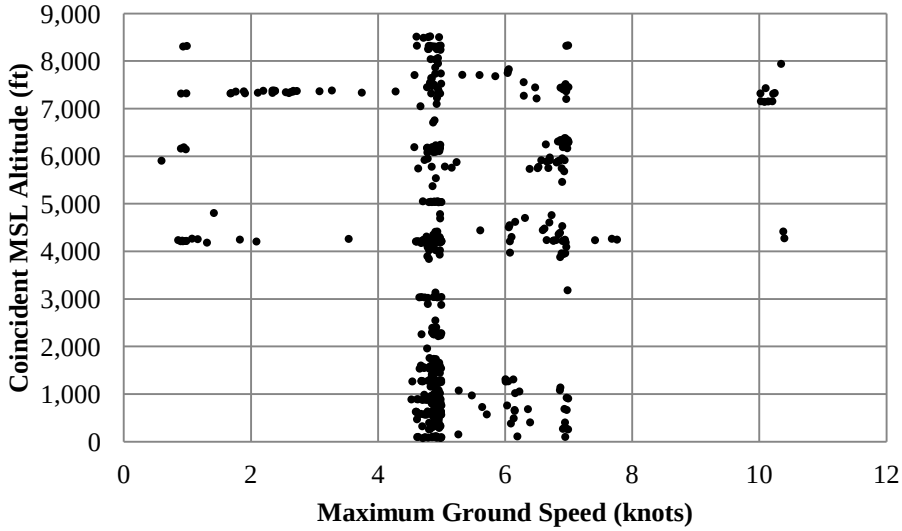

Figure 86. Maximum Ground Speed and Coincident MSL Altitude of the Start of Landing Phase

As previously stated, for the majority of start of landings the maximum MSL altitude comes at the point in which the helicopter transitions into the phase, and this is further substantiated by Figure 87. Taken at 0.01 nm, the majority of maximum MSL altitudes occurred within the first 60 feet (0.01 nm) of the phase, which is less than 1.5 helicopter lengths.

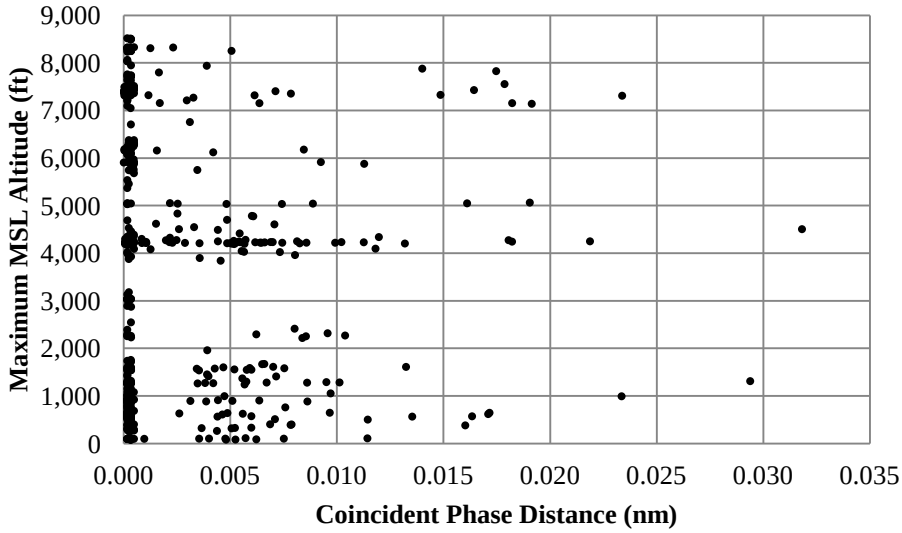

Figure 87. Maximum MSL Altitude and Coincident Phase Distance of the Start of Landing Phase

Figure 88 shows there was little correlation in phase duration and phase distance. This shows that the individual conditions of the landing position dominated the length of time and the distance covered during the landing operation.

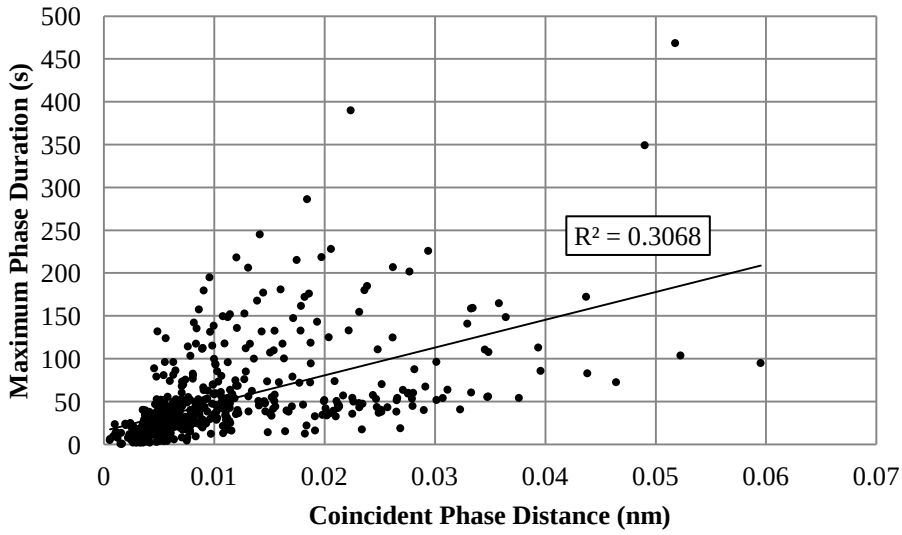

Figure 88. Maximum Phase Duration and Coincident Phase Distance of the Start of Landing Phase

g. Hover Phase Usage Statistics

Hover phases displayed many of the same statistical characteristics as stationary phases, in terms of the usage data, as presented in Table 29. This was expected since hovers were stationary phases which had been reclassified

based on accelerometer data. However, some differences were present, mostly due to the fact that the helicopter moved while in hover.

Table 29. Usage Statistics of the Hover Phase

Phase	Average Duration (s)	Max Duration (s)	Average Distance (nm)	Max Distance (nm)	Max Altitude (ft)	Max GS (knots)
Hover	101.11	1074.13	0.02	0.11	9153.98	10.85

Maximum MSL altitude during hover phases occurred across an array of ground speeds, with groupings at about 0, 5, 6, and 10 knots. The cases with ground speeds greater than 5 knots were due to program separation logic. In these cases, the helicopter accelerated and increasing climbed, but the variations in the data did not cross the predefined thresholds that would initiate the program to transition to a new phase. This is also shown in the groupings displayed in Figure 90.

Figure 91 shows that maximum MSL altitude occurred across an array of distances into a hover. At some instances, maximum altitude during hover occurred at the point of transition into hover, as would be the case for those maximum altitudes at zero coincident distance; and some occurred as the helicopter was climbing out of hover. This indicated that, while sharing a similar pattern, hover phases had a large variance in altitude profiles.

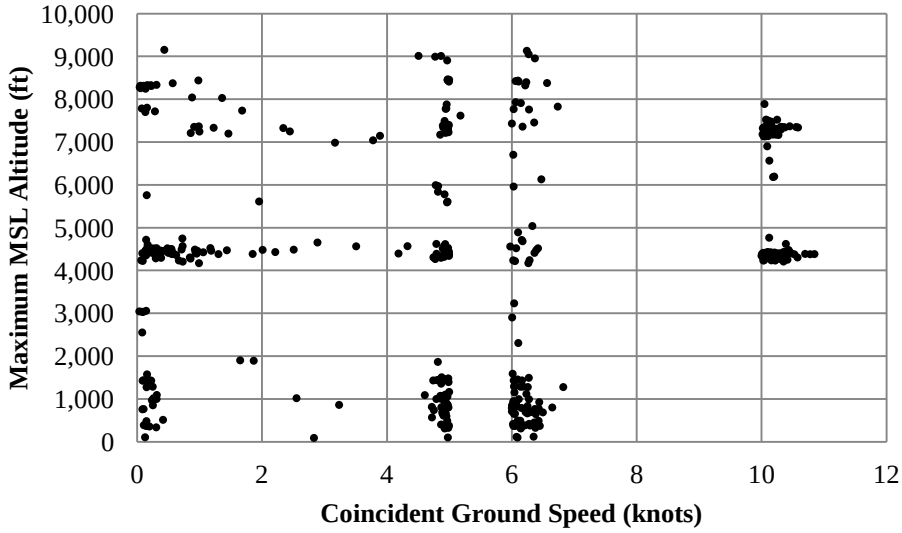

Figure 89. Maximum MSL Altitude and Coincident Ground Speed of the Hover Phase

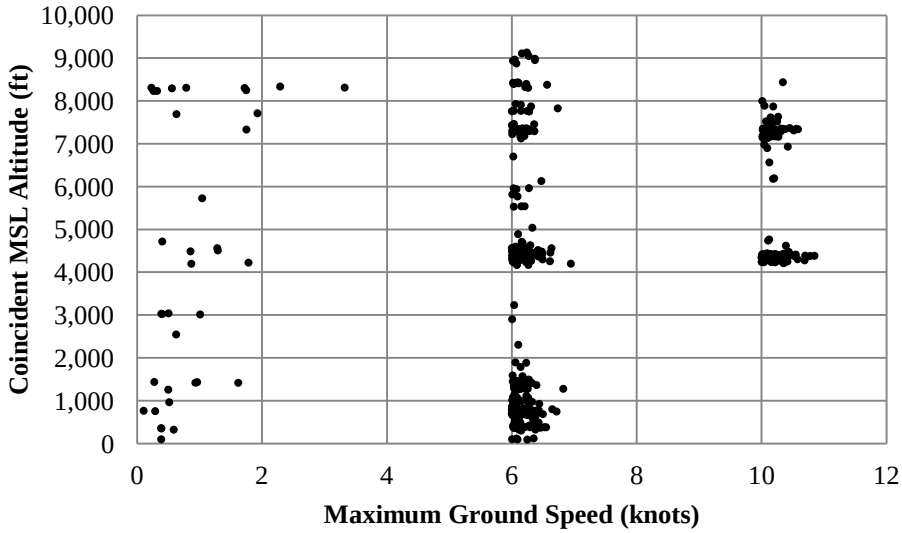

Figure 90. Maximum Ground Speed and Coincident MSL Altitude of the Hover Phase

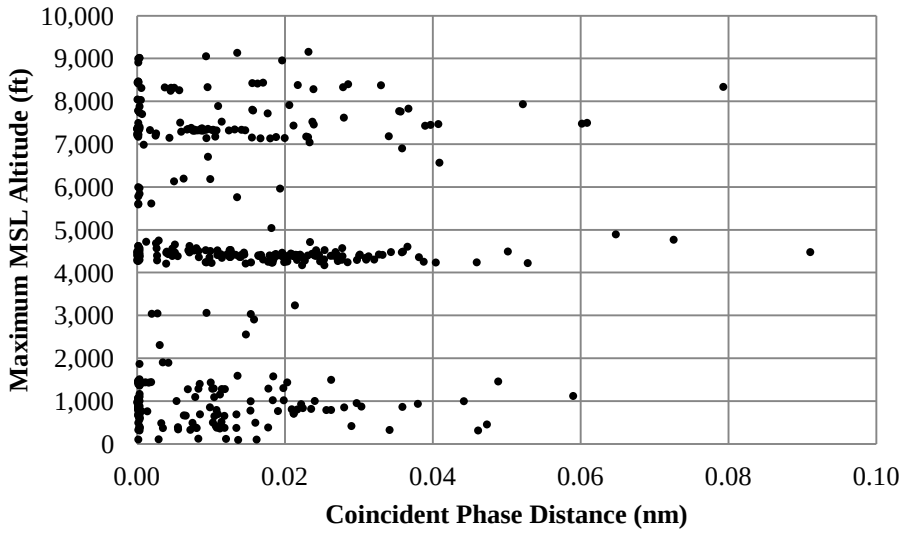

Figure 91. Maximum MSL Altitude and Coincident Phase Distance of the Hover Phase

Along with variation in altitude profiles, there was also little correlation in phase duration and distance, as shown in Figure 92. While a number of hovers had little variation from one another, as indicated by the tight grouping at less than 100 seconds and less than 0.03 nm, a large number with high variation showed many hover phases had unique profiles.

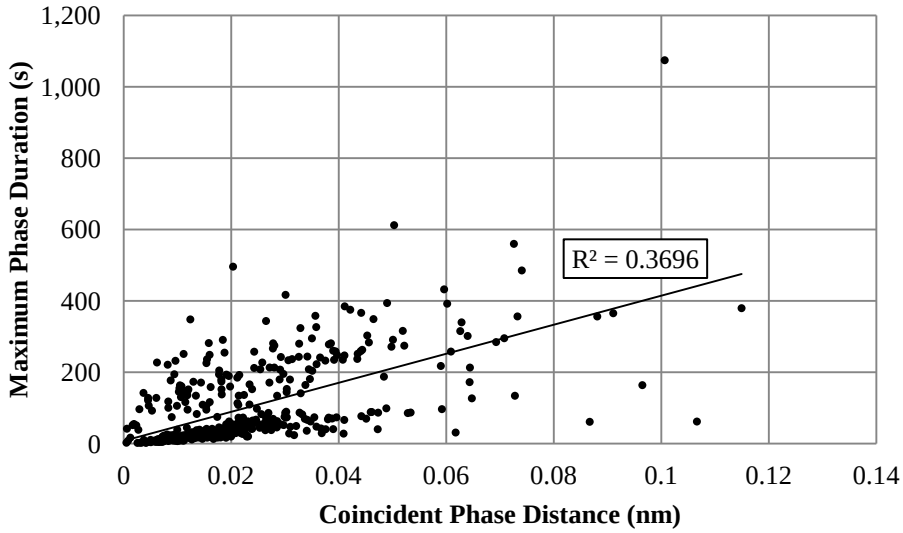

Figure 92. Maximum Phase Duration and Coincident Phase Distance of the Hover Phase

h. Bucket Fill Phase Usage Statistics

Bucket fill phases are one of two phase types unique to bucket missions, and share many characteristic similarities to hovers. The distinguishing factor of the bucket fills is the filling of a bucket at a source of water. In fact, this is the singular purpose of the phase. As seen in Table 30, the average duration of a bucket fill was 0.32 minutes, indicating that the time to fill the bucket was fairly brief.

Table 30. Usage Statistics of the Bucket Fill Phase

Phase	Average Duration (s)	Max Duration (s)	Average Distance (nm)	Max Distance (nm)	Max Altitude (ft)	Max KIAS (knots)
Bucket Fill	19.20	298.25	0.01377	0.16	9076.55	30.85

For the majority of bucket fills, the maximum MSL altitude occurred at the transition point either going into or coming out of the fill phase. The helicopter would descend to fill the bucket and then ascend to transport the water to the fire. There were four points in Figure 93, and seven in Figure 94 for which the helicopter accelerated and climbed past the airspeed threshold to prevent the phase separation program to mark the end of the bucket fill phase.

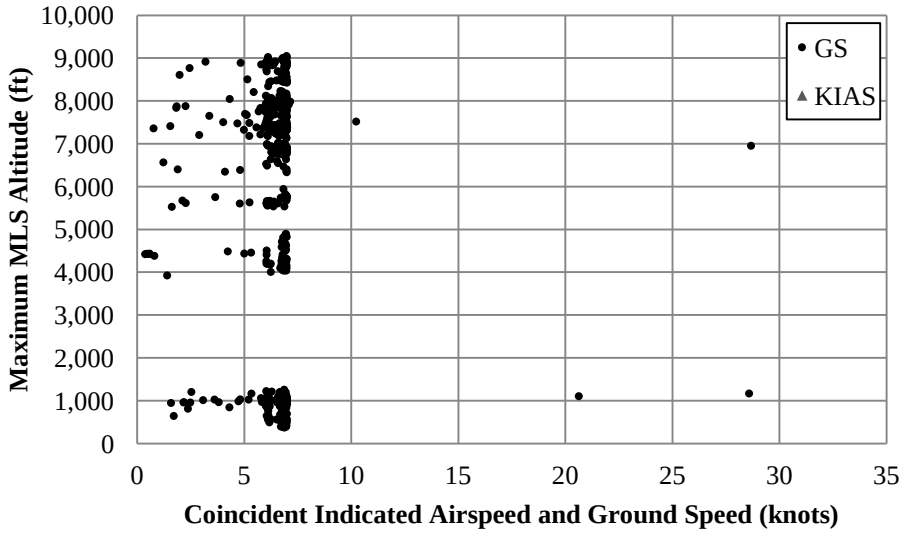

Figure 93. Maximum MSL Altitude and Coincident Ground Speed or Indicated Airspeed of the Bucket Fill Phase

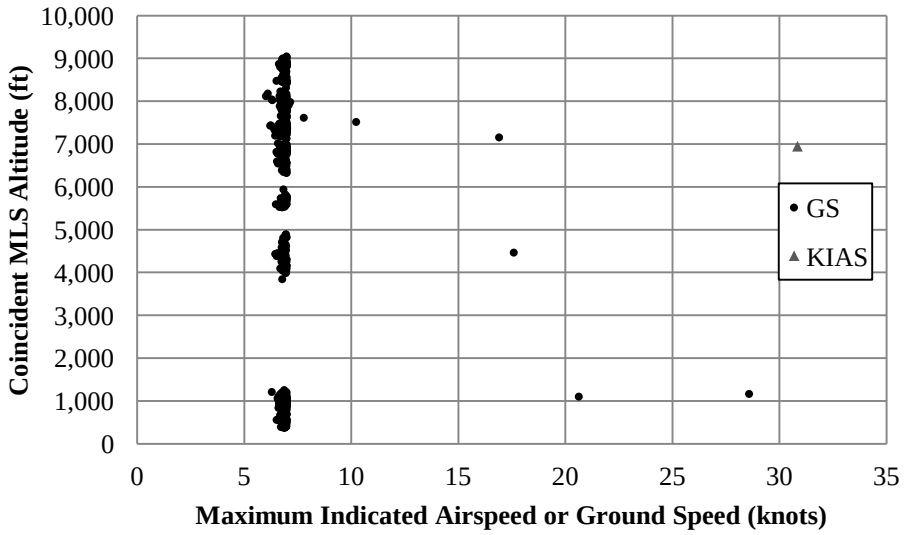

Figure 94. Maximum Ground Speed or Indicated Airspeed and Coincident MSL Altitude of the Bucket Fill Phase

With an average phase distance of 0.16 nm, Figure 95 indicates that maximum MSL altitude occurred at the beginning of the bucket fill phase in all but two instances.

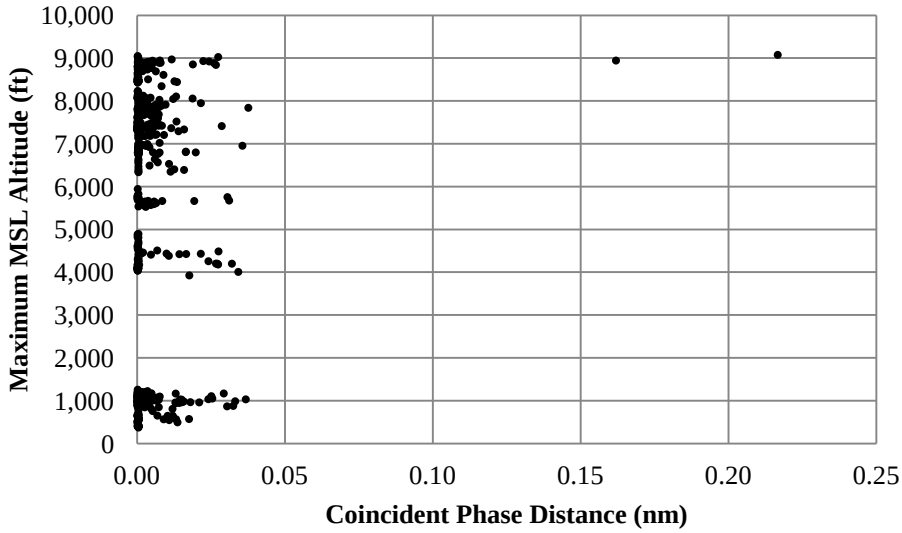

Figure 95. Maximum MSL Altitude and Coincident Phase Distance of the Bucket Fill Phase

The vast majority of bucket fills had good correlation between duration and distance. The instances that deviated from this were most likely due to situations in which the helicopter was required to spend longer than usual time over the body of water, though the exact cause of the increased fill time cannot be known from the flight data used in this study.

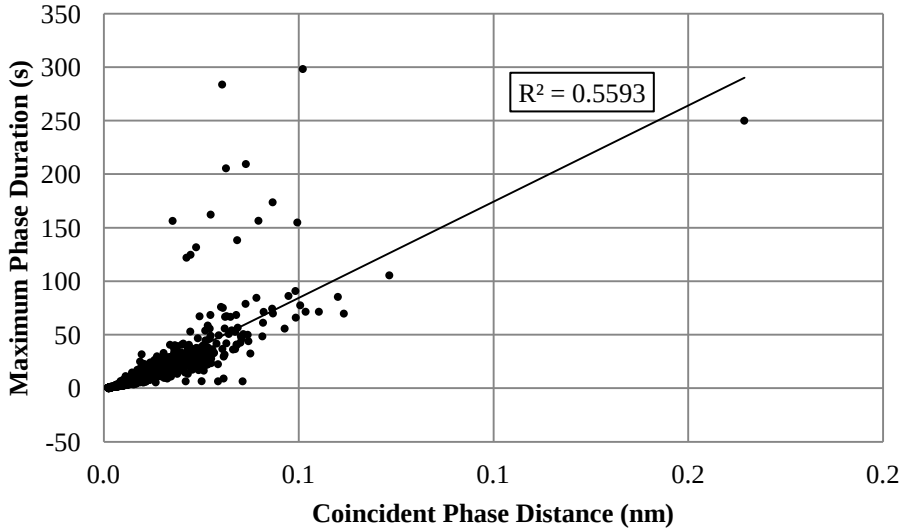

Figure 96. Maximum Phase Duration and Coincident Phase Distance of the Bucket Fill Phase

i. Bucket Drop Phase Usage Statistics

As shown in Table 31. Usage Statistics, bucket drops had an average duration of 7 seconds and maximum duration of 12.5 seconds, the lowest duration of all phase types. Given that it is the goal of the bucket drop to release the water as efficiently over a fire zone as possible, taking into account the type of vegetation, to help ensure extinguishing of the fire; the quickness was expected.

Table 31. Usage Statistics of the Bucket Drop Phase

Phase	Average Duration (s)	Max Duration (s)	Average Distance (nm)	Max Distance (nm)	Max Altitude (ft)	Max KIAS (knots)
Bucket Drop	7.13	12.50	0.03	0.28	9163.57	81.63

Figure 97 and Figure 98 show a wide array of airspeeds were attained during a bucket drop phase. The variation in airspeed could be attributed to the desired effect of the drop, that is, to efficiently cover a fire zone of some length or vegetation type with the contents of the bucket. It could be assumed that if there was a large fire zone, given the limited volume of water available, that the operator would be required to have a high airspeed to cover a longer. The inverse could be said about a small fire zone, requiring low airspeed to drop the contents of the bucket over the area efficiently, wasting as little water as possible on non-burning areas. Also, if the fire zone is made up of sparse vegetation, the drop would occur at higher airspeeds to increase area covered; as opposed to thick canopy, where water would be released at slow airspeeds or hovers to maximize penetration.

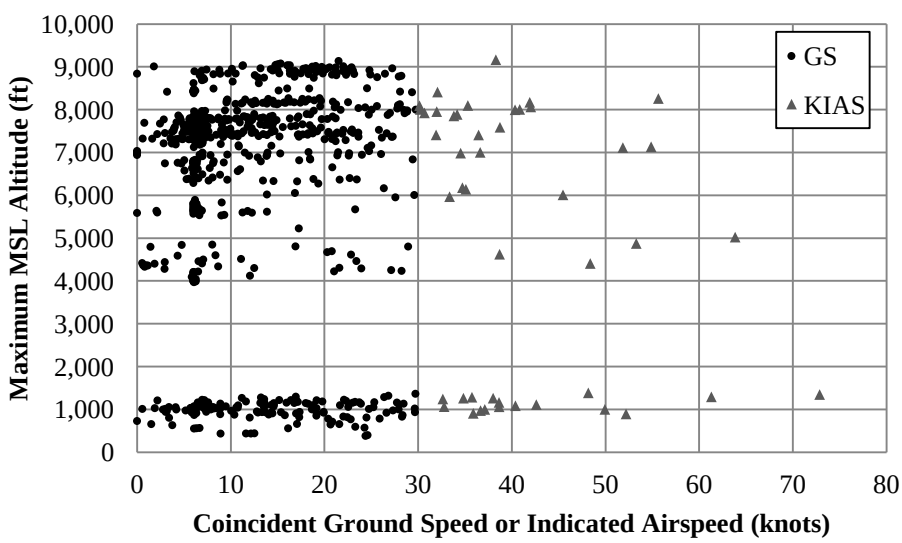

Figure 97. Maximum MSL Altitude and Coincident Ground Speed or Indicated Airspeed of the Bucket Drop Phase

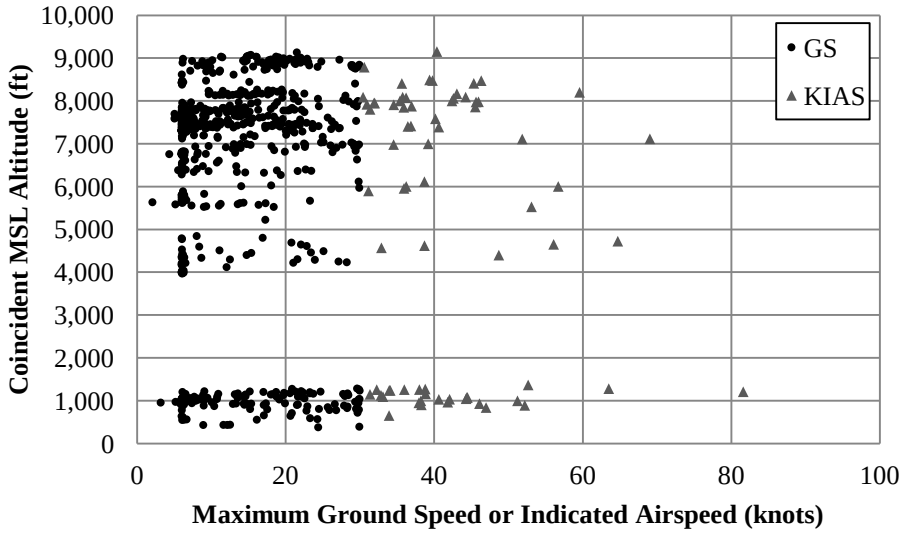

Figure 98. Maximum Ground Speed or Indicated Airspeed and Coincident MSL Altitude of the Bucket Drop Phase

Like many other phases, the maximum MSL altitude of the bucket drop occurs at the point at which the helicopter transitions into the bucket drop phase, as evident in Figure 99. While a majority of maximum MSL occurred at the initial point, there were a number of instances for which maximum altitude occurred at later points into the phase. This could have been caused by a number of factors, including dropping water on a hillside, requiring the helicopter to climb during the drop.

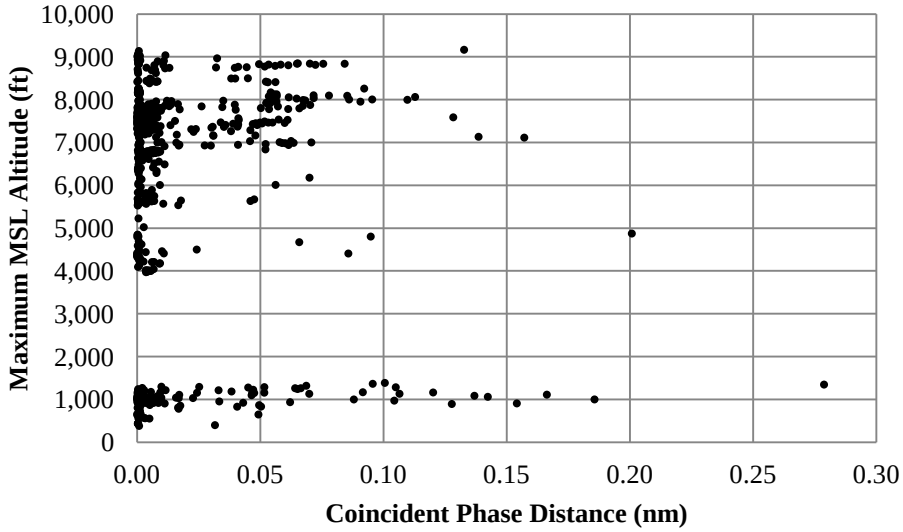

Figure 99. Maximum MSL Altitude and Coincident Phase Distance of the Bucket Drop Phase

In Figure 100 it is obvious that there was an absolute maximum duration for a number of flights across an array of phase distances. This was due to the programming logic used to determine the end of the bucket drop phase.

Certain parameters were searched for to determine when the phases began and ended within a certain time frame. If those parameters were not found, the end of the time frame was used as the end of the drop phase. There were two time frames used, and initial 6.25 seconds prior to the lowest airspeed and 6.25 seconds afterwards, totaling 12.5 seconds. It is for this reason that there were no drops exceeding 12.5 seconds in duration. If the lowest airspeed during the drop was very close to the threshold velocity for determining the beginning point of the phase, the time between the initial entrance into the phase and the lowest airspeed point would be zero. Furthermore, if the acceleration afterwards was low enough, the threshold to mark the end of the phase might was not crossed, resulting in the program using the maximum time of 6.25 seconds for the second half. With an initial time into the drop of zero seconds and a time out of drop of 6.25, the total time would be 6.25 seconds, thus resulting in the second line at the 6.25 second mark. As a result of this program logic restriction, the maximum duration of 6.25 and 12.5 seconds are not accurate.

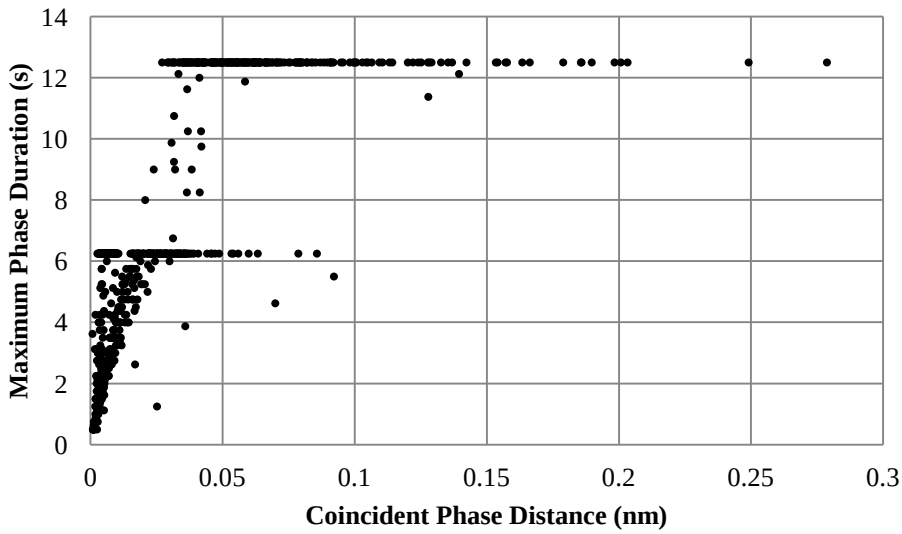

Figure 100. Maximum Phase Duration and Coincident Phase Distance of the Bucket Drop Phase

j. Helitorch Burn Phase Usage Statistics

The burn phase was unique to the helitorch mission type, during which the burning of a predefined target area occurred over an average time of 5.5 minutes, up to 10 minutes per burn. Because of the variation in target burn lengths, distances covered in the phase varied from 0.25 nm to the maximum distance of 3.63 nm displayed in Table 32.

Table 32. Usage Statistics of the Helitorch Burn Phase

Phase	Average Duration (s)	Max Duration (s)	Average Distance (nm)	Max Distance (nm)	Max Altitude (ft)	Max KIAS (knots)
Helitorch Burn	329.84	598.13	1.27	3.63	8482.89	46.40

Figure 101 shows that there were two primary maximum MSL altitude bands that helitorch burns were performed in, 7,500 ft and 8,400 ft. This would suggest that there were two areas in which target locations designated for burning were located.

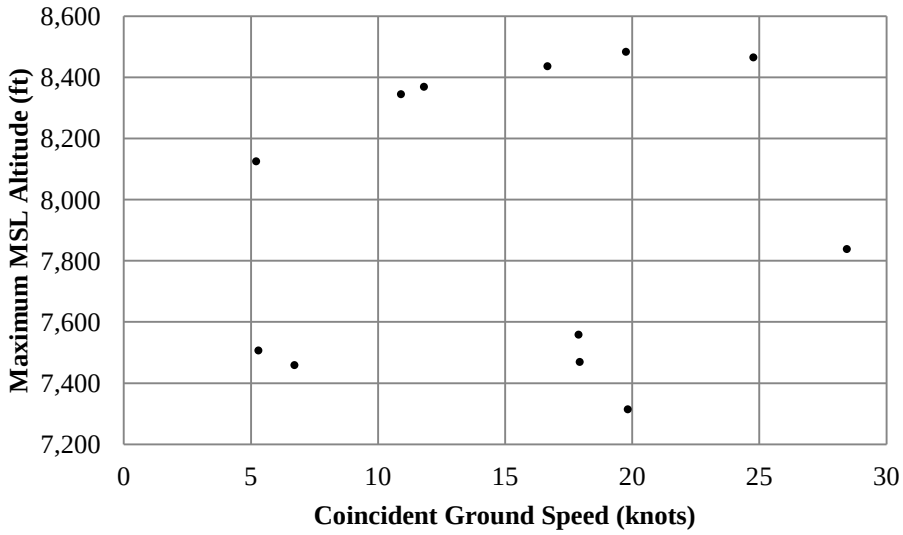

Figure 101. Maximum MSL Altitude and Coincident Ground Speed of the Helitorch Burn Phase

From Figure 102, approximately 75% of maximum airspeed was around 20 knots, with only four instances occurring outside this grouping. This would suggest that during most helitorch burn phases the operator remained within an imposed airspeed limit, only exceeding this for special circumstances.

It can be seen from Figure 103 that there was no particular point throughout all helitorch burns when maximum MSL altitude occurred. Given the variation in overall distances, there was no correlation between maximum MSL altitude and coincident distance into phase.

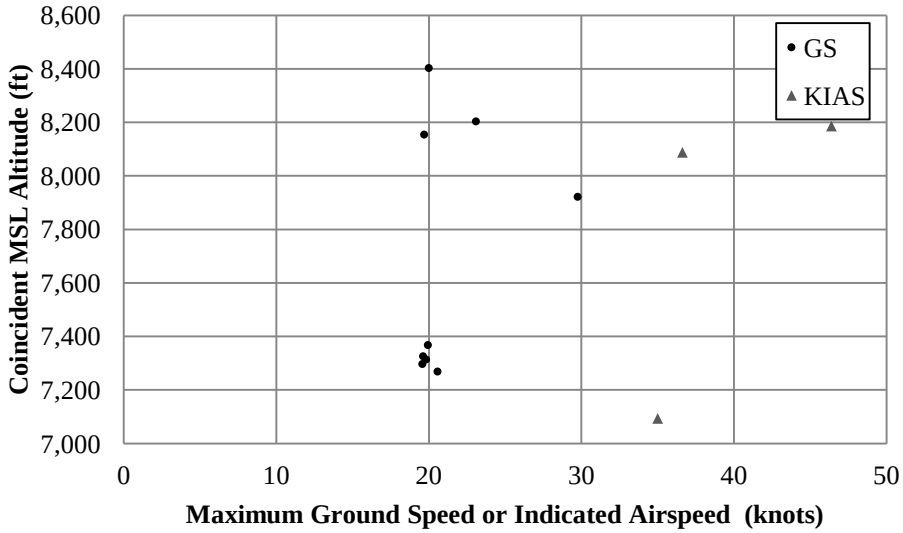

Figure 102. Maximum Ground Speed or Indicated Airspeed and Coincident MSL Altitude of the Helitorch Burn Phase

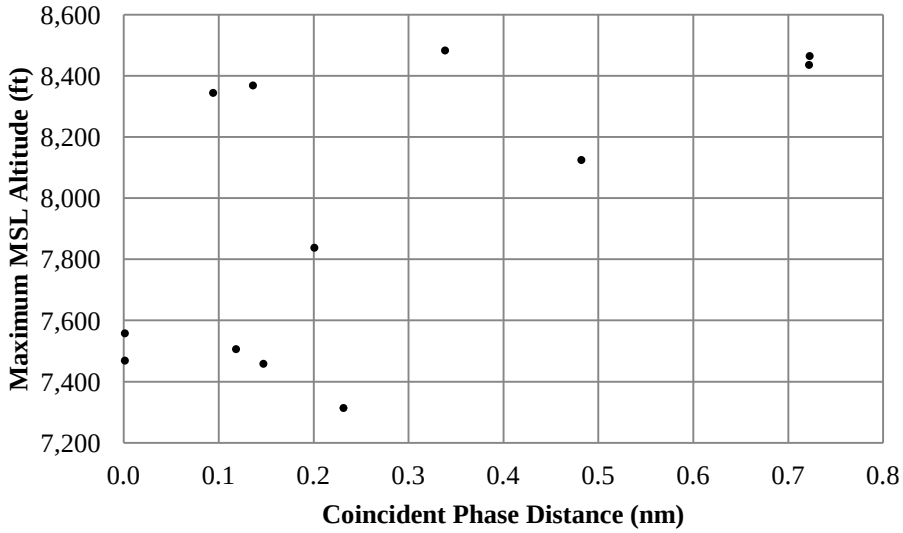

Figure 103. Maximum MSL Altitude and Coincident Phase Distance of the Helitorch Burn Phase

Figure 104 shows good correlation between phase duration and phase distance. Within the overall distance spread, there were three groupings that appeared; at 0.25 nm, just over 1 nm, and just less than 2 nm; with two individual cases at 0.5 nm and 3.7 nm. This suggested the duration spent in a helitorch burn phase was consistent with the length or vegetation type of the target burn area.

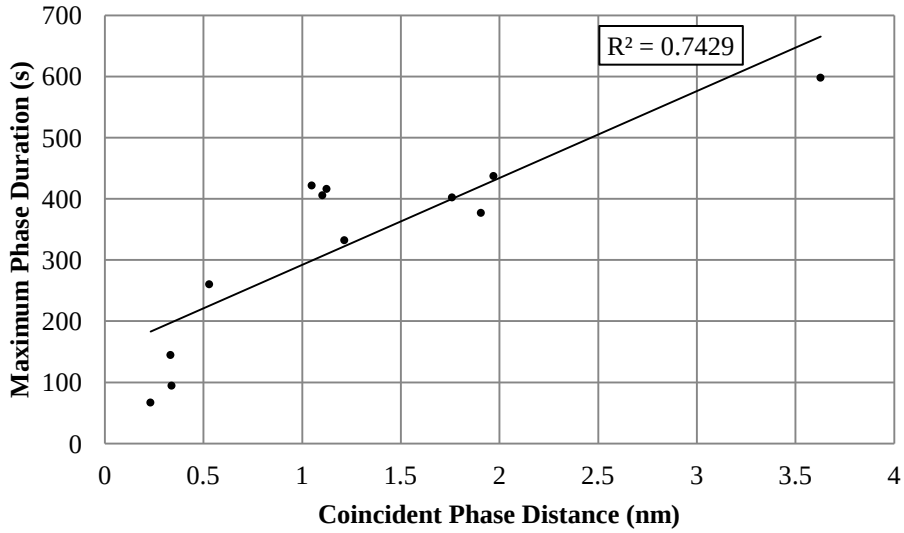

Figure 104. Maximum Phase Duration and Coincident Phase Distance of the Helitorch Burn Phase

D. Flight Loads

Along with determining general and mission usage statistics, it was also important to determine the magnitude, frequency, and classification of vertical loads experienced by the helicopter over the course of a mission. In the following sections, the general results of overall vertical flight loads, along with the results per mission, are presented, compared to previous studies, and discussed. Furthermore, statistics via classification are given to allow more detailed analysis into the vertical loads experienced by the helicopter.

1. General Usage Results and Comparisons

A primary goal of this study was to examine the difference between flight loads experienced by firefighting aircraft and their civilian or military counterparts. Figure 105 clearly shows that the firefighting 205A-1 experienced a greater quantity of flight loads than the UH-1H (the reader is reminded that the UH-1H is the military version of the 205A-1). At an incremental load factor of 0.3 g the 205A-1 experienced 93 times more loads per 1000 hrs than the UH-1H; at 0.6 g, this increases to 1,200 times more loads per 1000 hrs. It can also be seen that the 205A-1 experienced higher magnitudes of loads. The UH-1H never experienced an incremental load factor above +0.7 g [6], while the 205A-1 data contained recorded incremental load factors as high as +3.0 g. The reader, however, is cautioned on two caveats. First, the accelerometers were not placed at the c.g., which subjected the data to vibrations inherent in the helicopter, which may have artificially increased the magnitude of the vertical loads being experienced.

Secondly, the load separation criteria used is an un-scrutinized new method which differs from standard techniques, and should be met with some skepticism.

When the vertical flight loads were broken down by; it can be seen in Table 33 that the average positive incremental loads experienced were relatively the same for all missions, with ferry having a slightly lower average and recon having a slightly higher average. This trend was also present in negative loads with the difference between the highest and lowest averages being only 0.03 g. Since the averages were similar across all missions, it suggested that the loads experienced were independent of the mission being flown. The disparity between loads experienced during missions did increase when viewing the maximum and minimum loads, however these are more representative of extreme individual instances. There was no correlation between maximum loads experienced and the presence of external cargo. The highest load was associated during a passenger mission, followed by helitorch, then rappel. This indicates that the maximum and minimum loads were due to instantaneous flight characteristics rather than the mission being performed as a whole.

When the flight loads were broken down into the phases during which they occurred, as shown in Table 34, the descent phases had the largest values across all four categories. It is curious to note that stationary phases had an elevated average positive incremental flight load, as displayed in Table 34. This is most likely due to an initial loading experienced when the helicopter first launches.

Table 33. Mission Average, Maximum, and Minimum Incremental Load Factor

Mission	Average $+\Delta n_z$ (g)	Average $-\Delta n_z$ (g)	Max $+\Delta n_z$ (g)	Min $-\Delta n_z$ (g)
Bucket	0.65	-0.40	2.46	-1.19
Ferry	0.58	-0.37	2.21	-1.04
Passenger	0.65	-0.39	2.99	-1.12
Recon	0.69	-0.41	2.41	-1.11
Helitorch	0.66	-0.41	2.76	-0.79
Longline	0.65	-0.39	2.03	-0.94
Rappel	0.65	-0.38	2.49	-0.93

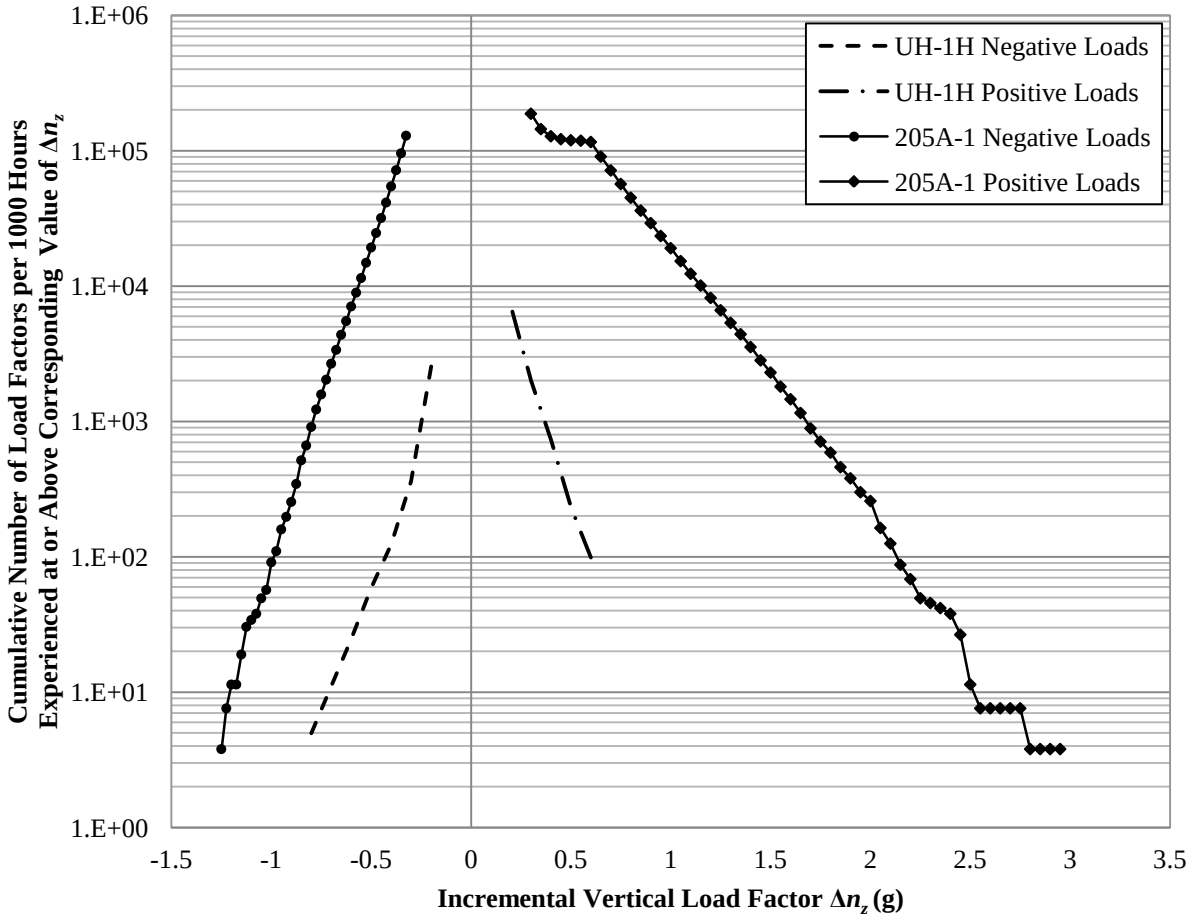

Figure 105. Model 205A-1 and UH-1H Cumulative Load Factor Comparison

Table 34. Phase Average, Maximum, Minimum Incremental Load Factor

Phase	Average $+\Delta n_z$ (g)	Average $-\Delta n_z$ (g)	Max $+\Delta n_z$ (g)	Min $-\Delta n_z$ (g)
Stationary	0.62	-0.35	1.31	-0.56
Start of Flight	0.56	-0.36	1.43	-0.56
Climb	0.62	-0.40	1.90	-0.98
Cruise	0.63	-0.38	2.49	-1.13
Descent	0.68	-0.40	2.99	-1.22
Start of Landing	0.53	-0.36	1.32	-0.61
Hover	0.60	-0.37	1.41	-0.70
Fill	0.42	-0.37	1.97	-0.71
Drop	0.56	-0.40	2.11	-0.86
Burn	0.60	-0.35	1.07	-0.58

2. Gust, Maneuver, and Change of State Induced Loads

While knowing the magnitude of a flight load experienced is useful, it does not provide insight into the circumstances during which the load occurred. It was therefore necessary to classify the loads to provide this insight. As previously discussed the flight loads were classified using a new method based on roll and pitch rates. The flight loads were separated into three categories: gust, maneuver, and change of state. For both positive and negative incremental flight loads, maneuvers made up the majority of occurrences, as can be seen in Figure 106. Gust, Maneuver, and Change of State Load Cumulative Load Factor Comparison and Table 35, making up nearly 76% of total occurrences. Gusts, however, made up less than 4% of occurrences and had the smallest averages for both positive and negative loads. When these results were compared to previous studies examining the impact of gusts on the flights of helicopters, it was found that these results matched those expected, in that the loads due to gusts were "of much lesser magnitude and frequency than maneuver loads." [7]

It can be seen in Figure 106 that, even for maneuvers, the negative incremental vertical load factor never exceeded -1.5 g. This is due to mechanical intolerances of the helicopter rotor system to large negative loads. If a helicopter were to experience a load less than -1 g n_z (-2 g Δn_z), it was reported that mechanical linkages could buckle, therefore negative loads were avoided by operators in flight.

By classical definition, a maneuver induced load is any load caused by the actions of the operator, and thus change of state induced loads would be classified as maneuvers. For purposes of classification, maneuvers and changes of state were treated separately, but for discussion of the results it is preferable to view them together. As can be seen in Table 35, combined maneuvers and change of state induced loads accounted for 96% of loads experienced. While the average incremental intensity of combined maneuvers and change of state induced loads are less than that of maneuvers alone, it can be seen in both Table 35 and Figure 106, that maneuvers dominated the intensity and cumulative number of loads per 1000 hours.

Table 35. N_z Disturbance Comparisons

Disturbance Classification	Percent of Total Occurrences	Average $+\Delta n_z$ (g)	Average $-\Delta n_z$ (g)
Gust	3.98%	0.36	-0.33
Maneuver	75.49%	0.70	-0.40
Change of State	20.52%	0.41	-0.37
Maneuver and Change of State	96.01%	0.66	-0.39

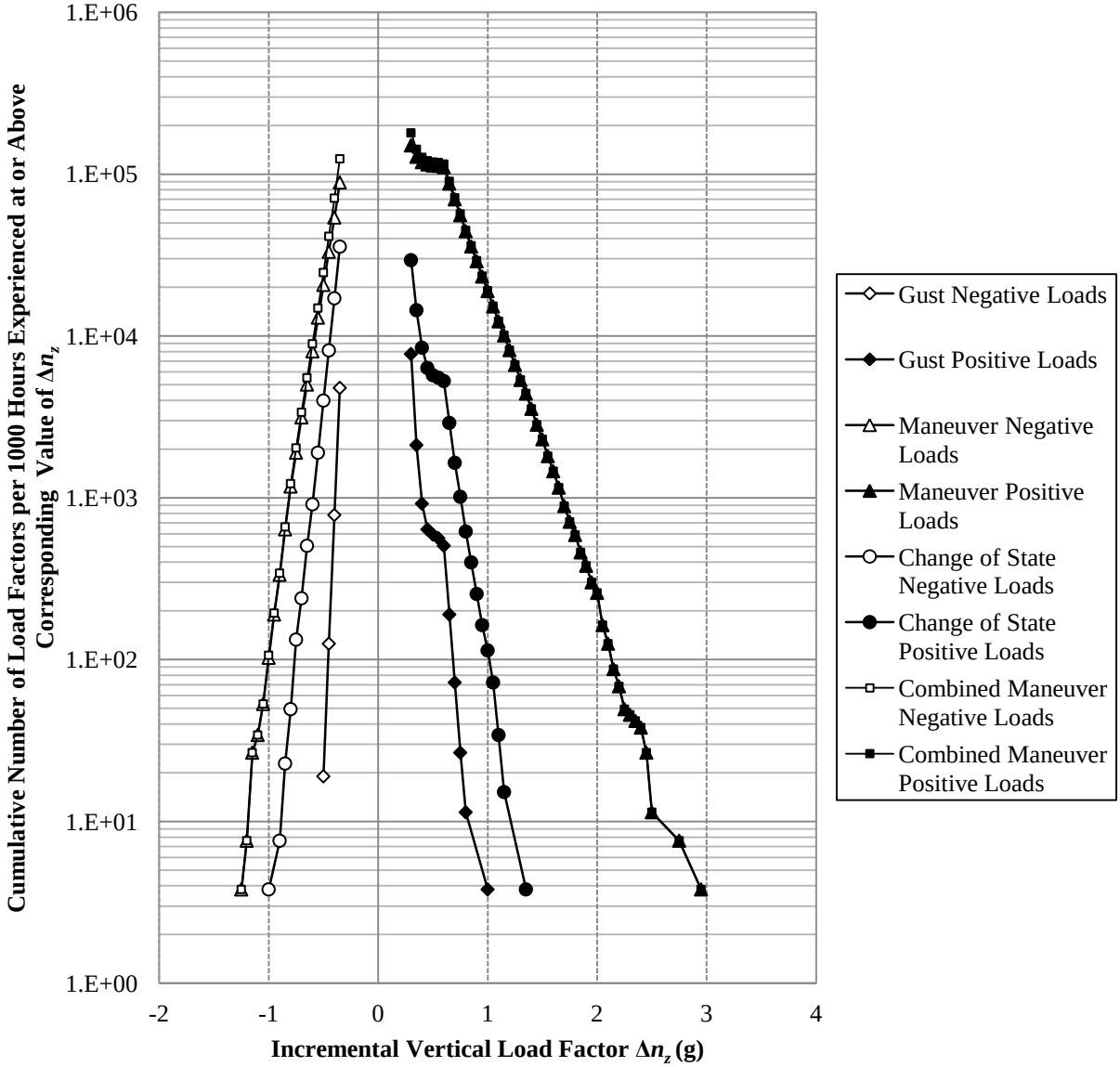

Figure 106. Gust, Maneuver, and Change of State Load Cumulative Load Factor Comparison

a. Gust Induced Vertical Flight Loads

The first thing that is noticed in Table 36 is that the average negative incremental vertical loads induced by gusts varied only by 0.008g for all missions. This indicated the uniformity of the loads caused by gusts. A similar uniformity occurred with positive incremental loads, with the difference between smallest and largest being only 0.03g. This suggested helicopter gust response was independent of the mission being performed. However, number of gusts correlated with the mission type. Bucket and helitorch missions had the largest number of average gusts,

followed by ferry and then passenger. Bucket and helitorch missions were flown in direct proximity of fire zones, exposing the helicopter to atmosphere that was more turbulent due thermal instability. With ferry and passenger, the cruise portion of the missions would occur at, presumably, higher AGL altitudes, and thus would be exposed to less turbulent air.

Table 36. Gust Induced Load Statistics by Mission Type

Mission	Average Number per Mission	Average $+\Delta n_z$ (g)	Average $-\Delta n_z$ (g)	Max $+\Delta n_z$ (g)	Min $-\Delta n_z$ (g)
Bucket	15.94	0.363	-0.334	1.013	-0.446
Ferry	13.01	0.355	-0.326	0.743	-0.491
Passenger	12.31	0.368	-0.326	0.812	-0.440
Recon	8.81	0.352	-0.328	0.728	-0.485
Helitorch	15.00	0.361	-0.329	0.756	-0.436
Longline	8.38	0.359	-0.332	0.783	-0.485
Rappel	6.55	0.344	-0.327	0.648	-0.462

Table 37 shows the breakdown of the loads by flight phase. Of note is the average positive incremental load of the stationary phase being the same as the maximum, this was due to the fact that there was only a single instance of a positive gust induced load occurring during a stationary phase.

Table 37. Gust Induced Load Statistics by Phase Type

Phase	Average Number per Phase	Average $+\Delta n_z$ (g)	Average $-\Delta n_z$ (g)	Max $+\Delta n_z$ (g)	Min $-\Delta n_z$ (g)
Stationary	0.01	0.610	-0.316	0.610	-0.328
Start of Flight	0.01	0.307	-0.338	0.318	-0.377
Climb	0.07	0.373	-0.327	0.707	-0.441
Cruise	1.92	0.351	-0.327	1.013	-0.491
Descent	0.09	0.377	-0.336	0.783	-0.485
Start of Landing	0.04	0.402	-0.329	0.675	-0.375
Hover	0.11	0.413	-0.338	0.727	-0.406
Fill	0.02	0.383	-0.346	0.809	-0.429
Drop	0.01	0.335	-0.331	0.424	-0.359
Burn	0.25	0.305	-0.328	0.305	-0.338

As can be seen in Figure 107, most gust loads occurred at airspeeds greater than 70 KIAS. Given that a larger number of gusts occurred during a cruise phase, it was expected that the majority of gust induced loads would occur at higher airspeeds due to cruise phases being longer and faster than other phases. It should be noted that there was an

absence of occurrences at approximately 0.50 g. Currently it is unknown why there was a lack of data points about this incremental load level.

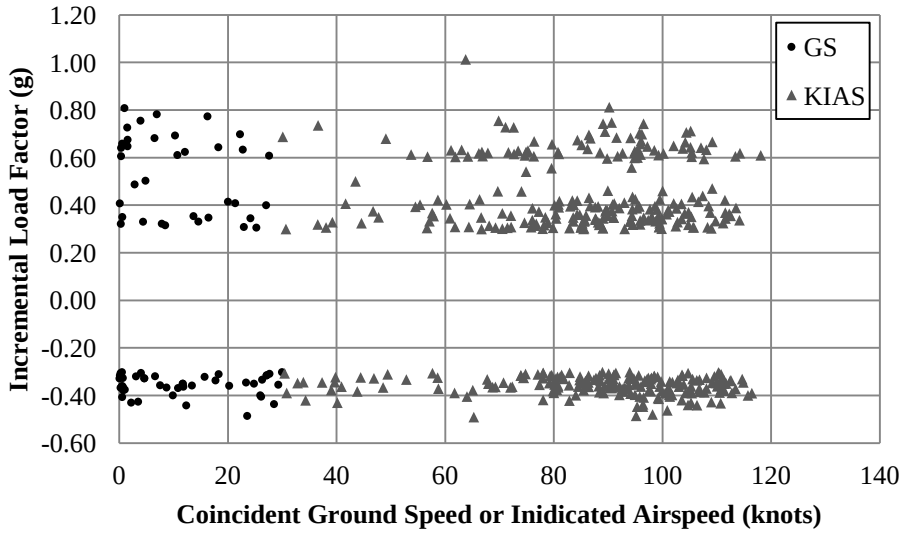

Figure 107. Maximum and Minimum Incremental Load Factors Due to Gusts and Coincident Ground Speed or Indicated Airspeed

Figure 108 shows the cumulative frequency distribution of gust induced loads by mission. As can be seen, across mission types, gust loading occurred in a similar manner, except for bucket missions at larger positive incremental loads. For positive incremental load factors greater than 0.7 g, the bucket mission experienced a higher frequency of loads than the other mission types.

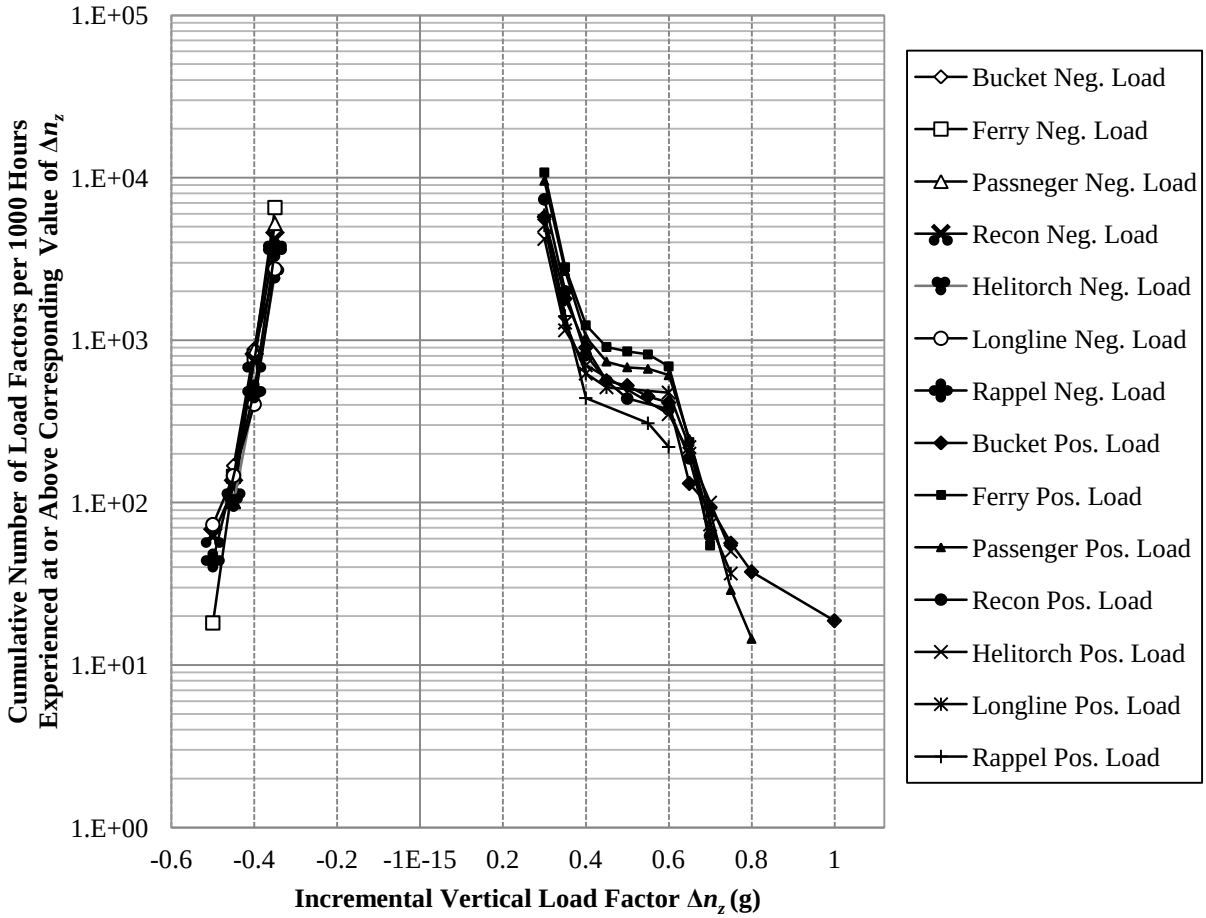

Figure 108. Gust Induced Cumulative Load Factor Comparision by Mission Type

b. Maneuver Induced Vertical Flight Loads

While not as uniform as gust induced loads, the average positive and negative incremental loads induced by maneuvers have a commonality in magnitude. Again bucket and helitorch had the highest average number of occurrences among the mission types, as shown in Table 38, followed by longline and reconnaissance. With an average number greater than 500 per mission, it would suggest that bucket and helitorch missions required more maneuvers to take place, which would be accurate considering the flight profiles of each of the missions. Bucket missions, for example, contain several low AGL phases (fill, drop, descent into drop, climb out of drop, and cruises between fills and drops) which would require increased maneuvering, thus leading to the larger number of occurrences during the mission.

Table 38. Maneuver Induced Load Statistics by Mission Type

Mission	Average Number per Mission	Average $+\Delta n_z$ (g)	Average $-\Delta n_z$ (g)	Max $+\Delta n_z$ (g)	Min $-\Delta n_z$ (g)
Bucket	592.90	0.688	-0.407	2.460	-1.189
Ferry	107.46	0.664	-0.377	2.211	-1.037
Passenger	153.05	0.732	-0.405	2.995	-1.119
Recon	248.10	0.740	-0.420	2.407	-1.112
Helitorch	549.89	0.703	-0.421	2.760	-1.216
Longline	302.85	0.699	-0.397	2.031	-0.937
Rappel	156.52	0.705	-0.394	2.492	-0.932

As can be seen in Table 39. Maneuver Induced Load Statistics by Phase Type, other than cruises, descent and burn phases had a relatively high average number of occurrences per phase. This was most likely due to the flight profile associated with these phases, such as the approach to landing which might require increased maneuvering to accomplish. Likewise with burns, maneuvering into proper alignment for an accurate drop would necessitate increased maneuvering of the helicopter.

Table 39. Maneuver Induced Load Statistics by Phase Type

Phase	Average Number per Phase	Average $+\Delta n_z$ (g)	Average $-\Delta n_z$ (g)	Max $+\Delta n_z$ (g)	Min $-\Delta n_z$ (g)
Stationary	0.03	0.665	-0.359	0.996	-0.513
Start of Flight	0.18	0.582	-0.356	1.430	-0.502
Climb	1.46	0.653	-0.408	1.900	-0.978
Cruise	23.52	0.715	-0.400	2.492	-1.134
Descent	7.50	0.712	-0.412	2.995	-1.216
Start of Landing	0.56	0.564	-0.363	1.318	-0.614
Hover	4.35	0.631	-0.373	1.408	-0.703
Fill	0.98	0.571	-0.373	1.972	-0.713
Drop	0.65	0.611	-0.402	2.112	-0.863
Burn	7.50	0.422	-0.357	1.070	-0.575

Figure 109. Maximum and Minimum Incremental Load Factors and Coincident Ground Speed or Indicated Airspeed shows a definite load factor grouping about certain airspeeds, approximately 40 KIAS, 70 KIAS, and greater than 80 knots. The average airspeed of cruises across all missions was 78.50 KIAS, and 34.06 KIAS for descents. It can also be seen that the magnitude of maneuver induced loads at greater than 80 KIAS decreases proportionally with an increase in airspeed. Above 100 KIAS there is a single instance of maximum incremental load being greater than 1.0g.

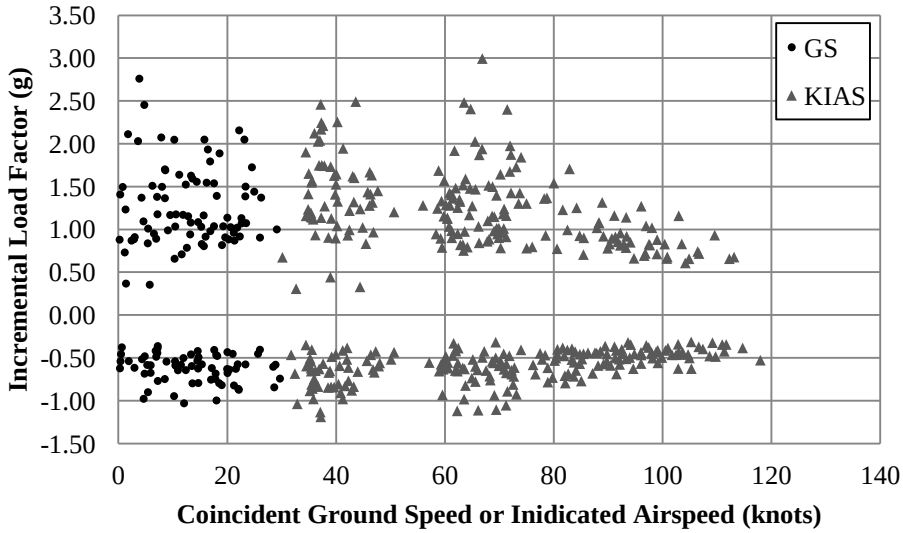

Figure 109. Maximum and Minimum Incremental Load Factors and Coincident Ground Speed or Indicated Airspeed Due to Maneuvers

The cumulative frequency of occurrences in Figure 110 shows a similar pattern of distribution across all mission types, excluding ferry missions, except at the outer ranges of the flight loads. This would suggest that while smaller magnitude maneuver loads were similar and independent of the mission type, for the more extreme values, the individual flight characteristics of the mission began to play an increased role in the frequency of occurrences. Ferry missions have a reduced number of maneuver induced loads as compared to the other mission types. Given the simplicity of the ferry flight profile, the mission would not require excessive maneuvering due to mission characteristics, thus reducing the number of maneuver induced loads.

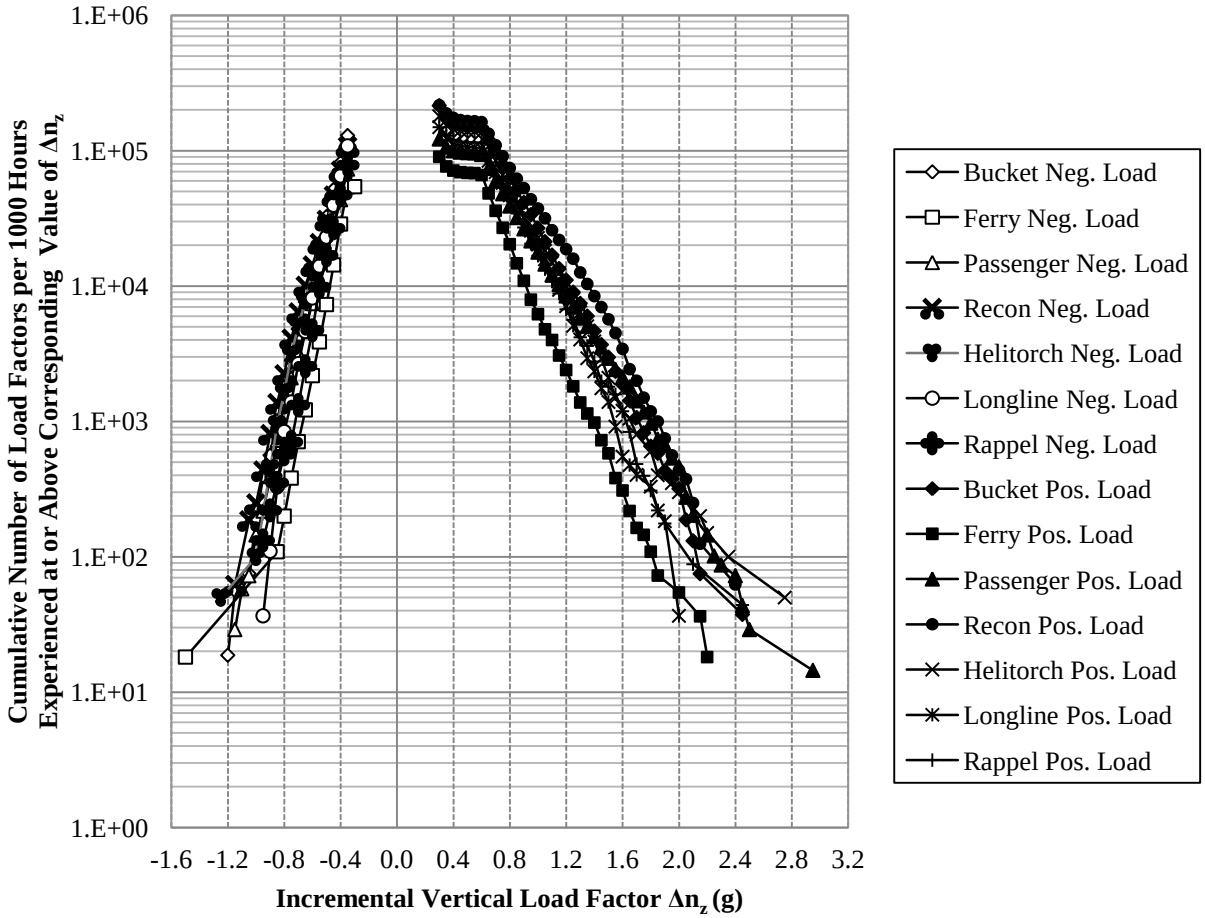

Figure 110. Maneuver Induced Cumulative Load Factor Comparision by Mission Type

c. Maneuver and Change of State Induced Vertical Flight Loads

As previously discussed, changes of state induced loads have classically been defined as maneuvers. Therefore, it is of use to see the effect of loads classified as change of state on maneuver induced loads as a whole. Like maneuver induced loads alone, bucket and helitorch missions had the highest average number of occurrences per mission, followed by longline then reconnaissance. As compared to maneuver induced loads alone, the average positive and negative incremental loads, as presented in Table 40, were reduced in magnitude by an average of 0.046g for positive, and 0.0096g for negative loads.

Table 40. Maneuver and Change of State Induced Load Statistics by Mission Type

Mission	Average Number per Mission	Average $+\Delta n_z$ (g)	Average $-\Delta n_z$ (g)	Max $+\Delta n_z$ (g)	Min $-\Delta n_z$ (g)
Bucket	717.29	0.654	-0.400	2.460	-1.19
Ferry	149.18	0.600	-0.369	2.211	-1.04
Passenger	203.38	0.666	-0.392	2.995	-1.12
Recon	310.76	0.695	-0.408	2.407	-1.11
Helitorch	661.56	0.673	-0.411	2.760	-1.22
Longline	379.88	0.658	-0.389	2.031	-0.94
Rappel	199.67	0.661	-0.385	2.492	-0.93

Beside cruise phases, the descent phase had a relatively higher average number of occurrences per phase, including the highest maximum and minimum incremental loads. When first determining the nature of change of state induced loads, it was noticed that they occurred when the helicopter was transitioning from a cruise to descent. Via Table 41, when compared to Table 39, it is evident that the majority of change of state induced loads occurred in the cruise phase, but that the last few would occur in the descent phase and that these final loads would be the highest of the group.

Table 41. Maneuver and Change of State Induced Load Statistics by Phase Type

Phase	Average Number per Phase	Average $+\Delta n_z$ (g)	Average $-\Delta n_z$ (g)	Max $+\Delta n_z$ (g)	Min $-\Delta n_z$ (g)
Stationary	0.04	0.625	-0.355	0.996	-0.51
Start of Flight	0.20	0.570	-0.357	1.430	-0.50
Climb	1.76	0.629	-0.401	1.900	-0.98
Cruise	31.71	0.649	-0.388	2.492	-1.13
Descent	8.91	0.684	-0.405	2.995	-1.22
Start of Landing	0.67	0.543	-0.361	1.318	-0.61
Hover	5.14	0.608	-0.370	1.408	-0.70
Fill	1.07	0.564	-0.373	1.972	-0.71
Drop	0.73	0.599	-0.400	2.112	-0.86
Burn	8.00	0.419	-0.355	1.070	-0.58

As can be seen in Figure 111, change of state induced loads were spread across the entire airspeed range, suggesting no correlation between change of state induced loading and airspeed. It can also be seen that change of state induced loads alone remained at magnitudes less than 1.5 g and greater than -1.0 g, and experienced similar grouping to that of maneuvers.

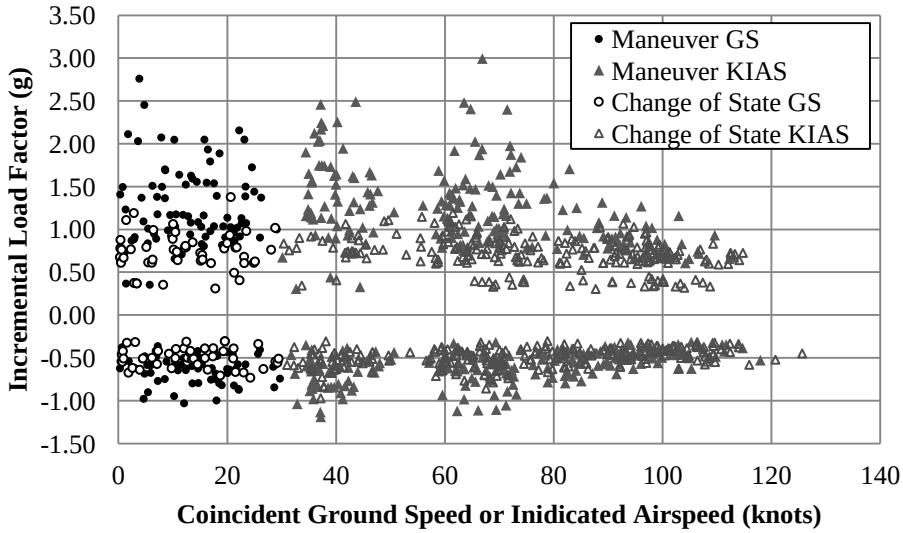

Figure 111. Maximum and Minimum Incremental Load Factors and Coincident Ground Speed or Indicated Airspeed due to Maneuver and Change of State

Figure 112 shows the cumulative occurrences of combined maneuver and change of state induced flight loads, and display a similar pattern of distribution across all mission types, except for outer ranges of the flight loads, much like gust and maneuver induced flight loads. However, recon missions showed a higher frequency of change of state loading for all positive incremental loads up to it maximum incremental load factor. Ferry missions also showed a further decrease in the number of cumulative load factors per 1000 hours when change of state induced loads were introduced.

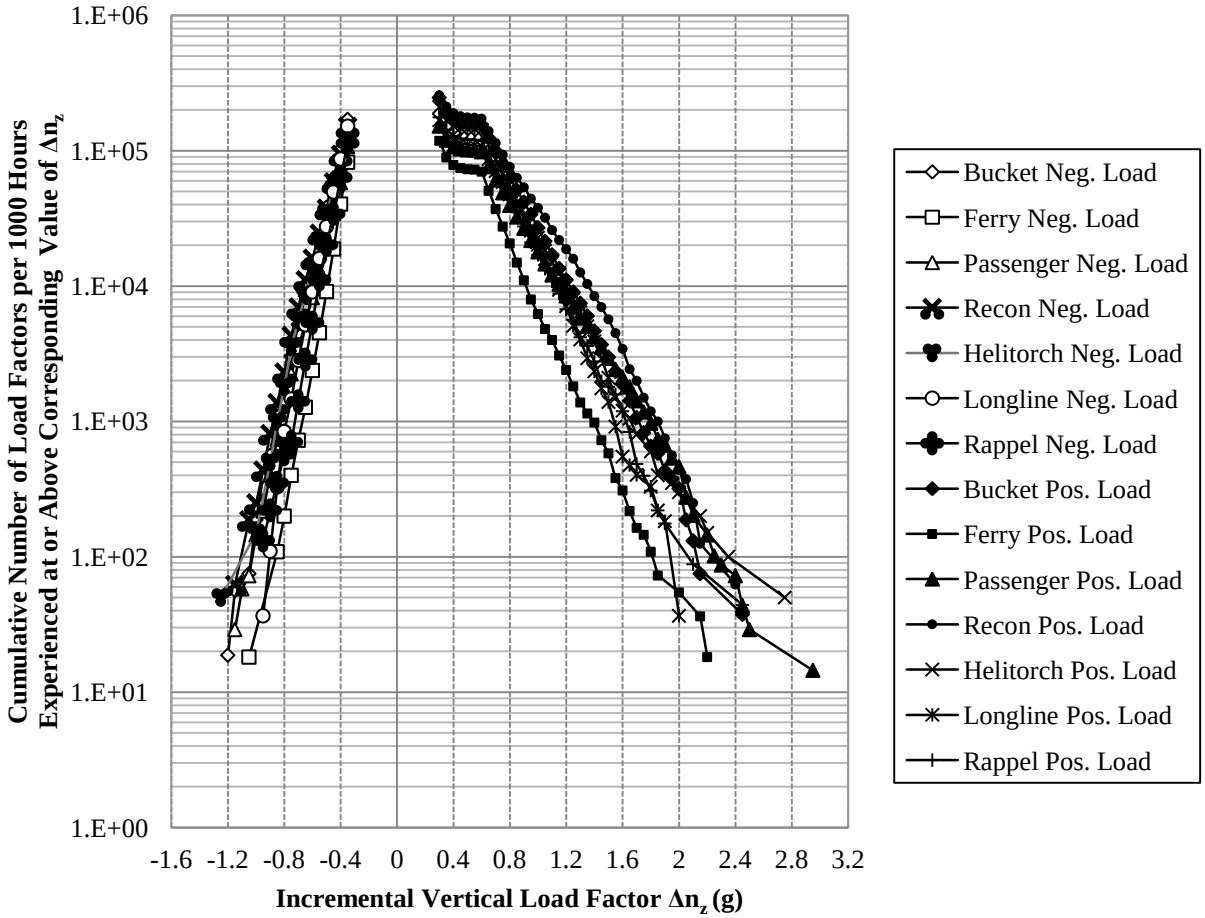

Figure 112. Change of State Induced Cumulative Negative Load Factor Comparision by Mission Type

CHAPTER 4

SUMMARY

An exploratory analysis was performed on 282 flights of a Bell Model 205A-1helitcopter used in firefighting operations. The flight data contained 263.46 hours of recorded time, covering 15,989 nm. Seven missions were identified, and each mission was divided into seven universal phases and three mission specific phases. Each mission and phase type was analyzed separately. Both usage data and loads experienced by the helicopter were examined.

For the usage of the helicopter, maximum altitude, indicated airspeed, and duration were examined for each mission and phase type. The normal distribution of flight duration and distance, along with maximum and minimum pitch and roll angles at the coincident indicated airspeed were also examined for each mission. The average flight profiles, such as average number of phase type per mission, were also discussed.

Vertical flight loads were separated for each data file using a new flight angle rates method, and were presented per 1000 hours overall and by type of load for each mission. The overall occurrences per 1000 hours was compared to the military counterpart of the helicopter to determine if loads experienced in firefighting roles were greater than those of a non-firefighting missions. The average numbers of loads, along with average and maximum and minimum loads were presented for each mission and phase. The V-n diagrams of the maximum and minimum flight loads were presented for gust, maneuvers, and combined maneuvers and change of state.

CHAPTER 5

CONCLUSIONS

A number of trends were noticed throughout the analysis of both the flight usage and for the vertical flight loading. For the overall mission usage, it was seen that the helicopter used in this study was required to perform a wide array of mission types. However, the helicopter was predominantly used in the transport of personnel or cargo not in direct conjunction with fire fighting operation; passenger missions accounted for 32% of total flights, followed by ferry missions, accounting for 26%. Missions operating primarily in fire zones were flown, but were not the primary focus of helicopter operations, as bucket missions accounted for 11%, helitorch for 3%, and rappel missions for 12%.

Trends were also observed in the flight profiles for each mission and phase type. Within each mission type, it was found that there were numerous V_{NE} exceedances for bucket, ferry, passenger, and longline missions. Longline displayed the highest average exceedance duration, largest average exceedance magnitude, and largest maximum exceedance magnitude. Despite the volume, the average magnitude of the exceedance beyond the +10% margin was less than 1.5 knots across all missions types. For each mission it was found that the correlation of maximum flight duration and coincident flight distance varied according to the mission profile. Specifically, it was found that missions which had a higher number of stationary or hovers (standard or specialized) had the lowest level of correlation. It was also shown that the majority of maximum pitch angles occurred at zero airspeed. Phase results showed that universal phases, primarily climb, cruise, and descent, had a wide variation in maximum airspeed attained during the phase. For cruise, despite the variation in maximum airspeed, there was good correlation between maximum phase duration and coincident phase distance.

In firefighting service, the data showed that this helicopter experienced far greater normal loading, both negative and positive, than its military counterpart. Smaller incremental load factors of the order of +0.3 g occurred about 90 times more frequently than those on a UH-1H when viewed at instances per 1000 hours. The maximum incremental load experienced by the UH-1H was +0.7 g during combat operations in Southeast Asia, while that of the present airframe approached +3 g during a passenger mission. In total, 92% of missions had maximum incremental loads greater than +0.75 g. This displays that this helicopter experienced more severe loading than its civilian or military counterparts. The results showed that the gust alleviation of the helicopter limited the number of gust induced loads, with an average of 11.43 gust induced loads occurring per mission. Maneuvers produced the highest number

and the largest magnitude of loads, with each mission experiencing 374.53 maneuvers per mission on average. The bucket missions had the highest frequency at an average of 717 maneuver loads per mission. For phases, while cruise phases had the highest average number per phase, descent phases exhibited the highest average magnitude and highest maximum loading.

CHAPTER 6

RECOMMENDATIONS

There are two primary areas of improvement that could increase the accuracy and completeness of future studies, data provided and program refinement. The placement of the accelerometers near the nose of the ship, instead of closer to the center of gravity, introduced some uncertainties in the conclusions presented here. Given the natural vibration of helicopters, coupled with the accelerometer placement, it is most likely that some of the loads recorded were higher than what the airframe actually experienced. Therefore, it is imperative to repeat this investigation after moving the sensors to a place closer to the center of gravity and less subject to airframe vibration. Along with the moving of the accelerometers, recording of the cyclic and collective control stick angles would allow for further insight into helicopter structural stress, as it has been noted that some control movements would not result in experiencing of a flight load.

The addition of several parameters would prove useful for the gathering of usage statistics and mission identification. The recording of AGL altitude could allow for superior phase separation, as it would allow clearly defining when the helicopter lifts off. Also, AGL altitude could be used to determine more complex phases, such as burn, which might not have consistent characteristics with the present data. Weight on hook is a desired parameter; this is primarily for the application of V_{NE} analysis. Missions with external cargo had a constant V_{NE} applied across the entire mission based on the assumption that external cargo was attached over the entire mission, though study of the ground speed traces suggested this might not be an accurate. With weight on hook provided, this inaccuracy could be eliminated.

For future studies, certain refinement of the program used for phase separation and identification, mission identification, along with vertical loading separation and classification, would be possible. While separation for basic phases was fairly reliable, identification of specialized phases, predominantly burns, proved problematic. Further refinement of parameters is needed to eliminate incorrect or missed phase identification. Because of placement of the accelerometers, a new and untested method of load classification was needed to provide initial insight into flight loads. However, using such a method may produce inaccurate results. Therefore, if accelerometers are placed correctly, a more refined and tested method of load classification could be used for future load analysis.

REFERENCES

REFERENCES

[1] Jewel Jr., J. W., Morris, G. J., & Avery, D. E., "Operating Experiences of Retardant Bombers During Firefighting Operations," NASA TM X-72622, Nov. 1974

[2] National Transportaion Safety Board, "Safety Recommendations A-04-29 through -33," April 23, 2004

[3] Tipps, D., Skinn, D., Rustenburg, J. S., "Statistical Loads Analysis of a BE-1900D in Commuter Operation," DOT/FAA/AR-00/11, 2008

[4] Hall, S. R., "Consolidation and Analysis of Loading Data in Firefighting Operations. Analysis of Existing Data and Definitition of Preliminary Air Tanker and Lead Aircraft Spectra," DOT/FAA/AR-05/35, October 2005

[5] Bramlette, R. B., "Exploratory Flight Loads Investigation of P-2V Aircraft in Aerial Firefighting Operations," Wichita Sttate University, M.S. Thesis in Aerospace Engineering, December 2008

[6] Johnson Jr., J. B., "Operation Use of UH-1H Helicopters in Southeast Asia," USAAMRDL-0062467, 1973

[7] Arcidiacono, P. J., Bergquist, R. R., & Alexander Jr., W. T., "Helicopter Gust Response Characteristics Including Unsteady Aerodynamic Stall Effects," AHS/NASA-Ames Specialists' Meeting on Rotorcraft Dynamics, February 13-15, 1974

[8] Taylor, J. W. (Ed.), "Bell Model 205A-1," *Jane's All the World's Aircraft* , p. 261. 1973-74

[9] Bell Helicopter, "Bell Model 205A-1 Flight Manual, Revision 16," May 1, 1998

[10] Heffernan, R., Precetti, D., & Johnson, W., "Vibration Analysis of the SA349/2 Helicopter," NASA-TM-102794, January 1991

[11] Hoblot, F. M., *Gust Loads on Aircraft: Concepts and Applications*, AIAA Education Series, AIAA. 1988

[12] Rustenburg, J. S., "Development of an Improved Maneuver-Gust Separation Criterion," UDRI-TM-2008-00008, January 2008

APPENDIX

APPENDIX

GUST AND MANUEVER N_Z PEAKS FOR VELOCITY FROM REFERENCE 6

Table 42. Gust N_Z Peaks for Velocity vs N_Z for Reference 6

	LESS	40	60	65	70	75	80	85	90	95	100	105	110	115	120	SUM
1.3																
1.2		5			1	3	7	2	2	2						22
0.8																
0.7		1	1		1	1	1	1	1	4						11
0.6						1	1									2
0.5																
SUM		6	1		2	5	9	3	3	6						35
Time	1196.3	729.7	409.9	476.1	565.2	850.0	1585.9	2429.4	2403.7	1148.5	292.9	55.2	17.5	1.7	0.0	12162.1

Table 43. Maneuver N_Z Peaks for Velocity vs N_Z for Reference 6

	LESS	40	60	65	70	75	80	85	90	95	100	105	110	115	120	SUM
1.7																
1.6		1		2	2	1	4	4	5		1					20
1.5		2	1		2	3	2	4	7	3		2	1			27
1.4	2	6	4	7	11	19	16	15	7	11	3		1			102
1.3	4	39	19	22	24	27	39	28	24	17	8	4	1	2		258
1.2	32	107	63	80	97	108	135	121	101	88	30	18	3	2		985
0.8																
0.7	10	40	21	31	39	53	53	72	60	40	21	1	2			443
0.6	1	6	2	1	2	2	5	6	4	7	1					37
0.5				1	2	2	3		1		1					10
0.4						3	2		2							7
0.2							2	2								4
Less						1										1
SUM	49	201	110	144	179	219	261	252	211	166	65	25	8	4		
TIME	1196.3	729.7	409.9	476.1	565.2	850.0	1585.9	2429.4	2403.7	1148.5	292.9	55.2	17.5	1.7	0.0	12162.1